University of Alberta

Integrated Affinity and Separation Based Methods on Microfluidic Devices

By

Abebaw Belay Jemere ⓒ

A thesis submitted to the Faculty of Graduate Studies and Research in partial fulfillment of the requirements for the degree of **Doctor of Philosophy**

Department of Chemistry

Edmonton, Alberta

Spring 2003

Canada

University of Alberta

Library Release Form

Name of Author: Abebaw Belay Jemere
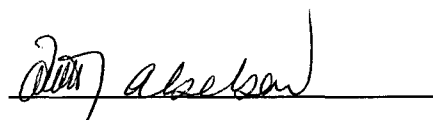
Title of Thesis: Integrated Affinity and Separation Based Methods in Microfluidic

Devices

Degree: Doctor of Philosophy

Year This Degree Granted: 2003

Permission is hereby granted to the University of Alberta Library to reproduce single copies of this thesis and to lend or sell such copies for private, scholarly or scientific research purpose only.

The author reserves all other publication and other rights in association with the copyright in the thesis, and except as herein before provided, neither the thesis nor any substantial portion thereof may be printed or otherwise reproduced in any material form whatever without the author's prior written permission.

12118-94 ST

Edmonton, AB, T5G 1J9
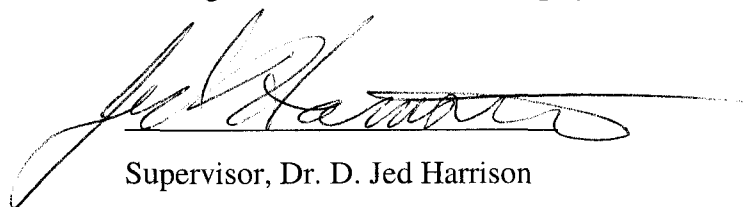
Canada

Date: December 5, 2002
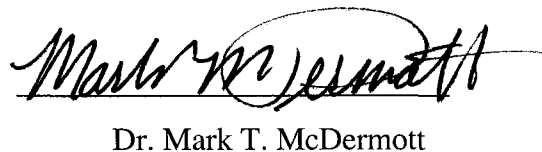
University of Alberta
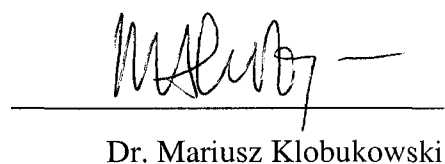
Faculty of Graduate Studies and Research
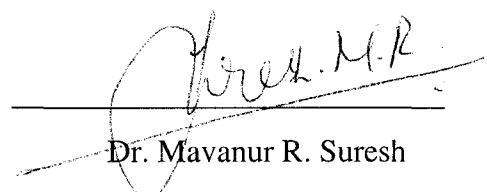
The undersigned certify that they have read, and recommend to the Faculty of Graduate Studies and Research for acceptance, a thesis entitled **"Integrated Affinity and Separation Based Methods on Microfluidic Devices"** submitted **by Abebaw Belay Jemere** in partial fulfillment of the requirements for the degree of **Doctor of Philosophy**.

Supervisor, Dr. D. Jed Harrison

Dr. Charles A. Lucy

Dr. Mark T. McDermott

Dr. Mariusz Klobukowski

Dr. Mavanur R. Suresh

External Examiner, Dr. Karen C. Waldron
Dept. of Chemistry, Université de Montréal

December 4, 2002

Date

Abstract

The development of miniaturized, microfabricated devices for chemical and biochemical analysis is a new and exciting application of micromachining technology. The ultimate goal of such systems is the development of an automated, portable and high throughput instrument capable of performing an assay on a routine basis. The results presented in chapter 2 of this thesis demonstrate the development and performance of a single channel automated instrument for immunoassay, a technique that is increasingly used in clinical diagnosis and environmental monitoring. The instrument performs the key elements of immuno-chemical analysis: sampling, injection, mixing, separation and detection within 3-5 min. The instrument incorporates a fluidic interface design to facilitate automated sample introduction into an electrokinetic microchip. On-chip mixing, reaction and separation of a protein biological threat agent simulant, ovalbumin, and Cy-5 labeled anti-ovalbumin could be performed with good quantitative results, independent of the operation of the sample introduction interface, which is connected with an external pump.

The thesis also explores the development of a facile method of trapping, rapidly exchanging, and utilizing micro beads within microfluidic devices. A two mask photolithographic and etching process is used to construct micro-weirs in a device substrate. The weirs act to retain the reagent-laden beads while allowing solution to flow through them. Columns ranging from 0.2 mm to 5 mm long were packed with ODS (octadecylsilane) beads and secured with either a "solvent lock" (for solid phase extraction, SPE) or a porous polymer plug technique (for capillary electrochromatography, CEC). Using a 0.2 mm long ODS column for SPE, neutral dyes, amino acids, and peptides were preconcentrated with preconcentration factors as high as 500. For a neutral BODIPY dye, we achieved a detection limit of 70 fM after preconcentration. In CEC, neutrals as well as charged analytes were separated with efficiencies up to 420,000 plates/m. Increasing the column length from 1 to 2 mm yielded ~1.8 times more theoretical plates than did the 1 mm column with the same flow rates. van Deemter plots were obtained for the three column lengths, showing increased plate height for the 5 mm length.

Indirect fluorescence detection of thiourea and of amino acids is demonstrated using a neutral indicator dye (BODIPY), with a detection limit of 10 μM for amino acids. The packed columns were also extended to show that size exclusion electrochromatography (SEEC) of biopolymers could be performed on chip using electrokinetic pumping. In SEEC, FITC-IgG and FITC-insulin were baseline separated with efficiency up to 139,000 plates/m.

Acknowledgments

I would like to express my gratitude to Professor D. Jed Harrison, my research advisor, for his consistent guidance, encouragement and support throughout the course of my thesis work. It has been a privilege for me to work under Prof. Harrison because his laboratory is well known for its pioneering work and scientific contributions in the area of microfluidics. I am very thankful for his patience in reading my thesis and bringing it to its current form. Also, I cannot forget the scientific knowledge I have gathered from all the conferences I have attended here in Canada and overseas, thanks to Prof. Harrison.

I cannot of course forget the past and present members of the DJH group. Thanks to all of you for the fun we had, and for sharing your experience and wisdom over the years. My special thanks go to Nighia Chiem and Richard Oleschuk, former Post Docs in the group, for their initial help in the techniques of immunoassay and bead based separations on-chip, respectively. Thank you to Dolores Martinez, Siew Bang Cheng, Justine Taylor, Michael Finot, James Kariuki and Said Attiya for the interest you showed to my work and for your friendship. Thank you to Fahima Ouchen for teaching me microfabrication at the University of Alberta student microfab. I should express my gratitude to Mrs. Arlene Figely for her personal advice, hospitality and efficiently handling any concerns that I may have had as a DJH group member.

My appreciation also extends to the technical support staff in the Chemistry Department especially to those of the electronic, machine and glass shops. Thank you to Dr. William Lee, from DRES, for your support and guidance in the DARPA project, and for your personal advice and hospitality. It was a great pleasure to work with you. My appreciation also goes to Murray Paulson from Dycor Technologies Inc. for his clever and endless help in the DARPA project. I would like to express my gratitude to the members of my candidacy and defence committee in the persons of Professors Charles Lucy, Mark McDermott, Mariusz Klobukowski, Mavanur Suresh and Karen Waldron.

I should express my deepest gratitude to my teachers from the early days of my school year. Special place is given to Dr. Ghirma Moges for convincing me to work in this new and exciting field of microfluidics.

Special thanks go to my friends and country mates. I cannot list all of your names, but you know how much I love you. In particular Hailu G/Mariam, Said Muhie, Alemayehu Berega, Asnake Tiruneh (and his family), Eshetu Getachew, Abebaw Gedefaw, Girma Hailu (and his wife, Fahime), Girma Abera (and his wife, Tigest) for your friendship and encouragement throughout my thesis work. Benyam Tesfaye and Daniel Zeilo for over 20 years of friendship.

Last but not least I should express my gratitude to my parents, sister, and brothers for your love and support. Mum, although you are not hear today to share in this moment, this proud moment is yours nevertheless. Roman Fabris, you have a special place in my heart. Your love, encouragement and being there for me in the good and bad times in the last four years was very instrumental for my success. I love you, Bella. And most importantly to God for giving me the courage and patience to persevere during the course of my research.

Dedicated to my late mother, whose unconditional love,
support and inspiration has made this dream come true.
You will be missed.......

Table of Contents

List of Figures and Tables

Figures

Tables

List of Abbreviations

Ab	antibody
Ag	antigen
Ag*	labeled antigen
Ab-Ag*	antibody-labeled antigen complex
ACN	acetonitrile
AO	acridine orange
BODIPY	4,4-difluro-1,3,5,7,8-penta methyl-4-bora-3a,4a-diaza-s-indicene
CE	capillary electrophoresis
CEC	capillary electrochromatography
CEIA	capillary electrophoretic immunoassay
CITP	capillary isotachophoresis
CLOD	concentration limit of detection
CZE	capillary zone electrophoresis
DARPA	US Defense Advanced Research Project Agency
DRES	Canadian Defense Establishment Suffield
EOF	electroosmotic flow
FITC	fluorescein isothiocyanate isomer I
HPCE	high performance capillary zone electrophoresis
HPLC	high performance liquid chromatography
IA	immunoassay
LC	liquid chromatography
LIF	laser induced fluorescence
MEKC	micellar electrokinetic capillary chromatography
µTAS	micro-total analysis system
ODS	octadecylsilane
PMT	photo multiplier tube
RSD	relative standard deviation
SEC	size exclusion chromatography
SEEC	size exclusion electrochromatography
SIC	sample introduction channel
SPE	solid phase extraction
TAS	total (chemical) analysis system

Chapter 1: Introduction

1.1 Miniaturized Total Analysis Systems

1.1.1 Total Analysis Systems, TAS

The desire for automated and portable analytical instrumentation in industrial process control, and in environmental and medical sciences was the main driving force for the development of the concept of a Total (chemical) Analysis System (TAS). Pioneered by the late H. Michael Widmer[1] at Ciba Geigy in Basel, Switzerland, a TAS ideally performs all the component stages of a complete analysis in an automated fashion. These stages can include sampling, sample pretreatment, chemical reactions, analytical separations, detection, and data analysis. An automated system with all the necessary steps integrated into a single unit would significantly reduce human involvement in this labour intensive process, thereby reducing the total analysis time and cost of an assay. Realizations of TAS have enabled enhancements in on-line monitoring of chemical parameters in both gas and liquid phase analysis.[1-4] Because the sample pretreatment step eliminates most interfering compounds in the matrix, the detector or sensor in a TAS need not be highly selective. However, significant drawbacks still remain to be solved. These include: slow sample transport, especially in liquid phase analysis, high reagent consumption, waste generation and long analysis times, as well as the need to fabricate interfaces between distinct components. Manz et al.[5, 6] proposed that improvements in overall analytical performance could be achieved by minimizing the scale on which the analysis is performed i.e. "downsizing" TAS to create a Micro-TAS (μ-TAS).

1

1.1.2 Micro Total Analysis System, μTAS

Miniaturization of existing chemical analysis systems using microfabrication technology was first introduced in 1975 by Terry et al.[7, 8] In that pioneering work, they integrated a gas chromatographic analyzer, including a 1.5 m long, 200 μm wide and 30 μm deep separation column and a split injector, on a 5 cm diameter silicon wafer. A thermal conductivity detector was also fabricated on a separate silicon wafer and mechanically clamped on the wafer containing the column. The native SiO_2 surface layer of the channel was first treated with an organosilane compound and then coated with a silicone oil (OV-101) stationary phase. Although this device managed to separate simple mixtures of gaseous hydrocarbon compounds in a matter of seconds, the significance of this work for liquid phase analysis was not exploited until 1990, when Manz et al.[6] recognized the benefits of miniaturization for liquid chromatography. In that report, they fabricated an open-tubular chromatographic column and a conductometric detector on a 5 x 5 mm silicon wafer, connected to an off-chip conventional LC pump and valves to perform high-pressure liquid chromatography. Unfortunately, no data was ever published of any LC separations performed with the device. Simultaneously, Manz et al.[5] suggested the concept of a "miniaturized total chemical analysis system, μ-TAS" which incorporates all sample-handling operations on a single planar chip. The main reason for the miniaturization of TAS is related to an enhancement of analytical performance, rather than a reduction of system size. Miniaturization of flow manifolds to reduce the transport distance between the sampling and detection point addresses not only the problems in TAS, but also renders shorter separation times and better resolution of the analytes, based on simple diffusion and hydrodynamic theory. Examples of improved performance using

2

small inner diameter capillaries and shorter capillary lengths have been reported.[9-11] Utilization of conventional pumps to deliver fluid in microchips was awkward, however. Most pumps are not well suited to deliver the low volume of solutions needed within chips, and in some cases high backpressures might be a problem.[4, 12]

Harrison and co-workers[13, 14] demonstrated, for the first time, the use of electrokinetic pumping for fluid handling in silicon and glass microchips in 1992. Those reports demonstrated the feasibility of using electroosmotic pumping for flow control in interconnected channel networks without the need for mechanically moving valves. The suitability of glass and to some extent silicon wafers for electroosmotic pumping and the electrophoretic separation of ions was explored. A detailed description of electroosmotic pumping will be discussed later in this chapter. The use of electroosmotic flow (EOF) for pumping in miniaturized analytical systems renders a number of benefits, such as a uniform flow velocity across a channel's cross-section, channel width independent linear flow velocity, and no problems with back pressure generated by the small chip channels. Moreover, valveless switching of fluid between channels could be achieved by switching the voltages applied to each channel. In the above two reports, Harrison and co-workers proved the concept of μ-TAS, integrated injection, separation, and detection within a single planar device. Since the first demonstration of fast capillary electrophoresis separation on microchip by the above authors, electrokinetic fluid handling in microchips has been utilized by a large number of researchers in the field of μ-TAS. Researchers have developed a basic set of microfluidic tools, which can be successfully applied to define and move small volumes of samples, as well as mix them or dilute them, as the case may be. During the last decade, the interest in μ-TAS has increased very rapidly

3

and the concept of μ-TAS as a chemical analysis platform has expanded to include analysis of biological samples. Many of these efforts have been detailed in recent reviews to which the interested reader is referred. These include reports of integrated chip-based separation methods,[15, 16] biochemical applications of microsystems,[17, 18] sample pretreatment on microchip devices[19] and the clinical potential of chip-based analysis systems.[20, 21] More comprehensive and detailed reviews of μ-TAS are presented by Manz and co-workers.[22, 23] In addition, more complete and up-to-date coverage of the area of μ-TAS can be found in the proceedings of the international symposium on μ-TAS.[24-28]

1.2 Motivation of This Work

Separation is a key element of many analytical methods. The first solution phase on-chip separations were performed using capillary electrophoresis, and the variants of electrophoresis have remained the dominant method studied to date. This situation is a distortion of that commonly found in analysis, in which adsorption, affinity and extraction methods are more common. Thus, it would be useful to extend the microfluidics toolbox to include a broader range of separation methods. This thesis is focused on an exploration of a range of separation methods integrated on-chip. These include homogeneous phase affinity CE or CE immunoassay (CEIA), as well as a variety of adsorbent phase methods such as reversed-phase capillary electrochromatography (CEC), solid phase extraction (SPE), and size exclusion electrochromatography (SEEC).

Before and during the course of this thesis work, others have explored a variety of capillary and microchip based separation methods. In the following sections that work

4

will be reviewed, and some basic background relevant to microfluidic separation chips will be presented.

1.3   Micromachining

Micromachining or microfabrication refers to the fabrication of 3-D mechanical microstructures and related devices in silicon or other materials using microelectronic fabrication technology.[29]   This technology was originally developed for fabricating electronic devices such as computer chips. Its use in chemistry was first demonstrated by Terry et al.[7, 8] when they micromachined a gas chromatograph in a silicon wafer. Major processes involved in micromachining include film deposition, photolithography, etching, and bonding.   These processes are shown in Figure 1.1, which outlines a standard one-mask micromachining procedure for etching channels into a glass wafer.

At present, miniaturized chemical systems are fabricated in a wide variety of substrates, such as silicon, glass, quartz, and plastic using different etching techniques. Each material has its own advantages and disadvantages. Polymers such as polymethylmethacrylate (PMMA) and polycarbonate (PC) are promising materials for microsystem technology, since they are applicable for mass replication technologies such as injection molding, hot embossing, casting or laser micromachining.[30, 31]   Silicon is a semiconductor and the application of high voltages (> 300V) to a silicon microchip is extremely difficult.   Silicon devices covered with insulating layers of thermal oxide and nitride have been shown to suffer from electrical breakdown problems that seriously limit the applicable voltages.[32]   Quartz is suitable for CE because it is a good electrical insulator and it is transparent to UV light, which is required for absorbance. Other glasses

5

that are less costly than quartz, such as Corning 0211, Pyrex and Borofloat may also be used, although they may have reduced optical qualities. Moreover, a large variety of surface modification methods developed for conventional CE and HPLC can easily be transferred to glass and quartz microchip devices. The major drawback of glass and quartz microchips relative to plastic devices is the time and labour intensive nature of the fabrication procedures. However, the chemical compatibility of glass often makes it more suitable than plastics.

As has been discussed by Fan et al.,[33] microfluidic device fabrication begins with the deposition of a thin layer of adhesive reactive metal such as Cr beneath a relatively unreactive metal such as Au that is used for photolithography. Usually a layer of Cr/Au coating (25/100 nm thickness) is sputtered onto the glass surface before spin coating with light sensitive photoresist. A photoresist is a polymer that becomes soluble (for positive photoresist) or insoluble (for negative photoresist) in developer solution after exposure to light. The desired pattern is then created by irradiating UV light through the opening(s) of the photomask; photolithographic patterning. A photomask is a plate with a user designed pattern that is transparent, while the background is opaque (or vice versa) to the light. The UV exposed photoresist film undergoes photochemical reactions, which change the physical and/or chemical property of the film.[34] Once the photoresist is developed and baked at high temperature (to increase the adhesion of the unexposed photoresist with the metal layer), the next step involves etching the metal layers and removing the rest of the photoresist. The gold and chrome layers are removed with an aqueous potassium iodide/iodine solution and a Cr etchant. After the metal layer is removed, the desired pattern is etched on the glass substrate using a mixture of

concentrated $HF:HNO_3:H_2O$ (22:14:66). The etching rate is controlled by controlling the time the substrate is soaked in the HF solution. The etching progress can be monitored by a profilometer. Following etching of the channel networks, the excess photoresist and the Cr/Au layer are removed using acetone and metal etchants, respectively. To complete the fabrication of a device, the etched substrate is bonded with a cover plate into which access holes are drilled. Permanent bonding can be achieved thermally at 400 – 650 °C using a programmable oven.

The above description involves the use of a single mask. When different etch depths or processes are required, a multiple mask approach is used. A multi-mask procedure involves reiterating the steps described above, taking into account how the recently patterned etch might influence the subsequent mask step.

7

Photoresist

Cr/Au layer

Glass

A

UV light

Photomask

Glass

B

Glass

C

Glass

D

Glass

E

Glass

F

Glass

G
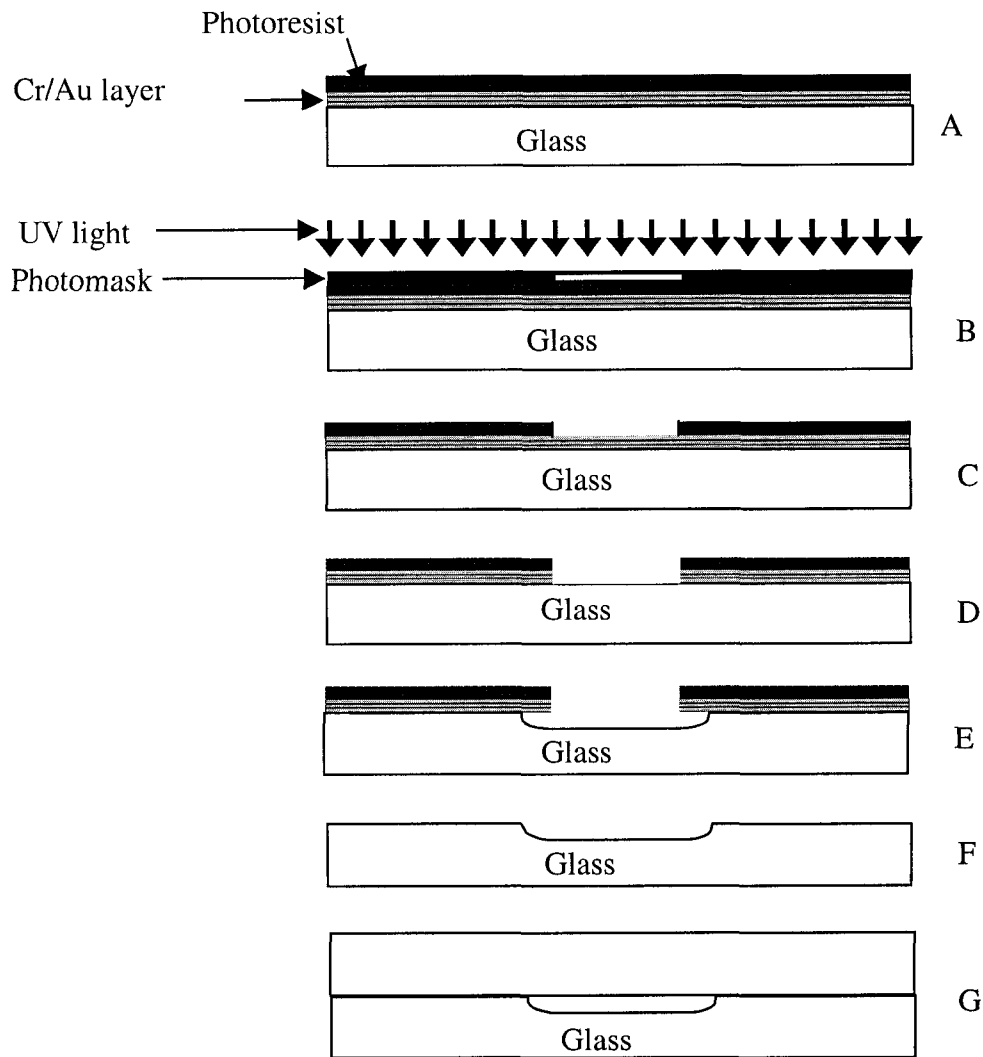
Figure 1.1   The sequence of device fabrication. (A) Glass/quartz plate
is coated with metal and photoresist; (B) Pattern is
transferred by exposing photoresist with UV light through
contact mask; (C) Exposed section of photoresist is
developed; (D) Exposed metal is etched; (E) Exposed glass
is etched; (F) Photoresist and metal are stripped off the
glass plate; (G) A glass cover plate with drilled access holes
is aligned and bonded with the etched glass plate; followed
thermal bonding.

8

1.4 Electrokinetic Based Separation Methods

1.4.1 Capillary Zone Electrophoresis

Capillary zone electrophoresis (CZE) was first demonstrated by Hjertén in 1967[35] when he separated charged compounds in a 3 mm i.d. glass tube. To minimize the adverse effect of the large inner diameter of the tube, he rotated the separation compartment about its longitudinal axis. Mikkers et al.[36] showed dispersion in CZE can be controlled by the use of narrow-bore tubes. The potential of this important separation technique was not, however, realized until Jorgensen and Luckas[37-40] published their work in early 1980 using 75 μm i.d. capillaries, which demonstrated the high resolving power of CZE and led to what is also called high performance capillary electrophoresis (HPCE). In CZE, separation of ions occurs in a free-flow, open tubular mode driven by electroosmotic flow and the inherent electrophoretic mobility of the analytes under the influence of an applied electric field. Separation is due to the differential electrophoretic mobility of the individual sample components. The separation of ions in CZE can be optimized by controlling the applied voltage, electrolyte composition, ionic strength and pH of the buffer, and surface coatings. Characterized by low sample consumption, high resolution, potential for automation and efficient separation, CZE has become more and more popular in academia and industry. The first commercial CZE machine was marketed in 1988 and since then many advances and applications have occurred. Many reviews and books present recent developments and applications of CZE,[41-47] to which the interested reader is referred.

9

1.4.1.1   Pumping in Electrokinetic Based Separation Methods

Typically, electrokinetic separations are made in capillaries filled with electrolyte solution (buffered at the desired pH), in which a sample is injected either electrokinetically (with voltage) or hydrodynamically (with a pressure gradient). When the two ends of the capillary are immersed into two buffer vials and an electric field is applied, the buffer ions will move relative to the stationary charged surface of the capillary via electroosmotic flow (EOF) and electrophoretic migration.[35, 37, 38]   A requirement for EOF is the presence of immobilized surface charges at the capillary wall in contact with the buffer. The surface of an uncoated fused silica capillary is negatively charged at a pH greater than 3, due to deprotonation of the surface generating $-SiO^-$. This surface charge leads to the formation of an electrical double layer by attracting oppositely charged ions from the buffer solution, and therefore leads to concentration and charge density gradients in the immediate vicinity of the capillary wall, as is illustrated in Figure 1.2. The positive character of the solution near the surface extends into a mobile diffuse region of the double layer. The interface between the silica wall and the bulk buffer inside the capillary has been extensively studied.[48]   Under the influence of an electrical field, solvated cationic species beyond a shear layer in the diffuse region of the double layer are electrically driven toward the cathode, dragging the bulk of the liquid in the capillary along. Thus, a flow is generated near the solid-liquid interface of the capillary wall. Because the flow is generated along the walls (i.e. the shear plane of the solid-liquid interface), the velocity profile of the EOF in the channel is flat. Unlike the parabolic flow pattern in pressure driven systems, the flat, plug-like flow pattern in EOF

10

results in very little dispersion and bandbroadening, leading to very high efficiencies in electrokinetic based separation methods.

In packed columns, as in capillary electrochromatography, which will be discussed later in this chapter, both the capillary wall and column packing carry surface charges that are capable of generating EOF. Most of the work in the literature, however, suggests that the column packing is responsible for the generation of most of the EOF,[49, 50] there is a greater total number of free silanol groups on the solid packing since it has a far larger surface area than the capillary wall. The EOF velocity in packed capillaries, however, is ~ 40-60 % slower than that in an open channel.[51, 52] This is caused, in part, by the lack of orientation between the interconnected channels and the capillary axis and because the observed velocity can be a function of column porosity. In addition, the modified surface of the silica packing particles, as compared with an unmodified surface, contains a reduced number of free silanol groups per unit area, leading to a decrease in EOF.

The application of an electric field in electrokinetic separation methods has an additional effect. It induces the separation of charged analytes due to the difference in their charge and size. This separation is referred to as electrophoresis. Although electrophoresis moves anions towards the anode and cations towards the cathode, all species are transported to the cathode because the electroosmotic flow is usually greater than the effect of the electrophoretic mobility of the ions. Typically, the surface charge is negative, leading to this net cathodal flow. Hence, the combined effects of electroosmotic flow and electrophoretic mobility of ions are responsible for separation and for pumping analytes towards the detection zone.

11
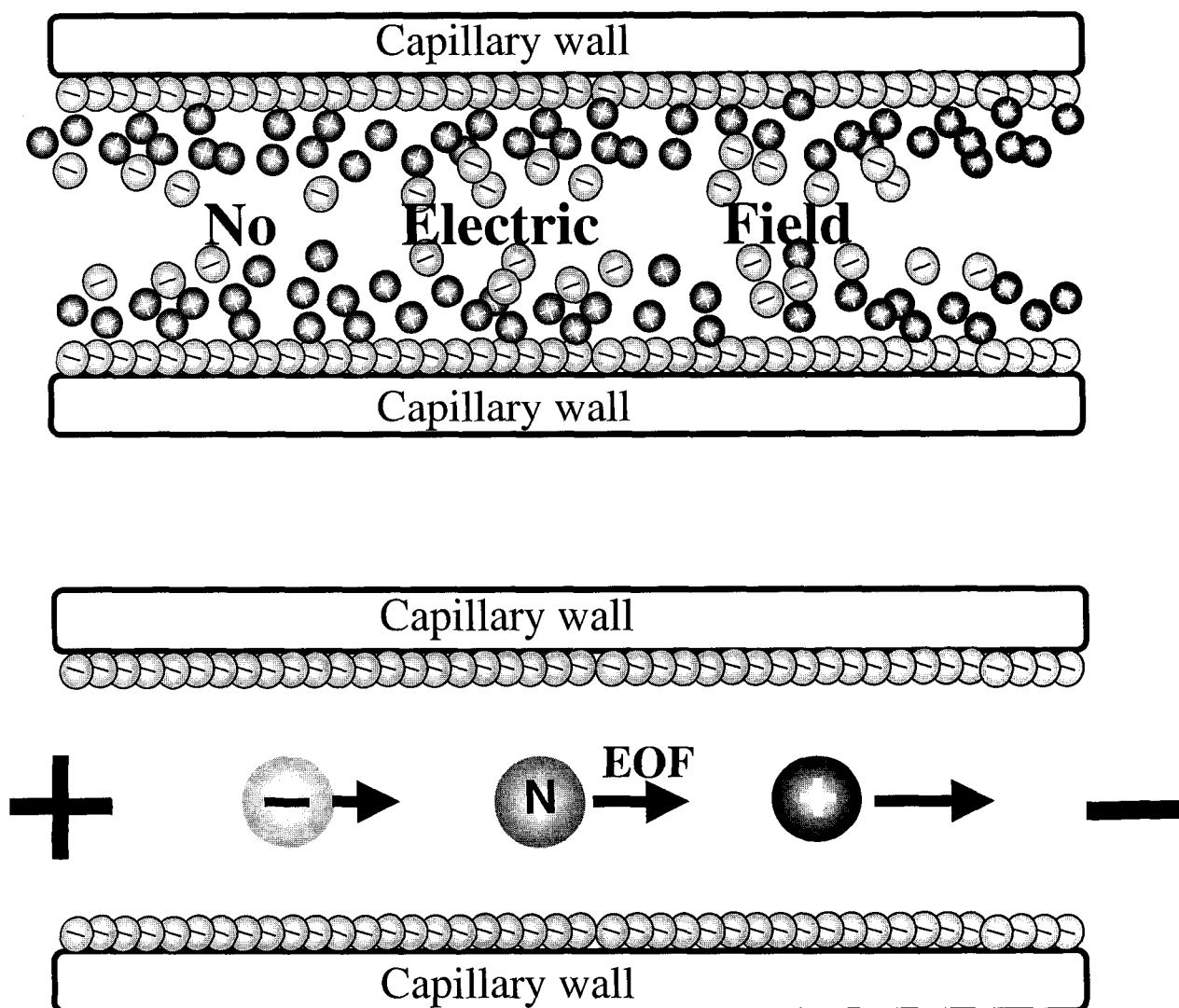
Figure 1.2   Schematic representation of electroosmotic flow. The top view shows the negatively charged glass surface and hydrated cations accumulating near the surface of the glass wall. The bottom view represents solvent flow towards the cathode upon application of electric field. The sizes of the arrows suggest the magnitude of the apparent mobility of the species.

12

1.4.1.2 Capillary Electrophoretic Immunoassay

Immunoassays are analytical techniques based on the specific reaction of an antibody and an antigen, for the determination of either reactant in solution. Immunoassays have become the method of choice for a wide variety of clinical, environmental, pharmaceutical, and chemical analyses due to their ability to quantitatively measure trace amounts of analyte (antigen) in complex mixtures whose constituents are often present at much higher concentration.[53, 54] The major drawbacks of currently available automated immunoassay systems are their bulky size, cost of instrumentation, and the fact that they are dedicated only for routine assays at fixed locations in large institutions. Thus, recent immunoanalytical research has been directed towards developing miniaturized, portable and automated immunoassay formats. Microchip based immunoassay systems, such as the one described in Chapter 2 of this thesis, can be smaller, less expensive, portable, and automated so that point-of-care testing (POCT) is possible.

The application of electrophoretic techniques to study interacting molecules began in 1960 when the equilibrium constants for the binding of Ca^{2+} and Zn^{2+} to serum albumin were determined with gel electrophoresis.[55] The high resolving power of electrophoretic methods compared to chromatographic methods (such as size exclusion chromatography) is a distinct advantage,[56, 57] but detection of the components of interest is not always straightforward. Since Grossmann et al.[58] and Lielsen et al.[59] first demonstrated the potential of capillary electrophoretic immunoassay (CEIA) based on the separation of free and bound forms of antigen or antibody by CE, it received attention as a method to perform the separation step needed in an immunoassay.[60-67] There are a number of reasons why CE might appear an interesting alternative to existing immunoassay

13

protocols. First, many immunoassays require the efficient removal of interfering biological matrix and the separation of free immunological reactant (antibody or antigen) from the immunological product (antibody-antigen complex) prior to quantitation. Due to the high resolving power of CE, it can be assumed that it can perform these steps efficiently in a single step. This avoids the multiple wash steps required in conventional immunoassay formats. In addition CE might allow simultaneous determination of many analytes, which is highly desirable in certain applications. The second advantage of CE in immunoassay comes from the minute volume requirement per assay. Furthermore, in CEIA fast separations (several minutes) can be achieved by the use of high electric field strengths. The initial CEIA methods, [60-67] however, required many minutes (5 – 15) for the separation as conventional CE methods were used.

At Transducers '95, Harrison's group[68] presented the first microchip based CEIA in which bovine serum albumin and anti-bovine serum albumin were mixed and reacted off-chip and the complex was separated from the reactants in a microfluidic device. A similar approach was used by Kounty et al.[69] for serum cortisol immunoassay with separation and detection of an off-chip reacted complex from the unreacted reagent. The greatest benefit of microchip based CEIA was first reported by Chiem and Harrison.[70, 71] In these reports, the antibody and antigen were mixed, reacted and the products separated on-chip, significantly reducing the assay time. Major advantages of microchip devices are their potential for automation and the fact that multiple channels of identical geometry can easily be fabricated on a single substrate, so that high throughput analyses are possible. A portion of this thesis focuses on the development, in collaboration with Defense Research Establishment Suffield (DRES) (Suffield, AB), Dycor Technologies

14

Ltd. (Edmonton, AB) and Micralyne (Edmonton, AB), of a robust and portable automated single channel based CEIA instrument for the determination of biowarfare simulation agents.[72] The instrument has been tested and characterized in Chapter 2 of this thesis. As another part of that project, Cheng et al.[73] developed a multichannel (6 parallel channels) microchip CEIA system that performs mixing, injection, separation and detection of immunoreagents and products simultaneously.

1.4.2 Micellar Electrokinetic Capillary Chromatography

Since the basis of separation in CZE is the differential electrophoretic mobility, which is proportional to the charge of the compound, neutrals cannot be separated by CZE. In order to separate neutral molecules by electrophoresis, charge must be introduced to them, usually by complexation with a charged ligand. In 1984, Terabe et al.[74] introduced micellar electrokinetic capillary chromatography (MEKC) in which separation is governed by differential micellar solubilization of analytes and their subsequent variation in electrokinetic migration. In MEKC, separation of neutral compounds occurs when they preferentially partition between the hydrophobic interior of molecular aggregates of surfactant molecules (micelles) and the aqueous phase. Although originally developed for the separation of neutral compounds, MEKC has increasingly been used for the separation of charged compounds that have similar electrophoretic mobilities, using both charged and neutral/zwiterionic surfactants.[75] In MEKC, separation of charged analytes could be obtained due to differences in both hydrophobic interactions and electrophoretic mobilities, as in CZE. MEKC has been successfully transferred into microchip format.[76-78] MEKC provides a CE-based alternative to liquid chromatography (LC). But it is not

15

as general or robust a method as LC, so does not provide a definitive LC-like method for microchip systems.

1.4.3 Capillary Electrochromatography

Capillary electrochromatography (CEC) is a recently developed variant of high performance liquid chromatography (HPLC) in which solvent transport is achieved by electroosmotic flow (EOF) rather than by applied pressure. As discussed above, EOF is generated by applying an electric field across the separation column. As in HPLC, the solutes of a given mixture can be separated based on differences in distribution ratios between two phases, the mobile and stationary phases. Compounds possessing charge can also be influenced by the applied electric field, leading to differential electrophoretic mobility, as in CE. Therefore, both charged and neutral analytes can be resolved according to their differential migration through the column, based on the analyte's sorption interaction with the two phases, or a combination of such interactions and the inherent electrophoretic mobility of the analytes.

The use of EOF as a pumping mechanism results in a number of important advantages for CEC over HPLC. These include: (1) EOF generates the needed pressure to address the high back pressure generated by a packed column, allowing the use of very small (<1 μm) particles; (2) EOF produces a 2-4 fold reduction in multipath band dispersion and mobile phase transfer resistance;[79] (3) it offers all the advantages of miniaturized separation techniques such as low solvent and sample consumption, increased mass sensitivity, and reduced analysis time.

16

Brief History of CEC

The history of CEC can be traced back 63 years to when Strain[80] published his work on the use of an applied electric field across an adsorption column. He demonstrated higher selectivity, due to the combined effects of electrophoretic and chromatographic separation forces. In 1974, Pretorius et al.[81] suggested the possibility of using EOF as a means of transporting solvent through an LC column rather than using pressure driven flow. They pointed out that with the use of EOF the efficiency of a chromatographic column would increase while back-pressure problems across the column would disappear. Significant progress in CEC began in the 1980s after Jorgensen and Luckas[38] demonstrated the use of EOF in capillaries and showed the possibilities of very high efficiencies. Later in 1987, Tsuda[82] reported on open tubular CEC using coated channels and recognized the factors that control the EOF as well as the importance of practical effects, such as bubble formation, in packed columns. The detailed theoretical and experimental contributions of Knox and Grant[51, 83] marked a recent renaissance of CEC. Recently, several contributions have been made to the further development of this important separation technique. The interested reader is referred to the recent reviews on CEC.[84-94]

1.4.3.1   CEC On-Chips

Although CEC would benefit from integration onto microchip structures, especially in terms of reduced separation/analysis time, this has been an area of limited research in microfluidics. Almost all separation processes adapted to microchips have been based

upon solution phase separations. As in a capillary, several possibilities exist for performing CEC on a microchip.

1.4.3.1.1   CEC with Open Channels

It is a relatively straightforward procedure to transfer open-tubular chromatographic experiments in capillaries to microchannels. In open-channel electrochromatography, the inside wall of the chip is coated with a stationary material. The first report on integrated open-channel electrochromatography came from Ramsey's group in 1994.[95] They coated the inside wall of a 5.6 μm deep microchip device with a reversed-phase C18 stationary material and separated three coumarin dyes. Later in 1998, the same group investigated open-channel electrochromatography in combination with gradient elution.[96] Under optimized conditions, they separated four neutral dyes within a 6 s elution window, with the chromatogram being completed in about 20 s. A strong influence of channel depth on column efficiency was observed, especially for channels deeper than about 5 μm. Smaller channel depths resulted in lower plate heights, while the minima for the van Deemter plot shifted towards higher velocities. Theoretical calculation from Reginer's group[97] supported the observed influence of channel depth on separation efficiency of open-channel electrochromatographic system.

The open-channel electrochromatographic approach, however, has a number of limitations. Channel widths of 2 μm or less are required to deal with the limited rate of mobile phase mass transfer.[98] Such small dimensions become increasingly susceptible to clogging. The very small phase ratio (i.e. the ratio of volume of stationary phase to

volume of the mobile phase) of these small channels will definitely limit sample capacity of the columns, therefore compromising efficiency.

Regnier's group[99, 100] introduced a totally new idea of performing CEC in microfluidic devices. They fabricated so-called collocated monolith support structures (COMOSS) separated by a rectangular support channels (1.5 μm wide and 10 μm deep) in quartz and PDMS. The support structures were then coated with reversed-phase stationary material and CEC separations of a tryptic digest of ovalbumin[99] and synthetic peptides[100] were demonstrated. Because the fabricated micro-columns still need to be coated with stationary materials to give proper retention, this approach can be considered a hybrid between an open channel and a packed channel CEC.

1.4.3.1.2   CEC with Monolithic Columns

Another approach being explored to perform CEC on-chip involves the use of porous polymer monoliths.[101-104] The preparation of monolithic columns in microchip channels is relatively simple, since a monomer solution with low viscosity is simply passed into the channels. Typical polymerization mixtures consist of methacrylate based materials.[101, 103, 104] The continuous polymeric bed is then created by thermally initiating the polymerization reaction[102] or exposing a segment of the filled channel to UV light.[101, 103, 104] Accordingly, there is no restriction as to the width of the channel, an issue in open channel electrochromatography. For microchip based CEC, photoinitation of the polymerization reaction is preferred over thermal reaction since the polymer cannot be localized in the latter approach. A microchip with channels completely filled with polymer may not be optimum, as it may be desired to have an open segment for injection

19

and detection. Column efficiencies of these microchip-based monolithic columns are in the range of 200,000 – 300,000 plates/m. The performance of monolithic columns depends on the pore size and distribution of the resulting polymer[105], which need to be controlled by fine tuning the proportion of the porogenic solvent used.

1.4.3.1.3   CEC with Packed Channels

In comparison with open channel CEC, packed columns in CEC have the advantage of higher capacity and larger retention capabilities. However, the number of publications on on-chip packed column CEC is very limited.[106-108] This has been ascribed to the difficulty of affixing frits to support conventional stationary materials (beads) in a portion of a network of micochannels and difficulties with manipulating beads on-chip. Ocvirk et al.[109] presented the first example of packed column LC wherein a split injector, a packed small-bore column, a frit, and an optical detector cell were all integrated onto a silicon chip. In that work two arrays of fine V-groove channels, 3 μm wide and 2 μm deep, retained the 5 μm ODS beads within the separation channel. The performance of this HPLC column was poor, suggesting poor packing of the μ-chip, or column overloading. Since then, Harrison's group reported a chip design that allows efficient packing of conventional stationary phases into a portion of a complex chip structure and demonstrated packed bed CEC on-chip.[106, 107] The chip design utilized a three-port system, with two weirs to trap beads in a restricted portion (200 μm long) of a chip layout. The microfabricated retaining frits resolved the problem of frit making seen in conventional CEC. Stationary materials could be readily exchanged. The details of this

20

chip design are described in Chapter 3 of this thesis. Ceriotti et al.[108] demonstrated fritless on-chip packed CEC on a PDMS device using tapered outlet geometry.

1.4.4 Size Exclusion Electrochromatography

Since Lindqvist and Storgard[110] and Lathe and Ruthven[111] first reported on the elution of biomacromolecules from Sephadex (an insoluble cross-linked polydextran gel) in an inverse order of molecular weight, size exclusion chromatography (SEC) has proven to be a powerful tool in the separation and characterization of both synthetic polymers and biopolymers.[112-114] In SEC, columns are packed with porous stationary phases and molecules are separated based on a simple concept of molecular size or hydrodynamic volume. Molecules that are larger than the pore size of the packing are excluded and remain in the mobile phase, thus eluting from the column first. Molecules that are smaller than the pore size, on the other hand, can penetrate or permeate throughout the pore maze and their progress through the column is retarded. Elution is, therefore, in the order of decreasing size.

It has been suggested that for CEC columns packed with porous particles an improvement of efficiency can be obtained as a result of a substantial electroosmotic solution flow through the pores of the particles.[115] It is to be expected that this enhancement is most obvious for macromolecules typically separated by size exclusion techniques. Since both synthetic polymers and biopolymers have naturally low diffusion coefficients, slow mass transfer in the mobile phase seriously limits the separation efficiency and speed in pressure driven SEC. Analysis times of well over 1 h are not uncommon.[112] Recently, size exclusion electrochromatography (SEEC) has been

21

introduced using conventional capillary columns.[116-122] In these reports, it was shown that SEEC can offer high speed and high efficiency molecular-size separations of synthetic polymers. So far, there is no report in the literature on integrated SEEC. Chapter 5 of this thesis reports on the potential of microfluidic devices for SEEC of biopolymers.

1.4.5 Analysis of Electrokinetic Separations

1.4.5.1 Measuring Electroosmotic Flow Velocity

As has been discussed in section 1.4.1.1, charged solutes traverse the separation column by both EOF and electrophoretic mobility. The apparent linear velocity of an ion, v_{app}, in an electric field is given by

$$v_{app} = (\mu_{eo} + \mu_{ep})E = \mu_{app} E = \mu_{app} V/L$$
$$v_{app} = v_{eo} + v_{ep}$$

1.11

where μ_{eo} is the mobility due to EOF, μ_{ep} is the inherent electrophoretic mobility of the ion, which can be in the same or opposite direction as the EOF, depending on the charge of the ion, μ_{app} is the apparent mobility of the ion ($\mu_{eo} + \mu_{ep}$), E is the electric field strength, V is the applied voltage, L is the length of the capillary, v_{eo} is the EOF velocity and v_{ep} is the electrophoretic flow velocity. μ_{ep} is proportional to the charge of the ion and inversely proportional to the frictional retarding force acting on it in solution. Therefore, the apparent velocity of neutrals is the same as the EOF velocity (v_{eo}) generated in the channel since μ_{ep} is zero.

22

The linear EOF velocity (mm/s) in an electrokinetic separation method can be obtained by measuring the time (t) required for a neutral marker to reach the detector in an electric field:

$$v_{eo} = L_d / t \qquad\qquad 1.12$$

where L_d is the distance from the injector to the detector.

In CEC and SPE, where a segment of the channel network is packed with stationary materials, the linear EOF velocity is not the same in the open and packed sections of the chip channel.[123-125] Each section has its own conductance and consequently different voltage drop and electric field strength since the current is conserved across the whole length of the channel. The voltage drop (ΔV) in a segment of the channel length L is the product of the resistance (R_L) of the particular segment and the current (i) passing through it:

$$\Delta V = i\, R_L \qquad\qquad 1.13$$

and R_L is given by

$$R_L = \rho\, L/A_L \qquad\qquad 1.14$$

where ρ is the resistivity of the buffer filling the channel and A_L is cross-sectional area of the channel segment. Due to the high resistance of the packed section of the channel compared to the open section, it is often assumed that most of the voltage drop is in the packed section of the channel,[123, 124] and thus the linear EOF velocity of the two sections are not the same. From the law of conservation of mass, however, the volumetric flow rate must be the same in both segments of the channel. The volumetric flow rate in a channel (mL/min) due to EOF can then be obtained from

$$F = v_{eo}\, A \qquad\qquad 1.15$$

23

where A is the cross-sectional area of the channel. Thus, volumetric flow rates are used instead of linear flow rates whenever considering electrochromatographic separations, in contrast to CE, in which linear flow rates are often more important.

1.4.5.2 Efficiency of Separation

The basis of separation in electrokinetic separation techniques is either the difference in electrophoretic mobility of ions under an applied electric field or chromatographic interaction with a stationary material or a combination of both. Thus, the basic equation proposed by Giddings [126] to calculate the number of theoretical plates can be borrowed to determine efficiency in electrokinetic separations. The number of theoretical plates, N, is defined as

$$N = L^2_d / \sigma^2_{tot} \qquad 1.16$$

where σ^2_{tot} is the total variance of a Gaussian peak and L_d is the distance from the injector to the detector. Since the total variance and peak width of a Gaussian peak are related by

$$W_b = 4\sigma_{tot} \qquad 1.17$$

and

$$W_{1/2} = 2.354 \, \sigma_{tot} \qquad 1.18$$

where W_b is the peak width at the base and $W_{1/2}$ is the peak width at half height maximum, equation 1.16 can be rearranged to give the following two equations so that N can be determined directly from an electropherogram or electrochromatogram:

$$N = 5.54 \, (L_d/W_{1/2})^2 \qquad 1.19$$

when $W_{1/2}$ is measured in units of length;

or

24

$$N = 5.54 \, (t/W_{1/2})^2 \qquad\qquad 1.20$$

if $W_{1/2}$ is measured in units of time; t is the retention or migration time of an analyte.

The corresponding rate of generation of variance per unit length or height equivalent to a theoretical plate, HETP, also simply called plate height, H, is given by

$$H = L/N \qquad\qquad 1.21$$

where L is the length of the separation channel. It is more practical to measure H as an index of separation efficiency, rather than N, as the individual components, which contribute to H may be identified, evaluated and combined to determine an overall value. In chromatography, it is also customary to express the efficiency of the column in terms of reduced plate height, h,

$$h = H/d_p \qquad\qquad 1.22$$

where d_p is the average diameter of the packing particles.

The total spatial variance of a sample zone as recorded by a detector (σ^2_{tot}) can be given by

$$\sigma^2_{tot} = \sigma^2_{col} + \sigma^2_{inj} + \sigma^2_{det} + \sigma^2_{oth} \qquad\qquad 1.23$$

where the subscripts denote contributions from the column, injector, detector, and other factors. The variance due to injection and detection arise from the finite volumes of the injector and detector, as well as the finite response time of the detection electronics. During sample injection, an additional contribution to band broadening due to dispersion of the sample has been identified and its variance is given by $2Dt_{inj}$,[127] where D is the molecular diffusion coefficient of the solute being injected. The contributions for the injector and detector for rectangular injection and detection systems are given by

$$\sigma^2_{inj} = l^2_{inj}/12 + 2Dt_{inj} \qquad\qquad 1.24$$

25

$$\sigma^2_{\text{det}} = l^2_{det}/12 + (\mu_{\text{app}}E\tau)^2 \qquad\qquad 1.25$$

where l_{inj} is the length of the injection plug, l_{det} is the length of the detector zone, t_{inj} is the injection time, and τ is the time constant for the detection system. The extra term in equation 1.23 is the variance due to non-ideal factors, including Joule heating, sample overloading, sample-wall interaction, and electrodispersion. Sample overloading only occurs at high analyte concentration. For microchip based electrokinetic separations with fluorescent detection, analyte concentrations are typically low ($\leq$ nM) and the band broadening due to sample overloading is minimal. Variance due to analyte-wall interaction can be minimized by an appropriate choice of buffer and, more importantly, by surface modification of the channel. Variance due to electrodispersion will arise due to differences in the conductivity of the sample and running buffers and can be minimized by matching the mobilities of the buffer constituent to the sample or by maintaining a running buffer concentration approximately two orders of magnitude higher than that of the sample.[128] Variance due to Joule heating effects is highly dependent on the ionic strength of the buffer system, the applied potential and the channel cross-section. With the small dimensions of microfluidic chip channels and the concentration of buffers used, the Joule heating contributing to band broadening is usually negligible.[10]

1.4.5.2.1   Column Contribution to Band Broadening

(A)   CZE

In CZE, the main contributor to in-column band broadening is longitudinal diffusion of analyte. The corresponding variance, σ^2_{LD} is given by

26

$$\sigma^2_{LD} = 2Dt \qquad\qquad 1.26$$

where D is the molecular diffusion coefficient of the solute and t is the separation time. Thus, the total spatial variance can be re-written as

$$\sigma^2_{tot} = 2Dt + 2Dt_{inj} + l^2_{det}/12 + l^2_{inj}/12 + (\mu_{app}E\tau)^2 + \sigma^2_{oth} \qquad 1.27$$

(B) CEC

In packed column CEC, additional terms appear in the equation for the total variance of a peak, each accounting for the different contributions to band broadening:[49, 129]

$$\sigma^2_{col} = \sigma^2_{disp} + \sigma^2_{f, diff} + \sigma^2_{i, diff} + \sigma^2_{t, diff} + \sigma^2_{kin} \qquad 1.28$$

where the subscripts denote axial (longitudinal) dispersion of the solute in the interstitial space, film resistance at the particle boundary, intraparticle diffusion, transchannel mass transfer, solute interaction kinetics with the stationary phase, respectively. Solute dispersion in the axial direction is given by

$$\sigma^2_{disp} = \sigma^2_{a, diff} + \sigma^2_{eddy, diff} \qquad\qquad 1.29$$

where $\sigma^2_{a, diff}$ is the contribution due to static diffusion in axial direction and $\sigma^2_{eddy, diff}$ is the contribution due to the flow velocity differences (eddy diffusion). Because of the plug-like flow profile of EOF, the contribution of transchannel diffusion is very small. The contribution of eddy diffusion to band broadening is very small, compared to pressure driven LC for example, because the flow velocity in CEC is largely independent of the channel width.

1.4.5.3   Resolution

The resolution of two peaks is given by

27

$$Rs = 2\left[\frac{t_2 - t_1}{W_1 + W_2}\right]$$
<div align="right">1.30</div>

where t_2 and t_1 are the retention or migration times of the two analytes and W_1 and W_2 are the peak widths at the base line. Thus, a desired separation of analytes in electrokinetic separation techniques can be achieved by optimizing the various factors that contribute to band broadening discussed above. The relative migration times of the two components can also be altered by using different stationary or mobile phases.

1.5 On-Chip Preconcentration Methods

Obtaining good concentration limits of detection when using optical detection has been a challenge in miniaturized capillary electrophoresis, due to the short path lengths engendered by the channel dimension and the low sample injection volumes. Laser-induced-fluorescence detection remains the predominant detection method for microchip CE, due to its relatively high sensitivity.[130] However, most compounds are not intrinsically fluorescent, and many of these are not easily labeled with fluorophores. Sample preconcentration is therefore a critical step for the determination of minute quantities of analytes for which the detection limits of the instrument may be poor. A number of on-chip preconcentration techniques have been developed, these are discussed below.

1.5.1 Capillary Isotachophoretic Preconcentration

Capillary isotachophoresis (CITP), introduced by Martin and Everaerts in 1970,[131] occurs when an electric field is applied to an electrolyte solution consisting of a sample solution

introduced as a zone between a leading and a terminating electrolyte, with each containing only one ionic species bearing the same charge as the sample ions to be separated. This technique can be used for sample preconcentration or as an analytical separation technique. The leading electrolyte is selected to have a mobility that is greater than that of any of the components of the sample to be separated and the terminating electrolyte must have a mobility that is less than that of any of the components in the sample mixture. When an electric field is applied, the sample ions separate over a given time into distinct zones located between the leading and terminating electrolytes, arranged according to their decreasing mobilities. After equilibrium is established, all of the ions migrate with the same velocity and the boundaries between the sample zones are very sharp due to self-focusing effects. The concentration in the sample zone is dictated by the concentration of the leading electrolyte. Therefore, preconcentration of ions in the sample can be tailored by adapting the leading electrolyte concentration. CITP has been integrated in planar devices for sample preconcentration applications.[132-134]

1.5.2 Field Amplification Stacking

Filed amplification stacking (FAS) in conventional capillary systems was first demonstrated by Mikkers et al.[36] and was intensively studied by Chien and Burgi.[135-139] In this technique, a long plug of sample containing sample ions prepared in a lower conductivity buffer is injected into a capillary that has been equilibrated with a higher buffer concentration. Sample preconcentration is achieved by generating a high electric field within the injected sample plug. When a voltage is applied, electrophoresis begins and ions in the low conductivity buffer will experience a higher electric field strength and

29

move much faster than the ions present in the higher buffer concentration region. When the ions reach the concentration boundary between the two buffer systems, their electrophoretic mobility is reduced as the field strength is lower in the high buffer concentration region, stacking sample ions at the boundary. FAS has been adapted to microchip system for stacking of analytes in 400 µm long, volume defined sample plugs[140] and for stacking of a full column's worth of sample.[140, 141]

1.5.3 Solid Phase Extraction

In solid phase extraction (SPE) analytes are retained by an appropriate stationary material and subsequently eluted in a more concentrated form. SPE has an additional advantage compared to the above two methods: the ability not only to concentrate but also to clean up the sample. The SPE process can be performed either on-line or off-line. On-line SPE for concentrating analytes for CE analysis, first introduced by Guzman et al.,[142] utilizes a small packed adsorbent inside the front end of the capillary to extract the analyte of interest and enrich the sample before releasing the material for CZE. The packing material can be a very selective adsorbent as in immunoaffinity chromatography or one that adsorbs analytes based on their hydrophobic interaction only (e.g. C18 phases). Figeys et al.[143] mounted an ODS SPE system between a microchip and an electrospray needle for frontal analysis of peptides in MS identification, but the SPE component was made in a capillary or similar cartridge external to the chip. The first truly integrated SPE system was an open-channel concentrator.[144] In that report, the authors coated the inside wall of the microchip channel with octadecyltrimethoxysilane (ODS) and demonstrated signal enhancement for a neutral coumarin dye C460. Dodge et

30

al.[145] has recently reported using the open-channel chromatography approach to selectively concentrate IgG on protein A coated chip channels.

One important parameter to control in the development of an SPE method is the breakthrough volume. This parameter limits the maximum sample volume that may be used in the SPE of samples with trace components and therefore limits the maximum preconcentration factor that can be achieved. The open-channel SPE approach has a limited stationary phase and is therefore inferior in performance compared to packed column SPE systems. In order to increase the surface area available to increase analyte adsorption, Harrison's group designed a three port system to trap chromatographic beads in a microchip and demonstrated CEC and SPE.[106, 107, 146] The chip structure described in these publications was packed with both selective (protein A coated beads) and reversed-phase (ODS coated beads) stationary phases. Since Harrison's group first report, Sato et al.[147, 148] have utilized a similar approach (based on a single weir design) to trap 45 μm beads in chip channels for selective sample clean up and preconcentration. Landers' group,[149] also employed a weir-controlled chamber to pack 5 – 15 μm silica beads, to extract nanogram quantities of DNA on-chip. Another possibility to conduct SPE on-chip is to use monolithic columns. In this technique, as for monolithic column CEC, a portion of a microfluidic device is filled with a monomer solution and polymerized to give a monolithic porous polymer within the microchip channels. Yu et al.[150] demonstrated the only report on the performance of such a column for on-chip sample preconcentration.

The various weir-based bead trapping methods and the monolithic column approach to SPE both have potential value, but in each case further exploration of the performance

31

of these devices is required in order to fully evaluate them. Chapter 3 of this thesis pushes the limits of detection of the double weir design to a very minute (down to 70 fM) concentration of analyte, using ODS beads, and evaluates quantitative performance. In order to evaluate the chip performance in the context of conventional SPE operating conditions and theoretical constraints, a brief discussion of the basics of SPE is given below.

The effectiveness of an SPE device for isolating and concentrating an analyte of interest from a mixture can be described by its breakthrough volume. The breakthrough volume is established from a breakthrough curve (or frontal chromatography), which is obtained by continuously pumping a sample of fixed concentration through the SPE bed at a constant flow rate. An example of such a curve is described in Chapter 3 of this thesis. During the initial sampling phase, the analyte of interest, possibly mixed with some matrix component, is quantitatively retained by the sorbent in the SPE bed, up to the point where the sample volume exceeds the retention capacity of the sorbent. Further sample entering the SPE bed will not be quantitatively retained and eventually the concentration of analyte at the outlet of the SPE bed becomes the same as the concentration of the analyte at the inlet, resulting in a sigmoidal breakthrough curve. A point in the curve at which the ratio of the concentration of analyte at the inlet to the outlet of the SPE device is a certain arbitrary number is defined as the breakthrough volume (V_B).[151-153] The point of inflection of the breakthrough curve corresponds to the chromatographic retention volume (V_R), since the first derivative of the breakthrough curve is a Gaussian distribution similar to the peak response observed during elution

32

chromatography.[154] Although it is difficult to precisely define the breakthrough volume

of an SPE bed, it can be conveniently estimated from plate theory as[155, 156]

$$V_B = V_R - 2\sigma_V$$

where σ_V is the volume standard deviation of the peak of the first derivative of the

breakthrough curve..

The primary goal of SPE is to obtain a high concentration factor, which is defined as

the ratio of sample volume to elution volume. The breakthrough volume, and hence the

concentration factor, for a particular analyte can be increased by using (i) a sampling

device that has a large holdup volume (i.e. large sorbent bed) and (ii) a sorbent material

that provides a high retention and fast kinetics for the analyte under the sampling

condition. However, there are a number of reasons to use short columns in SPE. These

includes (a) low pressure drop required in short packed columns (b) high flow rate is

often required as it permits the collection of large sample (c) most of all a small physical

plug during desorption step is advantageous for preconcentration.

Typically, there are two common causes of premature breakthrough in frontal

chromatography. The retention capacity of the sorbent bed is overloaded due to a high

concentration of either analyte or sorbed matrix component. Secondly, the sorbent bed

may fail to adequately retain the analyte due to very high flow rates used. Thus, it is

important to optimize these parameters for maximum efficiency of the sorbent. The

performance of the SPE bed studied in Chapters 3 will be evaluated with these factors in

mind.

33

1.6 Scope of The Thesis

The focus of analytical chemistry is the development of methods and instrumentation for the separation and quantitation of analytes. Most miniaturized separation systems developed so far have utilized open channel and solution phase approaches. The focus of this thesis work is to explore packed column separation methods for integrated assays. The integration of a variety of techniques based on packed columns that are complementary to CE will expand the capability of microfluidcs to analyze compounds that were beyond the scope of microchip based CE. These techniques may soon be added to the microfluidics arsenal, moving us ever closer to the true μ-TAS concept.

Chapter 2 reports on the development of a portable, automated immunoassay microchip platform. The instrument was developed in collaboration with other researchers as part of a large DARPA project. The instrument performs all the necessary steps of an immunoassay such as mixing, reaction, injection, separation and detection in automated fashion. This chapter involves characterizing and testing the chip design and the instrument.

Chapter 3 describes the development of an integrated SPE system using reversed-phase C18 beads. The three-port chip design that allows trapping of micro beads within a microfluidic device was first reported by Oleschuk et al.[106] In that report, the authors used a change in the composition of the buffer system after packing the bed to "lock" the beads within the bed. When used for SPE and CEC, this approach limited the range of solvent selection and the eventual formation of voids in the packed bed was observed. One of the key contributions of this thesis is the development of a physical plug, formed by polymerization, to trap the packed beads so that a wider variety of solvents and

34

operating conditions could be used. The use of polymer plug improved the packed bed stability and rendered improved separation efficiency than the previous report. Moreover, a chip design that originally could not be packed[106] was packed with methods developed in this thesis and the bed was secured using the polymer plug procedure. Chapter 3 also presents a much more detailed analysis, than reference 106, of the quantitative performance of a 330 pL, 200 μm long SPE bed, allowing quantitative comparison to other microfluidic designs. We show for the first time that sub-picomolar detection limits can be achieved for fluorescent dyes, and we also confirm that peptides and amino acids may be preconcentrated using these devices.

Chapter 4 demonstrates integrated packed column reversed-phase CEC of various column sizes (1- 5 mm long). The device, based on a three-port design, has an integrated cross injector for sample injection. Incorporation of an injector, and the use of columns longer than 0.2 mm were the key focus of this effort. The chapter presents a major extension of the first published CEC work in a packed bed.[106] In this chapter, we also developed an indirect detection method using a neutral additive to the mobile phase for native amino acids.

Chapter 5 is the first report on integrated packed column size exclusion electrochromatography. Procedures for packing a 2 mm long column are described, and van Deemter plot was developed. A mixture of two proteins was used as the test sample, and was separated as anticipated based on size.

Finally chapter 6 presents a summary of the preceding chapters and possible future work.

1.7   References

(1)   Widmer, H. M. *Trends Anal.Chem.* **1983**, *2*, VIII-X.

(2)   Widmer, H. M.; Erard, J. F.; Grass, G. *Intern. J. Environ. Anal. Chem* **1984**, *18*, 1-10.

(3)   Staehelin, J.; Graber, N.; Widmer, H. M. *Intern. J. Environ. Anal. Chem.* **1991**, *43*, 197-208.

(4)   Graber, N.; Ludi, H.; Widmer, H. M. *Sens. Actuators B* **1990**, *1*, 239-243.

(5)   Manz, A.; Graber, N.; Widmer, H. M. *Sens. Actutators B* **1990**, *1*, 244-248.

(6)   Manz, A.; Miyahara, Y.; Miura, J.; Watanabe, Y.; Miyagi, H.; Sato, K. *Sens. Actutators B* **1990**, *1*, 249-255.

(7)   Terry, S. C. Ph.D. Thesis, Stanford University, 1975.

(8)   Terry, S. C.; Jerman, J. H.; Angell, J. B. *IEEE Trans. Electron Device* **1979**, *ED-26*, 1880-1886.

(9)   Knox, J. H.; Gilbert, M. T. *J.Chromatogr.* **1979**, *186*, 405-418.

(10)   Monning, C. A.; Jorgenson, J. W. *Anal. Chem.* **1991**, *63*, 802-807.

(11)   Muller, S.; Schiedegger, D.; Haber, C.; Simon, W. *J. High Resolution Chromatogr.* **1991**, *14*, 174-177.

(12)   Manz, A.; Fettinger, J. C.; Verpoorte, E.; Lüdi, H.; Widmer, H. M.; Harrison, D. J. *Trends Anal. Chem.* **1991**, *10*, 144-149.

(13)   Harrison, D. J.; Manz, A.; Fan, Z. H.; Lüdi, H.; Widmer, H. M. *Anal. Chem.* **1992**, *64*, 1926-1932.

(14)   Manz, A.; Harrison, D. J.; Verpoorte, E.; Fettinger, J. C.; Paulus, A.; Lüdi, H.; Widmer, H. M. *J. Chromatogr.* **1992**, *593*, 253-258.

(15)   Bruin, G. J. M. *Electrophoresis* **2000**, *21*, 3931-3951.

(16)   Effenhauser, C. S.; Bruin, G. J. M.; Paulus, A. *Electrophoresis* **1997**, *18*, 2203-2213.

(17)   Jakeway, S. C.; de Mello, A. J.; Russell, E. L. *Fresenius J. Anal. Chem.* **2000**, *366*, 525-539.

(18)   Kopp, M. U.; Crabtree, H. J.; Manz, A. *Curr. Opin. Chem. Biol.* **1997**, *1*, 410-419.

(19)   Lichtenberg, J.; de Mello, A. J.; Verpoorte, E. *Talanta* **2002**, *56*, 233-266.

(20)   Coyler, C. L.; Tang, T.; Chiem, N.; Harrison, D. J. *Electrophoresis* **1997**, *18*, 1733-1741.

(21)   Verpoorte, E. *Electrophoresis* **2002**, *23*, 677-712.

(22)   Auroux, P.-A.; Iossifidis, D.; Reyes, D. R.; Manz, A. *Anal.Chem.* **2002**, *74*, 2637-2652.

(23)   Reyes, D. R.; Iossifidis, D.; Auroux, P.-A.; Manz, A. *Anal.Chem.* **2002**, *74*, 2623-2636.

(24)   van der Berg, A.; Bergveld, P., Eds. *Proc. μ-TAS '94 Workshop*; Kluwer Academic Pub.,: The Netherlands, 1994.

(25)   Widmer, H. M.; Verpoorte, E.; Bernard, S., Eds. *Proc. μ-TAS '96 Anal. Methods Instrum.*; Kluwer Academic Pub.: Basel, Switzerland, 1996.

(26)   Harrison, D. J.; van der Berg, A., Eds. *Proc. μ-TAS '98 Workshop*; Kluwer Academic Pub.: Banff, Canada, 1998.

(27)   van der Berg, A.; Olthuis, W.; Bergveld, P., Eds. *Proc. μ-TAS 2000 Symposium*; Kluwer Academic Pub.: Enschede, The Netherlands, 2000.

(28) Ramsey, J. M.; van der Berg, A., Eds. *Proc. μ-TAS 2001 Symposium*; Kluwer Academic Pub.: Monterey, U.S.A., 2001.

(29) Madou, M. *Fundamentals of Microfabrication*; CRC Press, Boca Raton, 1997.

(30) Effenhauser, C. S.; Bruin, G. J. M.; Paulus, A.; Ehrat, M. *Anal. Chem.* **1997**, *69*, 3451-3457.

(31) McCornick, R. M.; Nelson, R. J.; Alonso-Amigo, M. G.; Benvegnu, D. J.; Hooper, H. H. *Anal. Chem.* **1997**, *69*, 2626-2630.

(32) Harrison, D. J.; Glavina, P. G.; Manz, A. *Sens. Actuators B* **1993**, *10*, 107-116.

(33) Fan, Z. H.; Harrison, D. J. *Anal. Chem.* **1994**, *66*, 177-184.

(34) Weill, A., Ed. *The Physics and Fabrication of Microstructures and Microdevcies*; Springer-Verlag: Berline, 1986.

(35) Hjerten, S. *Chromatogr. Rev.* **1967**, *9*, 122-219.

(36) Mikkers, F. E. P.; Everaerts, F. M.; Verheggen, T. E. M. *J. Chromatogr.* **1979**, *169*, 11-20.

(37) Jorgenson, J. W.; Luckas, K. D. *Anal.Chem.* **1981**, *53*, 1298-1302.

(38) Jorgenson, J. W.; Luckas, K. D. *J. Chromatogr.* **1981**, *218*, 209-216.

(39) Jorgenson, J. W.; Luckas, K. D. *Clin. Chem.* **1981**, *27*, 1551-1553.

(40) Jorgenson, J. W.; Luckas, K. D. *Science* **1983**, *222*, 266-272.

(41) Altria, K. D. *J. Chromatogr. A* **1999**, *856*, 443-463.

(42) Kasicka, V. *Electrophoresis* **2001**, *22*, 4139-4162.

(43) Frazier, R. A. *Electrophoresis* **2001**, *22*, 4197-4206.

(44) Thormann, W.; Lurie, I. S.; McCord, B.; Marti, U.; Cenni, B.; Malik, N. *Electrophoresis* **2001**, *22*, 4216-4143.

(45)   Weinberger, R. *Practical Capillary Electrophoresis*; Academic Press, INC.: London, 1993.

(46)   Landers, J. P., Ed. *Handbook of Capillary Electrophoresis*; CRC Press, Boca Raton, 1996.

(47)   Camilleri, P., Ed. *Capillary Electrophoresis, Theory and Practice*; CRC Press, Boca Raton, 1997.

(48)   Salomon, K.; Burgi, D. S.; Helmer, J. C. *J. Chromatogr.* **1991**, *559*, 69-80.

(49)   Dittmann, M. M.; Rozing, G. P. *J. Chromatogr. A* **1996**, *744*, 63-74.

(50)   Dittmann, M. M.; Rozing, G. P. *J. Microcolumn Sep.* **1997**, *9*, 399-408.

(51)   Knox, J. H.; Grant, I. H. *Chromatographia* **1991**, *32*, 317-328.

(52)   Yamamoto, H.; Baumann, J.; Erni, F. *J. Chromatogr.* **1992**, *593*, 313-319.

(53)   Bao, J. *J. Chromatogr. B* **1997**, *699*, 463-480.

(54)   Gosling, J. P. *Clin. Chem.* **1990**, *36*, 1408-1427.

(55)   Waldmann-Meyer, H. *J. Biol. Chem* **1960**, *235*, 3337-3345.

(56)   Bog-Hansen, I. C. *Anal. Biochem.* **1973**, *56*, 480-488.

(57)   Cann, J. R. *Anal. Biochem.* **1996**, *237*, 1-16.

(58)   Grossman, P. D.; Colburn, J. C.; Laurer, H. H.; Neilsen, R. G.; Riggin, R. M.; Sittamalam, G. S.; Rickard, E. C. *Anal. Chem.* **1989**, *61*, 1186-1194.

(59)   Nielsen, R. G.; Rickard, E. C.; Santa, P. F.; Sharknas, D. A.; Sittamalam, G. S. *J. Chromatogr.* **1991**, *539*, 177-185.

(60)   Schultz, N. M.; Kennedy, R. T. *Anal. Chem.* **1993**, *65*, 3161-3165.

(61)   Schultz, N. M.; Huang, L.; Kennedy, R. T. *Anal. Chem.* **1995**, *67*, 924-929.

(62)   Schmalzing, D.; Nashabeh, W.; Yao, X. W.; Mhatre, R.; Reginer, F. E.; Afeyan, N. B.; Fuchs, M. *Anal. Chem.* **1995**, *67*, 606-612.

(63)   Schmalzing, D.; Nashabeh, W.; Fuchs, M. *Clin. Chem.* **1995**, *41*, 1403-1406.

(64)   Shimura, K.; Karger, B. L. *Anal. Chem.* **1994**, *66*, 9-15.

(65)   Lausch, R.; Reif, O. W.; Riechel, P.; Scheper, T. *Electrophoresis* **1995**, *16*, 636-641.

(66)   Chen, F.-T. A.; Evangelista, R. A. *Clin. Chem.* **1994**, *40*, 1819-1822.

(67)   Chen, F.-T. A.; Pentoney, S. L. *J. Chromatogr. A* **1994**, *680*, 425-430.

(68)   Harrison, D. J.; Fluri, K.; Chiem, N.; Tang, T.; Fan, Z. H., *Transducers '95 - Eurosensors IX, The 8th International Conference on Solid-State Sensors and Actuators, and Eurosensors IX*, Stockholm, Sweden 1995; pp. 752-755.

(69)   Kounty, B. K.; Schmalzing, D.; Taylor, T. A.; Fuchs, M. *Anal. Chem.* **1996**, *66*, 18-22.

(70)   Chiem, N.; Harrison, D. J. *Clin. Chem.* **1998**, *44*, 591-598.

(71)   Chiem, N.; Harrison, D. J. *Anal. Chem.* **1997**, *69*, 373-378.

(72)   Lee, W. E.; Jemere, A. B.; Attiya, S.; Chiem, N.; Paulson, M.; Ahrend, J.; Burchett, G.; Bader, D. E.; Ning, Y.; Harrison, D. J. *Journal of Capillary Electrophoresis and Microchip Technology* **1999**, *1/2*, 51-59.

(73)   Cheng, S. B.; Skinner, C. D.; Taylor, J.; Attiya, S.; Lee, W. E.; Picelli, G.; Harrison, D. J. *Anal. Chem.* **2001**, *73*, 1472-1479.

(74)   Terabe, S.; Otsuka, K.; Ichikawa, K.; Tsuchiya, A. A.; Andot, T. *Anal. Chem.* **1984**, *56*, 111-113.

(75) Chan, K. C.; Muschik, G. M.; Issaq, H. J.; Snader, K. M. *J. High Resolution Chromatogr.* **1994**, *17*, 51-52.

(76) Moore, A. W.; Jacobson, S. C.; Ramsey, J. M. *Anal. Chem.* **1995**, *67*, 4184-4189.

(77) von Heeren, F.; Verpoorte, E.; Manz, A.; Thormann, W. *Anal. Chem.* **1996**, *68*, 2044-2053.

(78) Kutter, J. P.; Jacobson, S. C.; Ramsey, J. M. *Anal. Chem.* **1997**, *69*, 5165-5171.

(79) Wen, E.; Asiaie, R.; Horvath, C. *J. Chromatogr. A* **1999**, *855*, 349-366.

(80) Strain, H. H. *J. Am. Chem. Soc.* **1939**, *61*, 1292-1293.

(81) Pretorius, V.; Hopkins, B. J.; Schieke, J. D. *J. Chromatogr.* **1974**, *99*, 23-30.

(82) Tsuda, T. *Anal. Chem.* **1987**, *59*, 521-523.

(83) Knox, J. H.; Grant, I. H. *Chromatographia* **1987**, *24*, 135-143.

(84) Bartle, K. D.; Myers, P. *J. Chromatogr. A* **2001**, *916*, 3-23.

(85) Pyell, U. *J. Chromatogr. A* **2000**, *892*, 257-278.

(86) Colon, L. A.; Maloney, T. D.; Fermier, A. M. *J. Chromatogr. A* **2000**, *887*, 43-53.

(87) Tang, Q.; Lee, M. L. *Trends Anal.Chem.* **2000**, *19*, 648-663.

(88) Fujimoto, C. *Trends Anal.Chem.* **1999**, *18*, 291-301.

(89) Schweitz, L.; Andersoon, L. I.; Nilsson, S. *J. Chromatogr. A* **1998**, *817*, 5-13.

(90) Cikalo, M. G.; Bartle, K. D.; Robson, R. R.; Myers, P.; Euerby, M. R. *Analyst* **1998**, *123*, 87R-102R.

(91) Robson, R. R.; Cikalo, M. G.; Myers, P.; Euerby, M. R.; Bartle, K. D. *J. Microcolumn Sep.* **1997**, *9*, 357-372.

(92) Rathore, A. S.; Horvath, C. *J. Chromatogr. A* **1997**, *781*, 185-195.

(93) Altria, K. D.; Smith, N. W.; Turnbull, C. H. *Chromatographia* **1997**, *46*, 664-674.

41

(94)   Crego, A. L.; Gonzales, A.; Marina, M. L. *Crit. Rev. Anal. Chem.* **1996**, *26*, 261-304.

(95)   Jacobson, S. C.; Hergenroder, R.; Kounty, B. K.; Ramsey, J. M. *Anal. Chem.* **1994**, *66*, 2369-2373.

(96)   Kutter, J. P.; Jacobson, S. C.; Matsubara, N. *Anal. Chem.* **1998**, *70*, 3291-3297.

(97)   Zhang, X.; Reginer, F. *J. Chromatogr. A* **2000**, *869*, 319-328.

(98)   Knox, J. H. *J. Chromatogr. Sci.* **1980**, *18*, 453-461.

(99)   He, B.; Ji, J.; Reginer, F. *J. Chromatogr. A* **1999**, *853*, 257-262.

(100)   Slentz, B. E.; Penner, N. A.; Reginer, F. E. *J. Chromatogr. A* **2002**, *948*, 225-233.

(101)   Yu, C.; Svec, F.; Frechet, J. M. J. *Electrophoresis* **2000**, *21*, 120-127.

(102)   Ericson, C.; Holm, J.; Ericson, T.; Hjerten, S. *Anal. Chem.* **2000**, *72*, 81-87.

(103)   Fintschenko, Y.; Choi, W.-Y.; Ngola, S. M.; Shepodd, T. J. *Fresenius J. Anal. Chem.* **2001**, *371*, 174-181.

(104)   Throckmorton, D. J.; Shepodd, T. J.; Singh, A. K. *Anal. Chem.* **2002**, *74*, 784-789.

(105)   Svec, F.; Peters, E. C.; Sykora, D.; Frechet, J. M. J. *J. Chromatogr. A* **2000**, *887*, 3-29.

(106)   Oleschuk, R. D.; Shultz-Lockyear, L. L.; Ning, Y.; Harrison, D. J. *Anal. Chem.* **2000**, *72*, 585-590.

(107)   Oleschuk, R. D.; Jemere, A. B.; Schultz-Lockyear, L. L.; Fajuyigbe, F.; Harrison, D. J., in *The Proc. μ-TAS 2000 Symposium;* van der Berg, A., Olthuis, W., Bergveld, P. (Eds.); Enschede, The Netherlands 2000; Kluwer Academic Publishers; 11-14.

42

(108) Ceriotti, L.; de Roij, N. F.; Verpoorte, E. *Anal. Chem.* **2002**, *74*, 639-647.

(109) Ocvirk, G.; Verpoorte, E.; Manz, A.; Grasserbauer, M.; Widmer, H. M. *Anal. Methods Instrum.* **1995**, *2*, 74-82.

(110) Lindqvist, B.; Storgards, T. *Nature (London)* **1955**, *175*, 511-512.

(111) Lathe, G. H.; Ruthven, C. R. J. *Biochem. J.* **1955**, *60*, XXXIV.

(112) Wu, C.-S., Ed. *Handbook of Size Exclusion Chromatography, Chromatographic Science Series*; Marcel Dekker, Inc.: New York, 1995.

(113) Barth, H. G.; Boyes, B. E.; Jackson, C. *Anal. Chem.* **1996**, *68*, 445R-466R.

(114) Barth, H. G.; Boyes, B. E.; Jackson, C. *Anal. Chem.* **1998**, *70*, 251R-278R.

(115) Stol, R.; Kok, W. T.; Poppe, H. *J. Chromatogr. A* **1999**, *853*, 45-54.

(116) Venema, E.; Kraak, J. C.; Tijssen, R.; Poppe, H. *Chromatographia* **1998**, *48*, 347-354.

(117) Peters, E. C.; Petro, M.; Svec, F.; Frechet, J. M. J. *Anal. Chem.* **1998**, *70*, 2296-2302.

(118) Venema, E.; Kraak, J. C.; Poppe, H.; Tijssen, R. *J. Chromatogr. A* **1999**, *837*, 3-15.

(119) Stol, R.; Poppe, H.; Kok, W. T. *J. Chromatogr. A* **2000**, *887*, 199-208.

(120) Stol, R.; Kok, W. T.; Poppe, H. *J. Chromatogr. A* **2001**, *914*, 201-209.

(121) Ding, F.; Stol, R.; Kok, W. T.; Poppe, H. *J. Chromatogr. A* **2001**, *924*, 239-249.

(122) Stol, R.; Pedersoli Jr., J. L.; Poppe, H.; Kok, W. T. *Anal. Chem.* **2002**, *74*, 2314-2320.

(123) Chodhary, G.; Horvath, C. *J. Chromatogr. A* **1997**, *781*, 161-183.

(124) Rathore, A. S.; Horvath, C. *Anal. Chem.* **1998**, *70*, 3069-3077.

43

(125) Cikalo, M. G.; Bartle, K. D.; Myers, P. *J. Chromatogr. A* **1999**, *836*, 25-34.

(126) Giddings, J. C. *Sep. Sci.* **1969**, *4*, 47-61.

(127) Seiler, K.; Harrison, D. J.; Manz, A. *Anal. Chem.* **1993**, *65*, 1481-1488.

(128) Heiger, D. *High Perfomance Capillary Electrophoresis: An Introduction*; Agilent Technologies: Germany, 2000.

(129) Dittmann, M. M.; Rozing, G. P. *LC-GC* **1995**, *13*, 800 - 808.

(130) Ocvirk, G.; Tang, T.; Harrison, D. J. *Analyst* **1998**, *123*, 1429-1434.

(131) Martin, A.; Everaerts, F. *Proc. Roy. Soc. London* **1970**, *A 316*, 493-514.

(132) Zhang, B.; Liu, H.; Karger, B. L.; Foret, F. *Anal. Chem.* **1999**, *71*, 3258-3264.

(133) Kaniansky, D.; Masar, M.; Bielcikova, J.; Ivanyi, F.; Eisenbeiss, F.; Stanislawski, B.; Grass, B.; Neyer, A.; Johnck, M. *Anal. Chem.* **2000**, *72*, 3596-3604.

(134) Prest, J. E.; Baldock, S. J.; Fielden, P. R.; Brown, B. J. T. *Analyst* **2001**, *126*, 433-437.

(135) Chien, R. L.; Helmer, J. C. *Anal. Chem.* **1991**, *63*, 1354-1361.

(136) Chien, R. L. *Anal. Chem.* **1991**, *63*, 2866-2869.

(137) Chien, R. L.; Burgi, D. S. *J. Chromatogr.* **1991**, *559*, 153-161.

(138) Chien, R. L.; Burgi, D. S. *J. Chromatogr.* **1991**, *559*, 141-152.

(139) Burgi, D. S.; Chien, R. L. *J. Microcolumn Sep.* **1991**, *3*, 199-202.

(140) Lichtenberg, J.; Verpoorte, E.; de Roij, N. F. *Electrophoresis* **2001**, *22*, 258-271.

(141) Li, J.; Wang, C.; Kelly, J. F.; Harrison, D. J.; Thibault, P. *Electrophoresis* **2000**, *21*, 198-210.

(142) Guzman, N. A.; Trebilcock, M. A.; Advis, J. P. *J. Liq. Chromatogr.* **1991**, *14*, 997-1015.

44

(143) Figeys, D.; Abersold, R. *Anal. Chem.* **1998**, *70*, 3721-3727.

(144) Kutter, J. P.; Jacobson, S. C.; Ramsey, J. M. *J. Microcolumn Sep.* **2000**, *12*, 93-97.

(145) Dodge, A.; Fluri, K.; Verpoorte, E.; de Roij, N. F. *Anal. Chem.* **2001**, *73*, 3400-3409.

(146) Jemere, A. B.; Oleschuk, R. D.; Taylor, J.; Harrison, D. J., in *The Proc. μ-TAS 2001 Symposium*; Ramsey, J.M., van der Berg, A. (Eds.); Monterey, U.S.A. 2001; Kluwer Academic Pub.; 510-502.

(147) Sato, K.; Tokeshi, M.; Odake, T.; Kimura, H.; Ooi, T.; Nakao, M.; Kitamori, T. *Anal. Chem.* **2000**, *72*, 1144-1147.

(148) Sato, K.; Tokeshi, M.; Kimura, H.; Kitamori, T. *Anal. Chem.* **2001**, *73*, 1213-1218.

(149) Wolfe, K. A.; Breadmore, M. C.; Ferrance, J. P.; Power, M. E.; Conroy, J. F.; Norris, P. M.; Landers, J. P. *Electrophoresis* **2002**, *23*, 727-733.

(150) Yu, C.; Davey, M. H.; Svec, F.; Frechet, J. M. J. *Anal. Chem.* **2001**, *72*, 5088-5096.

(151) Josefson, C. M.; Johnston, J. B. *Anal. Chem.* **1984**, *56*, 764-768.

(152) Lovkvist, P.; Jonsson, J. *Anal. Chem.* **1987**, *59*, 818-821.

(153) Wenzel, U. *J. Chromatogr. A* **2001**, *928*, 1-12.

(154) Fritz, J. S.; Macka, M. *J. Chromatogr. A* **2000**, *902*, 137-166.

(155) Werkhoven-Goewie, C. E.; Brinkman, U. A. T.; Frei, R. W. *Anal. Chem.* **1981**, *53*, 2072-2080.

(156) Hennion, M.-C.; Coquart, V. *J. Chromatogr.* **1993**, *642*, 211-224.

45

Chapter 2: Automated Microchip Platform for Immunoassay Analysis[*]

2.1 Introduction

Microchip-based fluidic devices can be fabricated on a variety of substrates such as glasses,[1-5] plastics,[6] silicon,[7] and polymers[8] and have been demonstrated for bioanalyses such as immunoassays,[9-13] DNA assays,[14-17] serum protein screening,[18] and cell responses.[19, 20] Recent work has shown that a wide range of chemical processing can be built into microchip platforms.[21, 22] Technological advancements are being directed toward developing complex and automated processing on a single chip. However, to utilize microfluidic technology for analytical instruments, there are requirements for system integration on two levels. One level is the integration of chemical function on the chip. Since an analytical process is a set of defined steps that must be carried out in a fixed order, each step must lead into the next with respect to position on the chip and sequence of events. The other level is combination of peripheral system components for control and operation of the chip. This requires having the peripherals (such as high-voltage supplies, optical detection unit, external pump) under computer control, ready to respond to a predetermined set of software-based commands. In this way the analysis can be initiated by the operator. The peripheral components will respond by making the

---

[*] A version of this chapter has been published as Lee, W. E.; Jemere, A. B.; Attiya, S.; Chiem, N. H.; Paulson, M.; Ahrend, J.; Burchett, G.; Bader, D. E.; Ning, Y.; Harrison, D. J. *Journal of Capillary Electrophoresis and Microchip Technology*, **1999**, 1/2, 51 - 59

46

chip perform the analysis, collecting the data from the analysis, and resetting the system for the next run.

This chapter describes the development of an automated microchip-based platform for immunoassay analysis, which is ultimately intended for use in the field to detect biological threat agents. For a demonstration, we have developed an immunoassay for the protein ovalbumin, which is used in field trial testing and evaluation of aerosol collectors and environmental monitoring systems. Capillary electrophoresis (CE) has emerged as a useful tool for immunoassays[23-26] and is well suited for microchip applications. Prof. Harrison's laboratory has developed microfluidic devices capable of performing immunoassays that can be applied to the determination of threat agents. In these devices samples and immuno-reagents are mixed homogeneously within 30–60 μm wide flow channels and then separated electrophoretically in order to determine sample concentration.[10, 11] Reagent consumption on the order of 0.1-10 nL per assay has been achieved, which is of critical importance for reduced maintenance of a field-based instrument. In this assay, a fluorescently labeled monoclonal antibody was reacted with ovalbumin and the product was separated by CE and detected by laser-induced fluorescence detection (LIF). The channel networks in the device were fabricated on micromachined glass plates. Electroosmotic pumping was used for quantitative injection of reagents and for liquid transport on the chip at velocities up to 1 cm/s. Thus, by voltage control alone, chemical processing can be carried out within a single manifold of channels on-chip through electroosmosis and electrophoresis.

The prototype automated microfluidic system, which has been developed by several researchers in a collaborative DARPA-funded project, enables the on-chip operation of

47

the key elements in analysis: injection, mixing, separation, detection, quantitation, and elimination plus direct-time data display. Researchers who collaborated on the prototype automated single channel microfluidic immunoassay project included William E. Lee, Abebaw B. Jemere, Said Attiya, Nghia H. Chiem, Guifeng Jiang, Murray Paulson, Jack Ahrend, Gary Burchett, Douglas E. Bader, Yuebin Ning and D. Jed Harrison. The instrument was designed to connect to a large-volume aerosol sample collector for environmental monitoring, although any low-pressure fluid delivery apparatus would be suitable for use with the microchip system. Compact peripheral subsystems were developed, so that all of the components could be engineered into a single box 30 x 35 x 50 cm. The unit consists of a programmable high-voltage subsystem for electroosmotic pumping and CE, coupled to a rapid wafer exchange, fluidic, and electrical interface to the chip. The fluid interface was designed to allow the use of a miniperistaltic pump to deliver analyte solutions from an external reservoir to the chip. Detection was accomplished with a built-in, compact, confocal epiluminescence LIF microscope utilizing a 635 nm diode laser. The operational control of the system was carried out by an on-board microprocessor under the command of Windows™ (Redmond, WA, U.S.A)-based software in a notebook computer. The microchip and instrumentation for this system was developed by the team above. The system was fully tested and characterized by this author, Abebaw B. Jemere. All data presented here was obtained and analyzed by this author, and the operational protocols were developed by this author.

48

2.2 Experimental Section

2.2.1 Materials

A 10^{-7} M stock solution of non-reactive Cy5 dye (Beckman Instruments, Fullerton, CA) was prepared by dissolving 200 pmole of dye in 2 ml de-ionized water. All solutions used with Cy5 were prepared by dilution of the stock solution in pH 9.0 tris/borate buffer. The tris/borate buffer, containing 20 mM tris and 100 mM boric acid (Sigma-Aldrich, St. Louis, Mo), was adjusted to pH 9.0 with 1 M NaOH. Chicken egg ovalbumin and monoclonal antiovalbumin (ascites fluid) were from Sigma-Aldrich. The antibody was labeled with bisfunctional NHS ester of Cy5 dye (Amersham Life Sciences, Pittsburgh, PA) using an affinity protected labeling procedure described elsewhere.[27] Other reagents were analytical grade, purchased from Sigma-Aldrich. Aqueous solutions were made from Milli-Q UV Plus Ultra-pure water (Millipore, Mississauga, ON), and all solutions were filtered using 0.22 μm pore nylon syringe filters (Nalgene, Rochester, NY) prior to use.

2.2.2 Device Fabrication

Devices were fabricated in 4 x 4", 600 μm thick Corning 0211 glass (Corning Glass Works, Parkridge, IL, USA) using two single mask microlithographic patterns and a previously described HF/HNO$_3$ etchant[3, 10] at Micralyne (formerly called the Alberta Microelectronics Corporation, Edmonton, AB). Devices consisted of two glass plates bonded together, one with an etched channel network and the other with holes drilled in it (cover plate). The cover plate also contained an etched sample introduction channel (SIC). One mask pattern was used to produce a channel network etched to a depth of 13

49

μm and a trapezoidal cross-section with a top width of 65 μm, and a bottom width of 26 μm, as depicted by the thin lines in Figure 2.1. The heavy lines in Figure 2.1 depict 13 μm deep and 275 μm wide channels produced using the same pattern. Designing various cross-sections for the device provides a built-in control of the voltage drop in each channel segment. For example, the major potential drop can be applied in the active separation channel from point A to point D rather than in segments that connect the reservoirs. The other pattern resulted in a sample introduction channel on the cover plate etched 300 μm deep, 1 mm wide, and 1.8 cm long. To make a complete device, both plates were cleaned, access holes aligned with channels, and bonded, as described previously.[11] The region at the top of the separation channel formed a double T-injector,[2, 28] as shown in the expanded diagram. The center-to-center distance between the two arms of the injector was 491 μm, corresponding to an injection volume of about 290 pL.

2.2.3 Instrumentation

Figure 2.2 shows a photograph of the prototype automated immunoassay instrument tested and characterized in this work. The instrument is comprised of three peripheral subsystems: a high-voltage power supply, a fluidic interface, and an epiluminescence confocal microscope.

50

2.2.3.1 High-Voltage Power Supply

A pair of power supplies (UltraVolt, Inc., Ronkonkoma, NY) was equipped with ripple strippers, mu-metal shielding and aluminum cases to minimize the supply noise. The power supplies had a range of 0-3 kV and 0-10 kV. Reed relay switches (Kilovac, Santa Barbara, CA) were used to deliver voltages to gold-plated electrodes for controlling the fluidic processing on the microchip. The high-voltage supply was always turned off prior to switching the relay to eliminate hot switching. A bleeder resister was used to terminate the high-voltage power supplies. The voltage decayed to under 100 V within 300 msec. This procedure prevented arcing at the relay contacts and protected the electronic components in the system. It also improved the formation of sample plugs at the separation channel. The rapid decay of voltage promptly stopped the electroosmotic flow and provided better fluidic control on the chip.

51
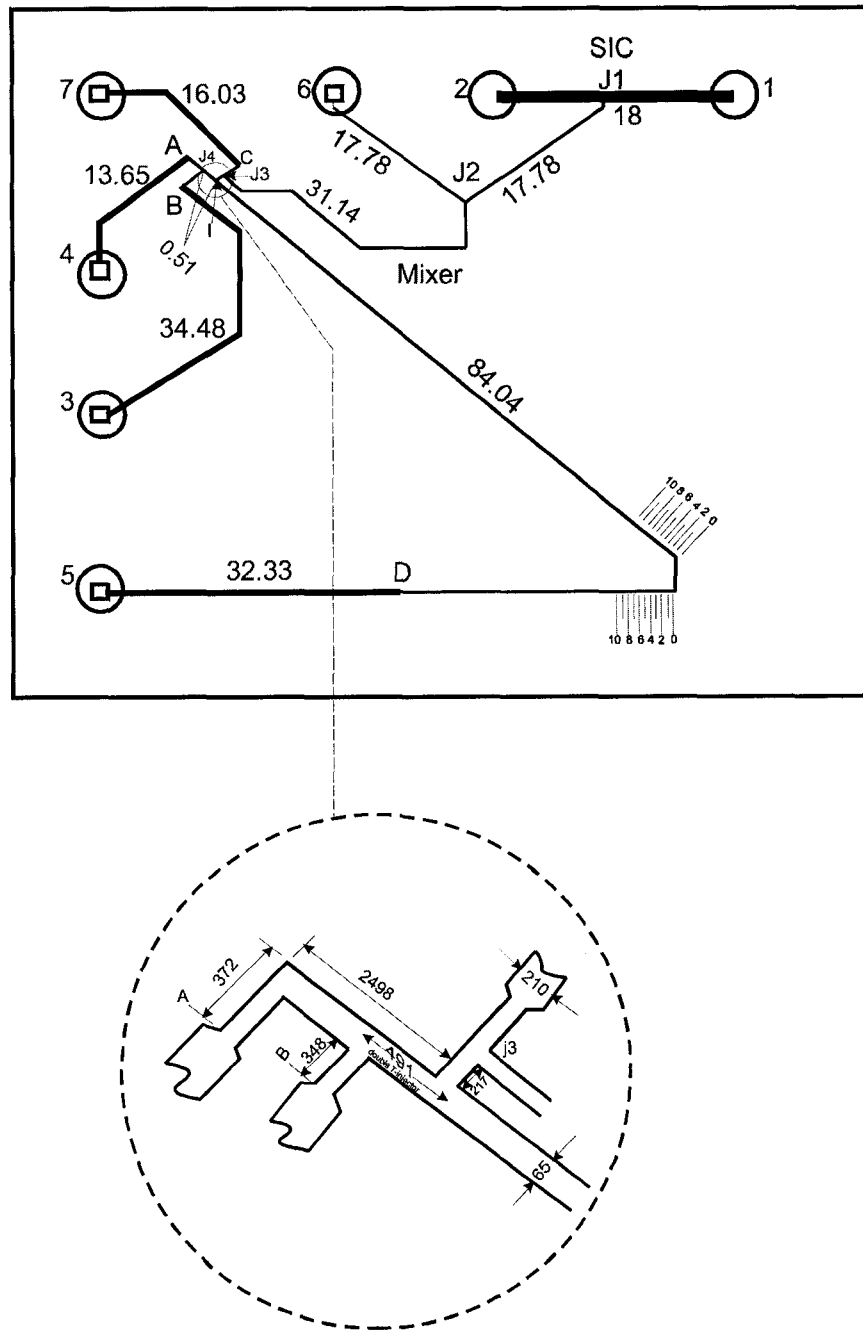
Figure 2.1 Schematic layout of microchip design. All dimensions are in millimeters in the main figure and in micrometers in the expansion, and reservoirs are numbered for reference. Different line thickness indicates relative channel widths. The double T-injector is shown in the inset and is 65 μm wide and 491 μm long. The drawing is not to scale.

52

2.2.3.2 Electrical and Fluid Interface Plates

A fixed, reusable interface plate for electrical and fluidic connections was fabricated from sheet acrylic (Cadillac Plastics, Edmonton, AB). The electrical leads from the high-voltage power supply were connected to gold plated spring pin electrodes (Interconnect Devices Inc., Kansas City, KS) through the sides of the interface plate and were held in place by threaded screw press-fittings. Electrical contact with the fluid reservoirs was made through the gold plated electrodes.

A disposable fluid interface was molded onto the chip. Threaded flange-free liquid chromatography mini-couplers (for 1/16" o.d. tubing, Valco Instruments, Houston, TX) were used as fluid reservoirs as suggested in Figure 2.3. The reservoir vials were bonded to the chip over the access holes using double-sided tape and then reinforced at the base with 5-min epoxy glue. After bonding, a mold was placed over top of the wafer and epoxy-encapsulating resin (Sealtronics #221AC-7V, Industrial Formulators of Canada, Burnaby, BC) was poured to a depth of 5 mm and allowed to cure for 24 h. A small amount of lampblack (0.25% w/w, Industrial Formulators) was added to make the resin opaque. The minicouplers were used for both fluid reservoirs and pressure fittings to the SIC. This design provided a leak-free interconnection to the chip. The chip assembly was mounted on an XYZ translation stage (Newport Instruments, Irvine, CA) so that it could be positioned and aligned with respect to the optical system. Sample was delivered to the chip by means of a miniperistaltic pump (Instech Laboratories model P-625/900, Plymouth Meeting, PA). The fluid lines for delivering the sample were 0.020" i.d. silicone tubing (Instech) connected to the interface chip by the flange-less minicouplers (Valco), as shown in Figure 2.3. The fixed interface plate was held on a levered cam and

53

was lowered into place on the disposable interface plate by the operator. When lowered, the gold electrodes rested in the fluid reservoirs to make the electrical connections. The high-voltage connection for the SIC was made off-chip in the sample tube. The sample fluid in the silicone tubing completed the circuit.

2.2.3.3 Fluorescence Detection Unit

The unit has a compact, epiluminescence confocal microscope (see Figure 2.4). A solid-state laser (Power Technologies, Mabelvale, AR) having a circular Gaussian beam profile and a nominal power output of 8 mW at 635 nm was used as the excitation source. The actual wavelength of the diode laser was determined to be 642 nm. The diode laser generated a significant amount of out-of-band radiation, a phenomenon similar to discharge glow in gas lasers, which was eliminated with a 640 (10)-nm band-pass filter (Melles Griot, Ottawa, ON). The laser beam was focused on the capillary channel perpendicular to the plane of the microchip with a 40x aspheric lens, 0.55 N.A., infinite focal length (New Focus Optics, Santa Clara, CA), that had a working distance of 2.7 mm. The emission was collected with the same aspheric lens, projected through an achromatic negative focal length lens (–25 mm f.l., Edmund Scientific, Barrington, NJ) onto a heat-reflecting filter (Roland Optics, Corvena, CA) that was used as a low cost beam splitter. The split-beam then passed through a filter-set consisting of a 665 nm short wave cut-off filter (Roland Optics), a three-cavity 675 (10)-nm band-pass filter (Melles Griot), and a 400-μm pinhole (Melles Griot) to the photomultiplier tube (PMT) (HC 577301, Hamamatsu Corp., Bridgewater, NJ). The PMT had a multi-alkali photocathode, which enhanced the sensitivity in the red and near-IR portion of the

54

spectrum. The narrow spread of the light, less than 40 nm, allowed the use of a chromatic optical design, that is, a single lens in the microscope objective. Thus, with the single-lens objective and the negative focal length element, a compact (4 x 8 x 13-cm) low cost optical unit was achieved.
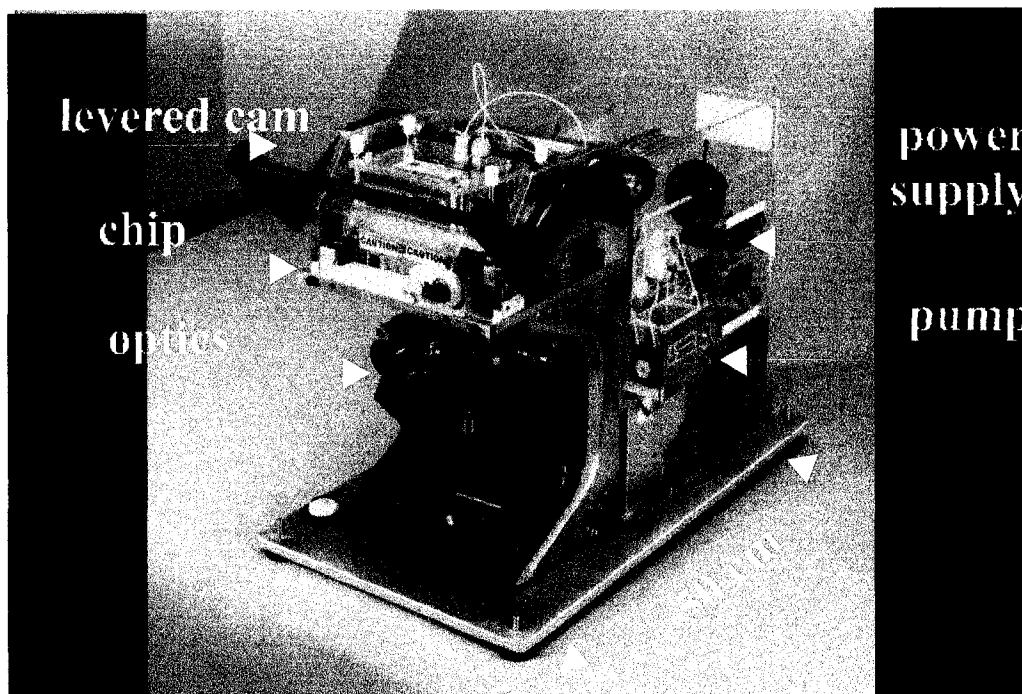
Figure 2.2. Photograph of the prototype automated immunoassay instrument.

55
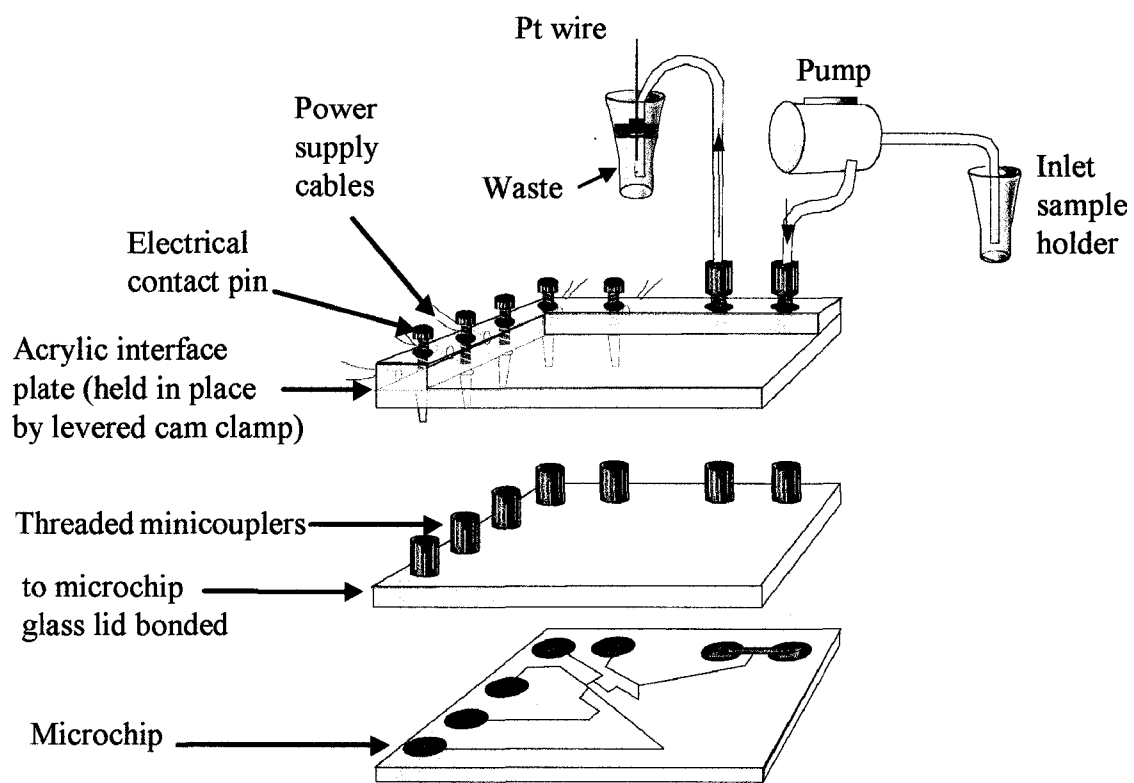
Figure 2.3. Interconnection assembly for automated immunoassay plate.

56

Microchip ⟶

40x microscope objective,
0.55 N.A.

675 nm-10 nm
band pass filter

Pinhole

-25 mm f.l. achromatic lens

Dichroic mirror

PMT

640 nm-10 nm
band pass filter

RG 665, sharp
cutoff filter

8 mW 635
nm diode
laser
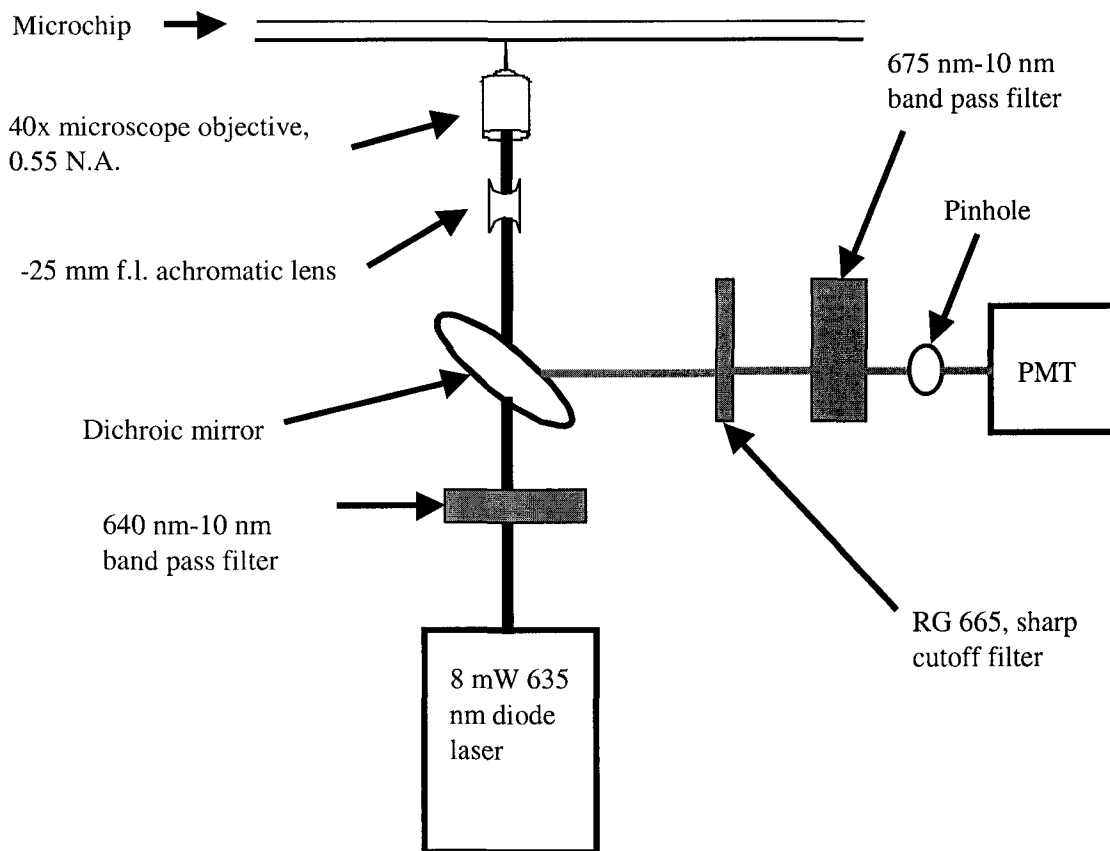
Figure 2.4 Layout of epiluminescent, confocal microscope for diode laser-induced fluorescence detection of the red absorbing dye, Cy5.

2.2.4 Chip Conditioning and Ovalbumin Immunoassay

As in conventional fused-silica capillaries, the micro-channels of the devices must be conditioned with NaOH solution and the separation buffer prior to use. New chips were first filled with de-ionized water, which moved by capillary action and wetted the channels. 0.1 M NaOH replaced all but one reservoir and house vacuum was applied to empty reservoirs for 1 hr. Because the channels were interconnected, the flow of NaOH solution was in the direction of the negative pressure. After flushing the channels with NaOH, reservoirs were rinsed with the separation buffer and the chip was conditioned in

57

the same way as with NaOH solution. Washing the devices with 0.1 M NaOH for 1 hr, followed by 20 min in 0.1 M HCl before their first use, produced devices with similar electroosmotic pumping rates. At the end of each day, the reservoirs were emptied and channels were flushed with de-ionized water for 15 min using house vacuum, and were then stored filled with de-ionized water. The water was removed by vacuum prior to introducing buffer and sample solutions. Care taken to avoid trapping air in the reservoirs during filling eliminated any problems with bubbles in the channels later. When required, the channels could be cleaned and conditioned by flushing under house vacuum with 0.1 M NaOH for 5 min and buffer for 5-30 min.

The buffer used for the immunoassay was composed of 50 mM tricine pH 8.0, 26 mM NaCl, and 0.01% Tween 20 (w/v). The antibody solution consisted of Cy5-labeled anti-ovalbumin diluted to 38 µg/mL in buffer. Ovalbumin was dissolved in buffer solution at 10-100 µg/mL. Approximately 300-500 µL of the sample solution was added to the off-chip sample tube and pumped through the SIC at 66 µL/min. Sample solution was pumped for an initial 2-3 min to flush the sample from the previous run.

2.3   Results and Discussions

2.3.1   Evaluation of the sample introduction channel

For continuous monitoring, such as in process control, the world-chip interface represents a challenge.[29, 30] Fluid flow resistance may be used to control the magnitude of pressure driven flow within each channel in a network of intersecting channels. This concept has been used to develop a sample introduction channel in which flow from an outside environment may be interfaced to a chip without perturbing the composition of the

58

channels within the microfluidic device.[12, 28] In order to deliver analyte fluids to the chip, a low flow-resistance interface was constructed on-chip. The large sample introduction channel was fabricated 0.3 mm deep, 1 mm wide and 1.8 cm long as shown in Figure 2.1. The other channels on the chip were 13 μm deep and 65 μm wide. Thus, the large difference in channel dimensions provides a large difference in resistance to solution flow. In this way, sample can be pumped through the low-resistance sample channel without the risk of contamination of the narrower chemical processor portion of the channel network. Successive samples were introduced to the SIC using a miniature peristaltic pump to draw sample from the sample tube through external tubing. The tubing length to the sample tube was not optimized, so that a total of 3 min was used to flush the sample line and SIC at a flow rate of 66 μL/min. No carryover of dye or proteins was observed with this loading protocol.

The microfluidic device was designed to perform automated chemical analysis, in which an antibody would be mixed with an antigen on-chip, the mixture would be incubated, and affinity probe capillary electrophoresis[31] would be performed to determine the antigen concentration. For such an application, it is important that no sample shall leak from the SIC during injection and separation while the pump is continuously supplying the analyte. A solution of hydrolyzed reactive Cy5 dye was continuously pumped through the SIC, while potentials were applied to the device to first withdraw sample from the SIC and mix at point J2 (Figure 2.1) with Cy5 labeled anti-ovalbumin from reservoir Ab. Injection at the double-T, followed by separation, was also performed with the pump on. The electropherograms shown in Figure 2.5 illustrates the reproducibility of individual sample introduction and separation steps. The peak heights

59

for the labeled antibody (Ab*) showed a 3 % RSD, while the primary Cy5 peak exhibited a 1.5 % RSD. Both peaks showed migration times variation of less than 0.5 % RSD. These results confirm that the SIC design allows complex steps such as mixing, injection plug formation, and separation to be performed simultaneously with continuous sample transit through the SIC, without perturbing the analysis.

The interface plate provided a quick and rapid means of exchanging devices within the unit. Chips were easily removed from the instrument when they needed thorough cleaning, refreshing reagents and/or buffer, or when they stop properly functioning. Opening the lever arm, seen near the top in Figure 2.2, allowed rapid insertion of a chip within the unit. Electrical contact to the fluids prefilled in the plastic reservoirs on the chip was easily made simply by lowering the arm again. Fluid contact from the peristaltic sample pump line to the SIC was made simultaneously. This fluid interface design was very effective. Initial difficulties with high voltage leakage currents in the top interface plate were due to corona discharge and were remedied by sheathing the upper portion of the electrodes with narrow gauge Teflon tubing.

2.3.2 Fluorescence Detection

Fluorescence detection provides the high degree of sensitivity required for microchip CE, where the sample volumes and hence the total number of detectable molecules are low. The epiluminescence microscope assembly used for LIF detection was mounted below the chip. The diode laser beam was aligned perpendicular to the chip using the translation adjustments on an optical stage. The eyepiece of the assembly could be rotated into place so that alignment could be made visually. Optimal alignment involved

60

focussing the laser beam at the axis of the channel and fine adjusting the translations to

minimize the background.
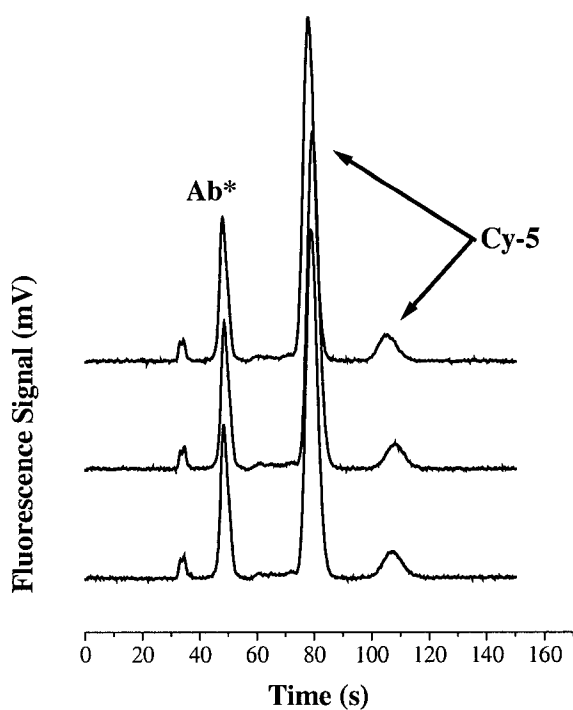
Figure 2.5. Electropherograms obtained for Cy5-labeled antibody (Ab*) and
hydrolyzed, reactive Cy5, mixed within the device at junction J2.
The Cy5 dye was introduced through the SIC and Ab* was
present in reservoir Ab, with the pump on continuously during
sample introduction, mixing, sample formation, and separation.
Sample was prepared in the running buffer consisting of 20 mM
Tris/100 mM borate, pH 9.0; separation voltage was 5 kV.
Traces are offset for clarity.

61

The performance of the optical unit installed in the platform was measured using nonreactive Cy5 dye. Serially diluted samples of the dye were introduced via the SIC and 290 pL sample plugs were injected electrokinetically. Figure 2.6 shows the calibration curve for peak area and peak height of nonreactive Cy5 over a range of 0.30 to 3 nM. A concentration limit of detection (S/N = 3) of 69 pM Cy5 was obtained; compared to the 100 pM limit we obtained for Cy-5 on a commercial Beckman P/ACE 5000 CE instrument with a 635 nm LIF unit.

The data in Figure 2.6 also demonstrated the ability of the SIC to provide sample delivery to the chip without carryover. The correlation between fluorescence signal and concentration of dye indicated the accuracy and reproducibility of the sample exchange.
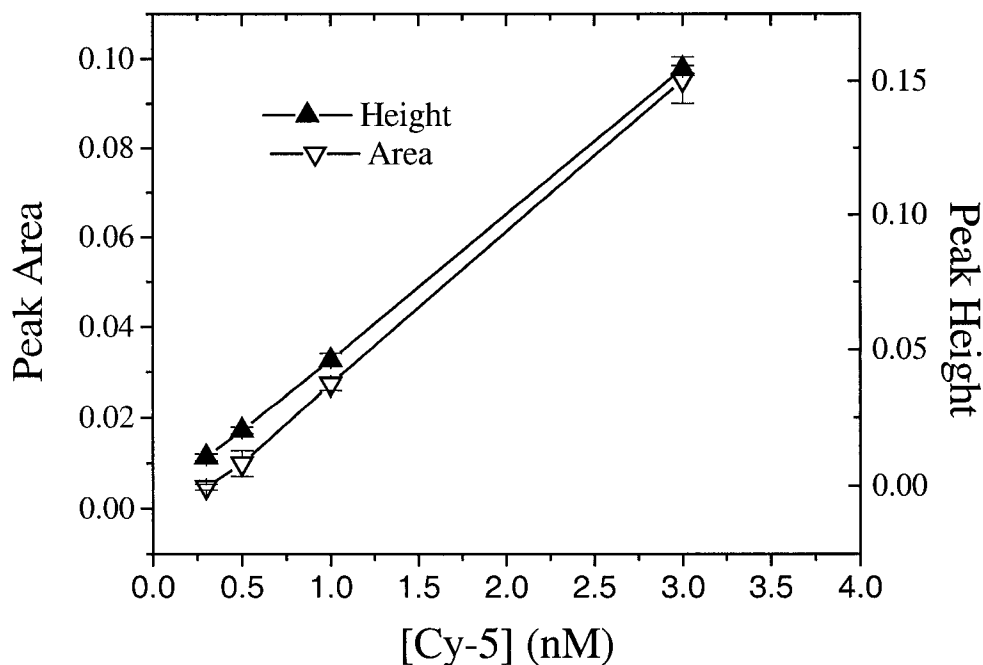
Figure 2.6. Calibration curve of serially diluted samples of the nonreactive
Cy5 dye, introduced via the SIC and injected electrokinetically
into the microchip device. The data points and bars represent
the mean and standard deviation for three consecutive
measurements (R^2 peak area = 0.99958; R^2 peak height =
0.99996).

2.3.3 Fluid Processing and Operation of Microchip

The pump in the prototype instrument can be used in both continuous (as shown above)

and stop-flow modes. In the stop-flow mode, once the SIC was filled, on-chip mixing

and reaction was followed by a capillary electrophoresis separation in a sequence of

timed events. Two programmable power supplies and a multistep program were used to

control the on-chip processes. Table 2.1 illustrates the timing sequences used, indicating

the magnitude and location of the potential applied, and the length of time it was applied

63

for. The first step was pumping of the sample through the SIC, followed by electrokinetic mixing of sample and antibody within the reactor channel. When the glass devices were well behaved, there was very little leakage during sample loading or separation. In that case, a simple two stage potential program was used, with potentials applied to the primary flow channels alone, as indicated by Program A, Table 2.1. With an older device, or after several hours of use and before reconditioning the channels, a more complex program was used to minimize leakage at the intersections. Program B in Table 2.1 illustrates the initial delivery of sample to reservoir B2 during mixing and filling of the 19 nL reaction channel. This was followed by loading of the injector, with plug shaping[2, 32] performed by application of voltages to all channels intersecting at the double-T injector. The fluid flow for loading the injector and plug shaping is shown in Figure 2.7a. Using the plug shaping procedure, reproducible injection volumes were obtained after about 15 s of injection at 1.2 kV, as shown in Figure 2.8 for a 40 nM Cy5 sample. A pre-separation step was performed to first move sample plug just past the double-T injector. Then potentials were applied to the side channels that contained sample to induce a side flow of buffer into the channels to push sample back and prevent leakage during the separation. The fluid flow for separation and detection is shown in Figure 2.7b.

In order for a set program to run a microfluidic chip repeatedly without human intervention, the migration time must be quite stable. In addition to the immediate reproducibility for replicate injections of ± 0.21 %, the long term change in migration time over 14 days on a single device varied by less than 3 % for a Cy5 sample. The variation in migration time between devices was about ± 2 %, when a rigorous cleaning

64

procedure involving both NaOH and HCl was applied. This reproducibility was judged to be adequate for allowing selection of stable operating parameters for routine operation of the devices.

Table 2.1 Voltage and relays switching matrix for fluidic control of microchip.

Program A

Step	Function	B1	B2	W1	W2	Ab	SO	SI	Time (s)
1	Sample input to SIC	-	-	-	-	-	-	P	180
2	Sample introduction, mixing, loading	-	-	V_L -1.2	-	G	G		15
3	Reaction (Stop flow)	-	-	-	-	-	-		60
4	Separation	G	-	-	V_H -7.0	-	-		80
5	Repeat steps 2 and 4								

Program B

Step	Function	B1	B2	W1	W2	Ab	SO	SI	Time (s)
1	Sample input to SIC	-	-	-	-	-	-	P	180
2	Sample introduction and mixing	-	V_L -1.2	-	-	G	G		30-60
3	Reaction (Stop flow)	-	-	-	-	-	-		60
4	Injection and plug shaping	G	-	V_L -1.2	G	G	G		15
5	Pre-separation	G	-	V_L – 0.5	V_H -5.0	-	-		0.6
6	Separation	G	V_L – 0.8	V_L – 0.8	V_H -7.0	-	-		80

*P = external pressure; - = floating voltage; G = ground; V_L = power supply variable from 0 to – 3kV; V_H = power supply variable from 0 to –10 kV. The power supply used and the voltage (in kV) it was set for are indicated in columns, B2, W1 and W2. SO and SI are the outlet and inlet ends, respectively, of the sample introduction channel.

65
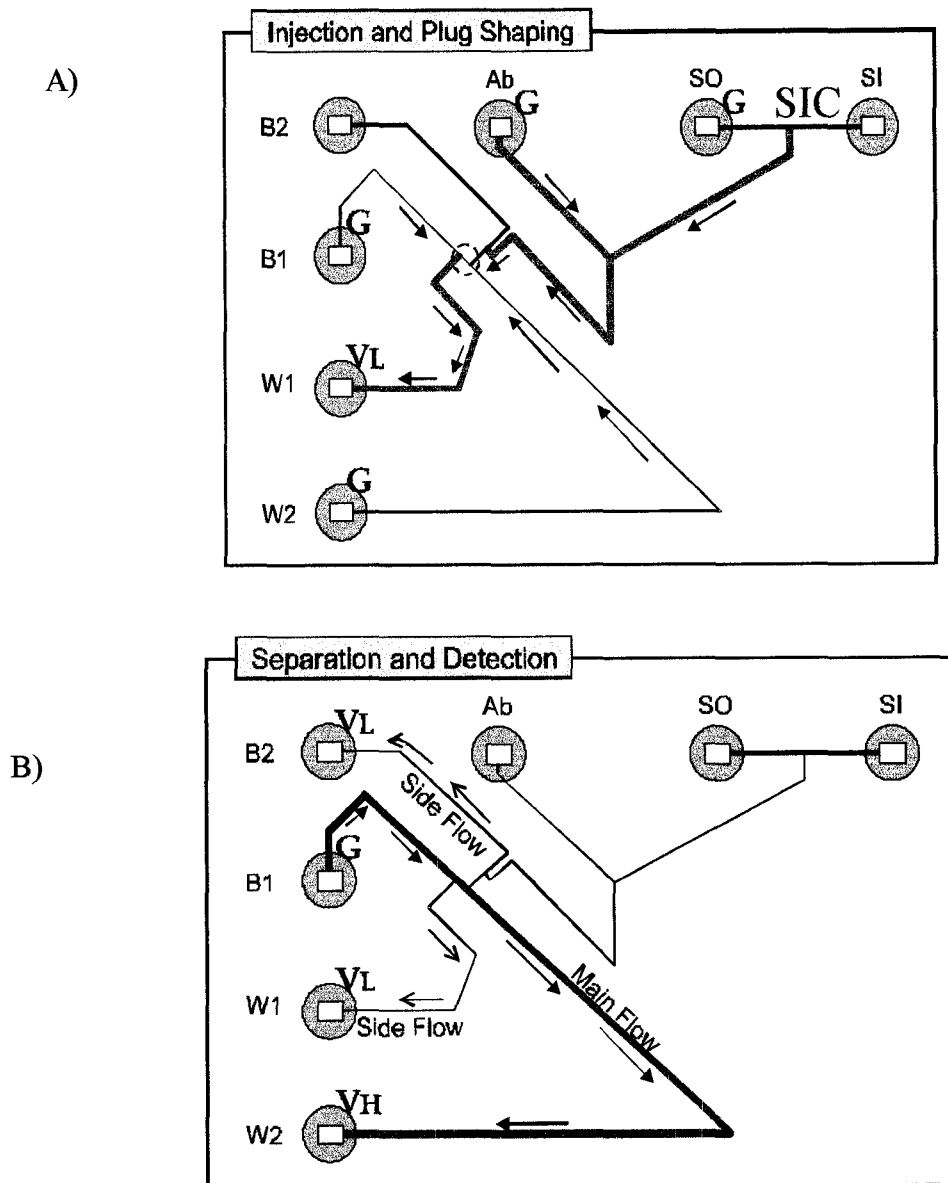
Figure 2.7 The on-chip processing was a sequence of timed events controlled by high voltages at the electrodes in the fluid reservoirs. A) Fluid flow for injection of the double-T and plug shaping, corresponding to step 4 in Table 2.1, program B. The double-T injector is shown in the dashed circle. B) Fluid flow for separation and detection, corresponding to step 6 in Table 2.1, program B.

66
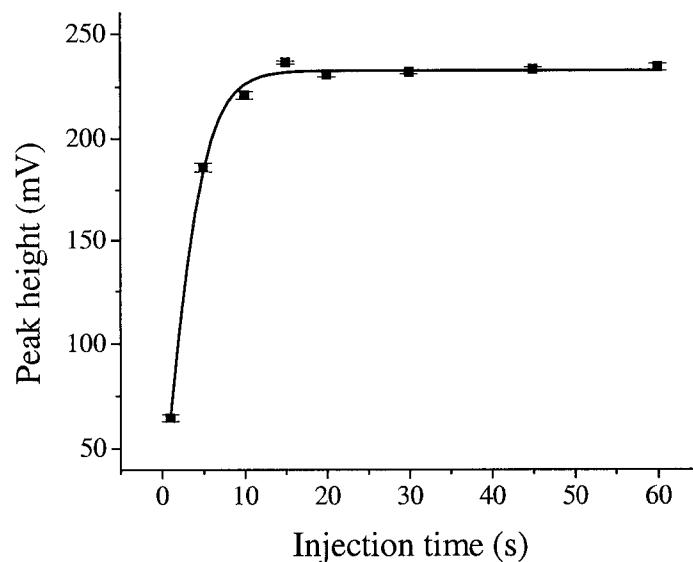
Figure 2.8. The peak height (representing volume of 40 nM Cy5 dye loaded into the 290 pL double-T injector) as a function of loading time. The injector was loaded using the plug shaping procedure of step 4 in Table 2.1, program B. The fluid flow during loading is shown in Figure 2.7a. The data points and bars represent the mean and standard deviation for five consecutive measurements.

2.3.4 Immunoassay of Ovalbumin

In the language of the chemist, homogeneous immunoassays are solution-phase reactions of antibody and antigen. Separation of antibodies from their antigen complexes using capillary electrophoresis can be a challenge, and the separation efficiency depends on the specific antigen/antibody pair.[33, 34] The labeling dyes used often play a role, since they will change the charge to size ratio of the labeled compounds. In this work we separated Cy5-labeled antibody to ovalbumin from the ovalbumin-antibody complex. The reaction of ovalbumin (Ov) and labeled anti-ovalbumin (Ab*) is given by the following:

67

$$Ab^* + Ov \rightleftharpoons Ab^*Ov.$$

To carry out the immunoassays, aliquots of Ov solution were placed in the sample tube (as depicted in Figure 2.3) and delivered to the SIC by the peristaltic pump. From the SIC, Ov was sampled electrokinetically, mixed on-chip with the Ab*, then injected and separated. Electropherograms of Ab* and a mixture of Ov and Ab* are shown in Figure 2.9. For Ab* alone, the peak appeared at 23 ± 0.2 s (n = 5). The small peak at 33 s was an impurity, most likely free Cy5 dye. For the Ov-Ab* mixture, the complex appeared at 26.5 ± 0.2 s (n = 5). Peak heights varied by 2-3 % (n = 5). The day-to-day variations in migration times were about 6 %. The free Ov peak was not observed, of course; however, Cy5-labeled Ov had a migration time of 35.6 ± 0.2 s (n = 5). In this chip assay, the free antibody and the complex peaks were fairly separated (resolution = 1.2). For a series of Ov samples (approx. 10–100 µg/mL) the peak heights varied linearly (R^2 = 0.9986), as illustrated in Figure 2.10.

A difficulty in CE separation of immunoassay products arises from protein adsorption on the capillary walls. Through the use of appropriate buffer systems sufficient resolution can be obtained within the microchip for immunoassays[10, 11] and clinical serum samples[18] without the need for channel coatings. The use of dynamic coating agents such as surfactants greatly simplifies the fabrication of the devices, and avoids durability problems associated with coating lifetimes. When protected from particulates and properly cleaned each day with NaOH and water, individual devices had lifetimes of 3 to at least 18 weeks.

68
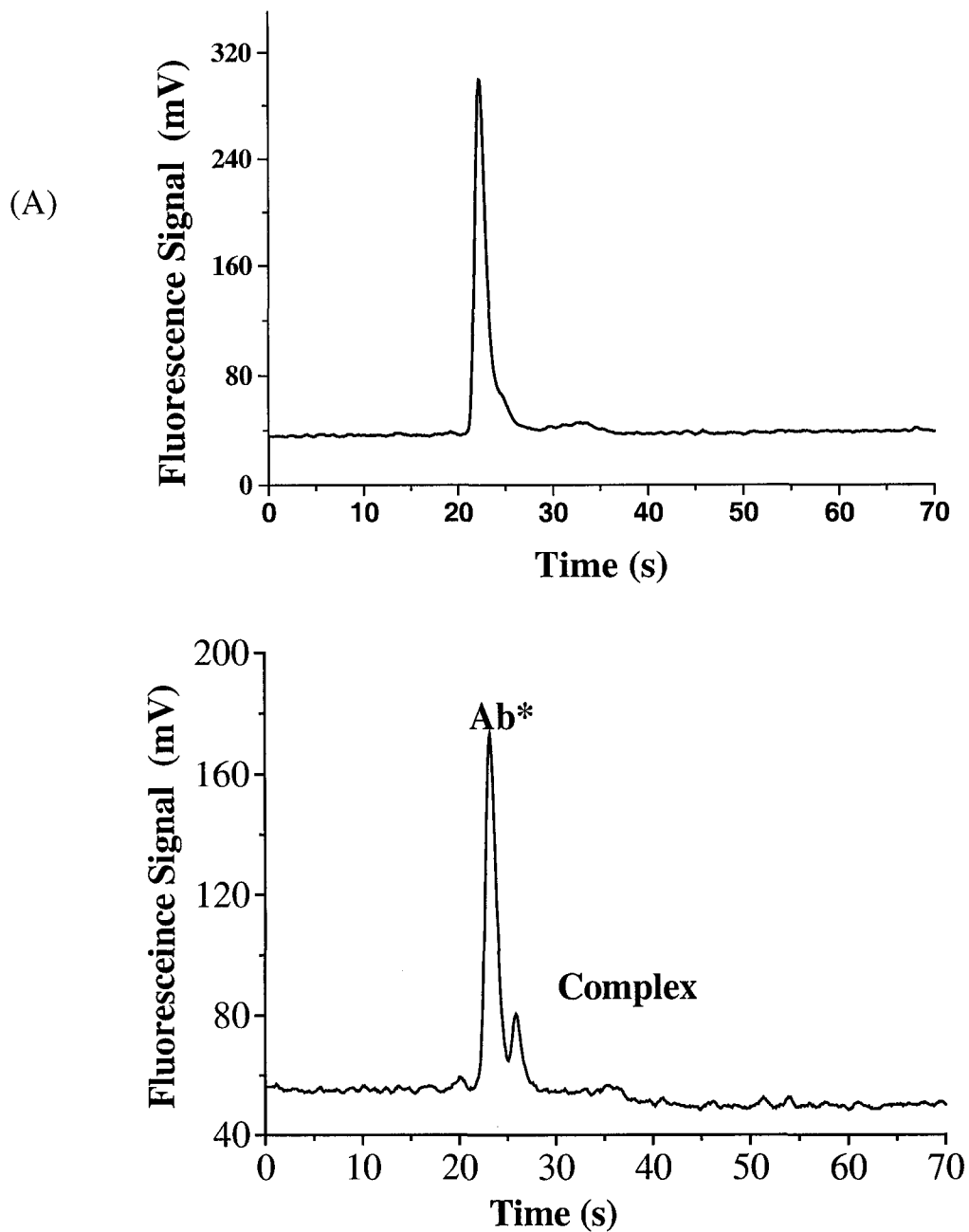
Figure 2.9 On-chip electropherogram of (A) 38 μg/ml labeled anti-ovalbumin
(B) a mixture containing 38 μg/ml labeled anti-ovalbumin and 10
μg/ml ovalbumin. The complex appears to the right side of the
antibody peak

69
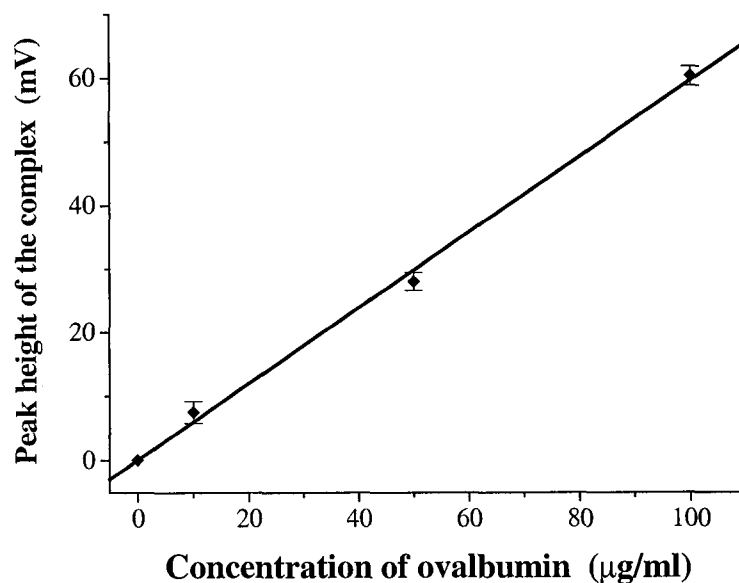
Figure 2.10. Calibration curve of on-chip ovalbumin assay. Samples of ovalbumin in varying concentrations were delivered to the sample introduction channel by peristaltic pump. The analysis from that point was completely automated. Total assay time was about 3 minutes. The data points and bars represent the mean and standard deviation for three consecutive measurements ($R^2 = 0.9986$).

2.3.5 Overall Instrument Evaluation

In order to perform chemical processes within a microfluidic chip, peripheral subsystems, such as lasers, detectors, power supplies and switches are required. Although the microchip devices are small, the use of conventional-sized peripherals can result overall in a large system, occupying a laboratory optical table. One of the goals of this work was to design more compact peripherals, so that the analytical instrument was potentially portable, rugged and stand-alone. The automated platform that is shown in Figure 2.2 has an overall size of 30 x 35 x 50-cm and operates with a standard 120-V AC supply.

70

This was accomplished in part through the use of small, low-current power supplies and high voltage relays to make an electrical subsystem that was about 20 x 20 x 10 cm in size. The greatest gain in shrinking the size of the instrument was in the design and construction of the epiluminescent confocal microscope for fluorescence detection. This unit contained the laser, detector, optics and alignment eyepiece and was 4 x 8 x 13-cm in size. We deliberately selected conventional optical sub-components because the demand for ultra-high sensitivity detection requires state of the art detection methods, which are difficult to achieve with integrated micro-optics or other novel solutions at this point. We obtained high performance of the optical unit at relatively low cost using standard optical elements.

The system and its sub-components were subjected to extensive testing over a period of about 10 months. Early problems with computer latch-up due to high voltage switching were resolved, and the optical detection system was improved to provide the present 69 pM detection limits for Cy5. The system will run continuously for 8-12 hours/day with no failures for periods of months at this stage. Assays carried out on the instrument were fast and easy to perform. The fluid interface plate design provides a convenient means of rapidly switching chips. The operator can change a chip within 1-2 min, and be ready to perform the next assay following 15-30 min of chip equilibration time. The low-resistance sample introduction channel provided a simple microfabricated solution to interfacing the chip to an external fluid flow. The transition from off-chip peristaltic (mechanical) pumping to on-chip electrokinetic injection was accomplished accurately and without leakage. There was no observed problem with sample carryover in the device for either Cy-5 or protein solutions.

71

2.4 Conclusions

This work, to our knowledge, was the first report of a stand-alone, automated, microfluidic-based instrument platform for immunoassays at the time of publication.[35] In this system the complete reaction process for immunoassays was performed on-chip. Automation was accomplished by organizing the assay as a set of defined chemical functions that could be executed precisely in a specific electrically controlled and electrokinetically driven sequence. The work reported here represents the first prototype stage in the development of an automated immunoassay instrument. In addition to the microchip-based processing, we were designing compact subsystems for optical detection and high voltage, plus fluidic interface and computer control. The results demonstrate the amount of automation and the rapid analysis times that can be achieved in a microfabricated device. The performance of the system is robust, with fluorescence detection limits of 69 pM, migration time reproducibility of $\pm$ 0.21 % between runs and $\pm$ 3% over 14 days, chip durability of many weeks, and stable system peripheral operation. The operator was required to change the sample solution in the sample tube after each run in the present design. However, with appropriate interfacing to an autosampler and less dead volume in the external fluid lines, such systems could form the basis of automated instruments for on-site environmental monitoring and point-of-care clinical analysis. The instrument also has the potential to be used in the screening of antibodies to determine affinity constants and in selection of suitable antibody producing hybridoma cells.

72

2.5 References

(1)   Harrison, D. J.; Manz, A.; Fan, Z. H.; Lüdi, H.; Widmer, H. M. *Anal.Chem.* **1992**, *64*, 1926-1932.

(2)   Harrison, D. J.; Fluri, K.; Seiler, K.; Fan, Z. H.; Effenhauser, C. S.; Manz, A. *Science* **1993**, *261*, 895-897.

(3)   Fan, Z. H.; Harrison, D. J. *Anal. Chem.* **1994**, *66*, 177-184.

(4)   Seiler, K.; Harrison, D. J.; Manz, A. *Anal. Chem.* **1993**, *65*, 1481-1488.

(5)   Schultz-Lockyear, L. L.; Coyler, C. L.; Fan, Z. H.; Roy, K. I.; Harrison, D. J. *Electrophoresis* **1999**, *20*, 529-538.

(6)   McCormick, R. M.; Nelson, R. J.; Alonso-Amigo, M. G.; Benvegnu, D. J.; Hooper, H. H. *Anal. Chem.* **1997**, *69*, 2626-2630.

(7)   Taylor, T. B.; Winn-Dawn, E. S.; Picozza, E.; Woudenberg, T. M.; Albin, M. *Nucleic Acids Research* **1997**, *25*, 3164-3168.

(8)   Effenhauser, C. S.; Bruin, G. J. M.; Paulus, A.; Ehrat, M. *Anal. Chem.* **1997**, *69*, 3451-3457.

(9)   Kounty, B. K.; Schmalzing, D.; Taylor, T. A.; Fuchs, M. *Anal. Chem.* **1996**, *66*, 18-22.

(10)   Chiem, N.; Harrison, D. J. *Anal. Chem.* **1997**, *69*, 373-378.

(11)   Chiem, N.; Harrison, D. J. *Clin. Chem.* **1998**, *44*, 591-598.

(12)   Attiya, S.; Jemere, A. B.; Tang, T.; Fitzpatrick, G.; Seiler, K.; Chiem, N.; Harrison, D. J. *Electrophoresis* **2001**, *22*, 318-327.

(13)   Cheng, S. B.; Skinner, C. D.; Taylor, J.; Attiya, S.; Lee, W. E.; Picelli, G.; Harrison, D. J. *Anal. Chem.* **2001**, *73*, 1472-1479.

(14) Simpsons, P. C.; Roach, D.; Woolley, A. T.; Thorsen, T.; Johnston, R.; Sensabaugh, G. F.; Mathies, R. A. *Proc. Natl. Acad. Sci. U.S.A.* **1998**, *95*, 2256-2261.

(15) Wolley, A. T.; Lao, K.; Glazer, A. N.; Mathies, R. A. *Anal. Chem.* **1998**, *70*, 684-688.

(16) Jacobson, S. C.; Ramsey, J. M. *Anal. Chem.* **1996**, *68*, 720-723.

(17) Kopp, M. U.; de Mello, A. J.; Manz, A. *Science* **1998**, *280*, 1046-1048.

(18) Coyler, C. L.; Mangru, S. D.; Harrison, D. J. *J. Chromatogr. A* **1997**, *781*, 271-276.

(19) Li, P. C.; Harrison, D. J. *Anal.Chem.* **1997**, *69*, 1564-1568.

(20) Salimi-Moosavi, H.; Szarka, R.; Andersson, P.; Smith, R.; Harrison, D. J. *Transducers '98 International Conference on Solid State Sensors and Actuators*; Hilton Head Island, Cleveland, U.S.A.; 1998, pp. 350-353.

(21) Manz, A.; Becker, H., Eds. *Microsystems technology in chemistry and life science*; Springer-Verlag: Berlin, 1998.

(22) Harrison, D. J.; van der Berg, A., Eds. *Proc. μ-TAS '98 Workshop*; Kluwer Academic Pub.: Banff, Canada, 1998.

(23) Landers, J. P., Ed. *Handbook of Capillary Electrophoresis*, 2nd ed. ed.; CRC Press, Boca Raton, 1996.

(24) Shintani, H.; Polonsky, J. *Handbook of Capillary Electrophoresis Applications*; Blackie Academic and Professional: London, 1997.

(25) Li, T.; Kennedy, R. T. *Electrophoresis* **1997**, *18*, 112-117.

(26) Effenhauser, C. S.; Bruin, G. J. M.; Paulus, A. *Electrophoresis* **1997**, *18*, 2203-2213.

(27) Attiya, S. Ph. D. Thesis, University of Alberta, 2000.

(28) Effenhauser, C. S.; Manz, A. *Anal. Chem.* **1993**, *65*, 2637-2642.

(29) Raymond, D. E.; Manz, A.; Widmer, H. M. *Anal. Chem.* **1994**, *66*, 2858-2865.

(30) Wolley, A. T.; Hadley, D.; Landers, P.; de Mello, A. J.; Mathies, R. A.; Northrup, M. A. *Anal. Chem.* **1996**, *68*, 4081-4086.

(31) Shimura, K.; Karger, B. L. *Anal. Chem.* **1994**, *66*, 9-15.

(32) Jacobson, S. C.; Hergenroder, R.; Kounty, B. L.; Warmack, R. J.; Ramsey, J. M. *Anal. Chem.* **1994**, *66*, 1107-1113.

(33) Grossman, P. D.; Colburn, J. C.; Laurer, H. H.; Neilsen, R. G.; Riggin, R. M.; Sittamalam, G. S.; Rickard, E. C. *Anal. Chem.* **1989**, *61*, 1186-1194.

(34) Schmalzing, D.; Nashabeh, W. *Electrophoresis* **1997**, *18*, 2184-2193.

(35) Lee, W. E.; Jemere, A. B.; Attiya, S.; Chiem, N.; Paulson, M.; Ahrend, J.; Burchett, G.; Bader, D. E.; Ning, Y.; Harrison, D. J. *Journal of Capillary Electrophoresis and Microchip Technology* **1999**, *1/2*, 51-59.

Chapter 3: An Integrated Solid Phase Extraction System for Sub-Picomolar Detection *

3.1 Introduction

Since its introduction, the concept of miniaturizing biochemical analysis by integration of analysis steps within micro total analysis systems (μ-TAS) has attracted considerable interest.[1-3] A key application of μ-TAS devices is the integration of both sample preparation and analysis on chip.[4] One of the common steps in sample preparation is the preconcentration of dilute samples. It is desirable to be able to perform this step within a microfluidic device as part of a series of analysis steps. Field amplification stacking[5-7] and isotachophoresis[8-10] are two methods of sample preconcentration that are easily integrated into devices pumped by electrokinetic forces. However, these methods are not readily adapted to a wide variety of sample compositions, whereas solid phase extraction (SPE) onto a non-polar sorption phase has become widely employed.[11-14] Kutter et al.[15] reported the integration of SPE in a CE device by modifying the channel walls with octadecylsilane (ODS), obtaining a preconcentration factor as high as about 80 for 8.7 nM neutral Coumarin C460 dye. However, the available surface area limits the adsorption capacity of the coated channels. Prof. Harrison's group has introduced[16] an integrated SPE system that utilizes ODS beads loaded on-chip to preconcentrate hydrophobic samples, allowing the use of high surface areas for adsorption, yielding preconcentration factors of up to 500. More recently, Yu et al.,[17] using an integrated monolithic column for SPE, reported a concentration enhancement of 190 in an ion-

---

exchange concentrator and up to 1650 in a hydrophobic concentrator for a 10 nM protonated Coumarin 519 dye. In this chapter we present a much more detailed analysis, than in reference 16, of the quantitative performance of a 330 pL, 200 μm long SPE bed, allowing quantitative comparison to other microfluidic designs. We show for the first time that sub-picomolar detection limits can be achieved for fluorescent dyes, and we also confirm that peptides and amino acids may be preconcentrated using these devices. Landers et al.[18] have described some difficulties with instability of packed beds. Here we describe improved packing and bed stabilization procedures to avoid such problems in the double weir beds. These packed beds can also be used to perform capillary electrochromatography (CEC), through the choice of appropriate solvent elution strength. The CEC performance of the double weir beds show improved separation efficiency when using the new bed stabilization procedures.

3.2   Materials and Methods

3.2.1   Reagents

A pH 8.3 buffer was prepared by dissolving 5 mM ammonium acetate (Caledon Laboratories LTD, Georgetown, ON) in ultra pure water (Milli-Q UV Plus, Millipore Canada, Mississauga, ON) and adjusting to pH 8.3 with 0.1 M NaOH. This was used as the SPE and CEC loading buffer. The buffer was mixed with acetonitrile (BDH, Toronto, ON) in a 3:2 (v/v) ratio to form our most commonly used elution buffer for the SPE and CEC bed. BODIPY 493/503 (4,4-difluro-1,3,5,7,8-penta methyl-4-bora-3a,4a-diaza-s-indacene) was from Molecular Probes (Eugene, OR), and was prepared as a 0.1 mM stock solution in HPLC grade methanol (Fisher, Fair Lawn, NJ). Acridine orange

77

hydrochloride solution (EC No. 2006140, Fluka Chemie GmbH CH-9471 Buchs, Switzerland) was used as received. Before injection, BODIPY and acridine orange were diluted as required in the loading buffer. Ethylene dimethacrylate (EDMA) and 2,2'-azo-bis(isobutyronitrile) (AIBN) (Sigma-Aldrich Chemical Co., Milwaukee, WI), reagent grade 1-propanol and 1,4-butanediol (Caledon Laboratories Ltd. Georgetown, ON and Eastman Organic Chemicals, Rochester, NY) were used as received. Angiotensin II and leucine (Sigma-Aldrich) were labeled following a previously published procedure.[19] To 16 μL of 1 mM aqueous peptide, 43 μL of 0.1 M carbonate buffer (pH 9.5) was added, followed by 20 μL of 84 μg/mL alexafluor in acetonitrile. The mixture was vortexed for about 10 s and kept in a heating block at 35 °C for 4 h. The labeled angiotensin II solution was then diluted to 1 nM in a 25 mM borate buffer (pH 8.3 adjusted with 0.1 M NaOH) used for loading the bead bed. Leucine was labeled with FITC following the same protocol (but was left overnight in the dark to react instead of heated at 35 °C for 4 h) and diluted to 1 nM in 25 mM borate buffer, pH 8.3. All buffers were filtered through a nylon syringe filter (0.2 μm pore sizes, Nalgene, Rochester, NY) prior to use.

A reversed-phase chromatographic stationary phase, Spherisorb ODS-1 (Phase separations, Flintshire, UK), was used for the integrated SPE and CEC bed. The porous silica particles had a mean pore size of ~ 8 nm, and a particle diameter ranging from 1.5 μm (high abundance) to 4.0 μm (low abundance), as determined by scanning electron microscopy. A slurry of approximately 3 mg/mL of ODS-1 beads in acetonitrile was prepared to pack the SPE and CEC beds.

3.2.2 Chip Design and Bead Packing

The chip layout, fabrication and operating protocols were described previously.[16] Details of the device geometry and the reservoir-labeling scheme are shown in Figure 3.1. Microchip devices were fabricated in Corning 0211 glass (600 μm thick, Corning, NY) using a previously published chemical etching procedure.[16, 20] The weirs were etched 1 μm deep and the channels were 10 μm deep. After drilling 2 mm diameter access holes on a 600 μm thick, Corning 0211 glass cover plate, the etched substrate was bonded to it at room temperature.[21] The small channel originating from reservoir 3 was used to direct ODS beads into the chamber using electrokinetic[22, 23] or pressure injection.

The channels were conditioned with acetonitrile prior to use, since an initial aqueous flush often resulted in trapped air bubbles. Acetonitrile in reservoir 3 was then replaced with the ODS-bead slurry and a positive high voltage (~1 kV) was initially applied to the bead reservoir 3, with reservoirs 1 and 2 grounded. The bed was typically packed in 15–20 s, manually ramping the voltage down to 100 – 200 V during the last 5–10 s of packing. Once the chamber and a good portion of the bead introduction channel were packed with beads, the acetonitrile in reservoirs 1 and 2, and the excess slurry in reservoir 3, were replaced with the aqueous buffer. The voltage in reservoir 2 was then ramped manually from 200 V to 800 V over about 1 min, with reservoir 3 biased at 400 V and reservoir 1 grounded. The packed chamber was monitored with a 25 X microscope objective attached to a CCD camera (Sony model SSC-C370 with 0.5 X lens) to ensure that the acetonitrile was completely replaced by buffer and that the packing material did not shift or unpack during this procedure. The ODS beads could be seen to agglomerate

as the acetonitrile was expelled, creating a "solvent lock", and the change in the index of refraction at the buffer/acetonitrile interface was clearly visible.

3.2.3 Bead Entrapment

For the SPE experiments the "solvent lock" method described earlier[16] was used. For CEC, in order to immobilize the packed beads in the chamber, a monomer was introduced and polymerized *in situ*. The monomer solution was prepared by dissolving 200 μL of a mixture of EDMA and the free radical initiator AIBN (2 wt% AIBN per weight of EDMA) in 800 μL of a ternary solvent mixture (10 wt% H_2O, 40 wt% 1,4-butanediol, and 50 wt% 1-propanol), and stored at 4 °C.[24, 25] The mixture was purged with N_2 for 15 min to remove dissolved O_2. About 20 μL of the mixture was placed in reservoir 3 and suction was applied to reservoir 1 for about 2 min, while reservoir 2 contained water. The advancement of the monomer solution inside the bead introduction channel was visually monitored using a CCD camera and suction was stopped before the monomer solution reached the bed. Plastic caps were then placed over reservoirs 1 and 2 to prevent evaporation. The chip was subsequently cured in an oven at 60 °C for 24 h, and reservoirs 1 and 2 were topped up with H_2O after 12 h, if needed. After curing, acetonitrile was added to reservoir 3 and pulled towards reservoir 2 using vacuum, followed by an aqueous flush of the bead introduction channel. Devices were stored with H_2O in the channel at 4 °C with capped reservoirs, until use.

80
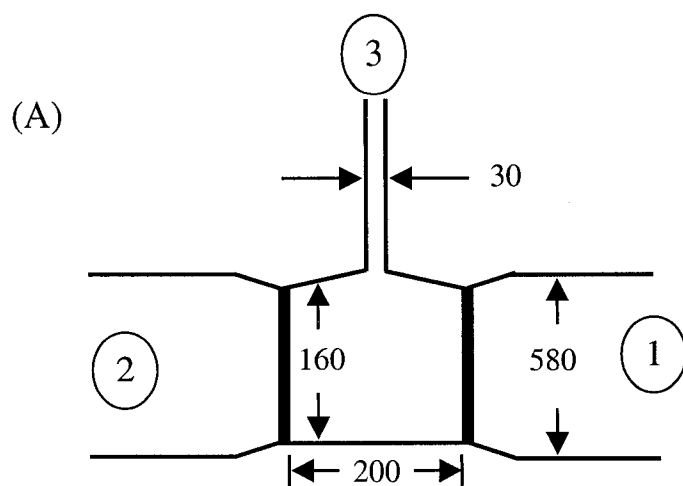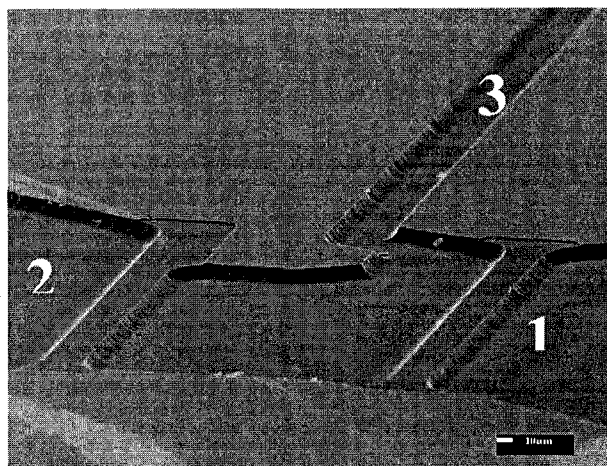
Figure 3.1.   (A) Drawing of top view of channel layout for symmetric side channel entrance design used for CEC. Chamber is ~330 pL, channels are 10 μm deep.   Dimensions illustrated are in microns, but are not to scale. The bead introduction channel is (3), the inlet sample/buffer channel is (2) and the outlet buffer channel is (1). (B) Image of the asymmetric cavity taken with scanning electron microscope, showing placement and hooked bead channel entrance. This device was used for SPE. Channel labeling is the same as in (A).

81

3.2.4 Chip Operation

Before use, loading buffer replaced solvent in all reservoirs, and the bed was equilibrated with buffer, while applying vacuum to reservoir 1. Samples were loaded onto the bed with an applied electric field from reservoir 2 to 1 (1 grounded), with reservoir 3 floating. Buffer was then introduced to reservoir 2 and a 1 min buffer flush was executed. Eluent buffer was then placed in reservoir 2 to release samples adsorbed on the bed, using the same voltage scheme as during sample loading.

Electroosmotic flow velocity during SPE studies was measured using a neutral BODIPY dye. After equilibrating the channels with the loading buffer, BODIPY in the same buffer was pumped into the bed with + 500 V applied on reservoir 2, reservoir 1 grounded and reservoir 3 floating. The fluorescence detector was positioned immediately upstream of the bed. From the time required for BODIPY to reach the detector and the electrical field used, the electroosmotic flow velocity was calculated.

In order to obtain the corrected retention time for CEC studies, the time needed for the eluent to reach the packed bed was measured by electrokinetically pumping neutral BODIPY dye, dissolved in the eluent buffer, into channels filled with aqueous buffer. The fluorescence detector was located just upstream of the bed for this determination. BODIPY was pumped with + 800 V applied on reservoir 2.

In order to determine the total capacity of the SPE bed, breakthrough curves were obtained for 10 nM aqueous solution of BODIPY dye pumped at an electroosmotic flow (EOF) rate of 0.20 μL/min. Fluorescence signal of BODIPY was recorded both at the inlet and outlet of the bed in separate runs. The breakthrough time was taken as the time needed for the signal downstream of the bed to reach 50% of its maximum (the inflection

82

point), less the time required for dye to reach the inlet of the bed. The time needed for dye to reach the inlet also allowed determination of the linear and volumetric flow rates.

3.2.5 Instrumentation

The computer controlled power supply and relay arrangement has been described elsewhere.[26] In-house written LabVIEW programs (National Instruments, Austin, TX) were used for computer control of the voltages and for data acquisition. The laser induced fluorescence detection system consisted of a 488 nm air-cooled Ar ion laser (Model 2214-105L, Uniphase, San Jose, CA), operated at 4 mW and associated focusing optics[16] (Melles Griot, Irvine, CA). Fluorescence emitted from BODIPY/acridine orange was collected using a 25X, 0.35 N.A. microscope objective (Leitz Wezlar, Germany). A 530 nm emission filter and a photo-multiplier tube (PMT) (R1477, Hamamatsu, Bridgewater, NJ) were used as a detector, positioned between the chamber and reservoir 1 (Figure 3.1) in the wide channel just next to the chamber. The weir was just out of the field of view. The PMT was biased to 550 V, while the PMT signal was amplified, filtered (25 Hz Butterworth) and sampled at a frequency of 50 Hz. Peaks used for calibration curves were further smoothed with a 13-point Savitzky-Golay smoothing function, included in Microcal Origin Software (Northampton, MA). Noise was measured as the standard deviation about the mean of the smoothed baseline (n = 100) for signal to noise (S/N) estimates.

83

3.3 Results and Discussions

3.3.1 Packing and Unpacking of the Chromatographic Material in the Bead Chamber

An integrated solid-phase extraction bed was prepared using a previously described double weir design to construct a cavity in which beads coated with a stationary phase could be trapped.[16] The 30 μm wide side channel forms part of a three-way junction, and was designed to feed beads into or out of the chamber created by the two weirs on either side of the side channel, as illustrated in Figures 3.1. Sample could then be delivered from reservoir 2, along the inlet channel, across the chamber, and on toward the outlet (reservoir 1). The volume of the chamber was 0.33 nL, while the inlet and outlet channels were 0.041 and 0.15 μL, respectively. The inlet and outlet channels had much lower flow resistance than the side channel, despite the weirs, given their wide dimensions (580 μm, tapering to 300 μm at the weirs). The flow resistance was manipulated by the selection of these channel dimensions in order to encourage flow between reservoirs 1 and 2, rather than into bead-introduction channel during sample loading and elution.

Electrokinetic packing of conventional capillaries has been demonstrated,[22, 23] and we have adapted the method for the microchip. The packing procedure involved applying a positive voltage to the bead reservoir, while grounding reservoirs 1 and 2, as discussed in the experimental. The applied voltage induced EOF to flow down the bead channel, carrying the beads into the cavity. At the early stage of packing, the beads entering the cavity contacted the weir structures on either side of the cavity shown in Figure 3.2a. The beads were unable to traverse the weir because the distance from the

84

top of the weir to the bottom of the cover plate (1.0 µm) was less than the diameter of the individual particles of the packing material (1.5 – 4.0 µm). The cavity continued to pack until it was entirely filled with chromatographic material, as shown schematically in Figure 3.3. Several authors have described the difficulties associated with reproducibly fabricating frits for retaining packing material in conventional capillaries.[27-29] The two weirs design of the microchip used in the present work overcame this problem, and the electrokinetic packing of the beads provided an even distribution of beads throughout the chamber with no observable voids. It was also possible to pack the cavity by applying vacuum at reservoirs 1 or 2.

Figure 3.2a shows an image of the bead cavity midway through the packing procedure, while Figure 3.2b shows the cavity 10 s later. If the beads did not pack tightly they were removed from the chamber by simply reversing the voltages and then repacking the bed. Once aqueous solution was introduced to the chamber, the reversed-phase beads tended to agglomerate and were more difficult to remove. In the SPE work subsequent removal of the beads was accomplished by flushing the aqueous solution out with acetonitrile, using either EOF or vacuum or a combination of the two. The ability to remove beads that have been packed enables one to refresh used stationary phases.

Once the chamber is filled, the beads were observed to flow down the sides and up the middle of the bead introduction channel (towards reservoir 3) mimicking the solvent back flow generated in a closed electrophoretic system.[30] In such a system, EOF is directed along the walls until it reaches the end of the chamber, where pressure causes the solution to reverse direction and flow back up the center of the bead introduction channel. Ramping the voltage down during the last few seconds eliminates significant bead back

85

flow. The use of negative pressure at reservoirs 1 or 2 can also be beneficial, as it causes the solution to flow towards the bead bed.

(A)

(B)
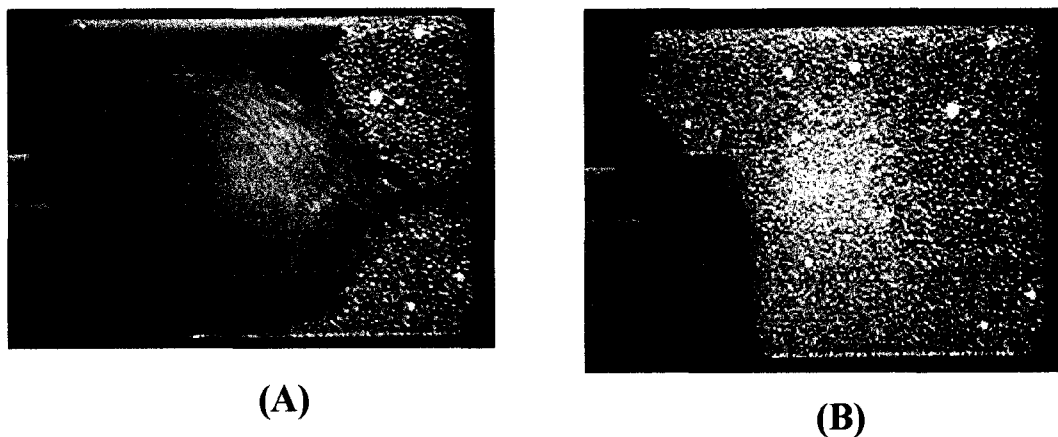
Figure 3.2.   Images of chamber (A) at an initial stage of electrokinetic packing and (B) after it is completely filled with beads.
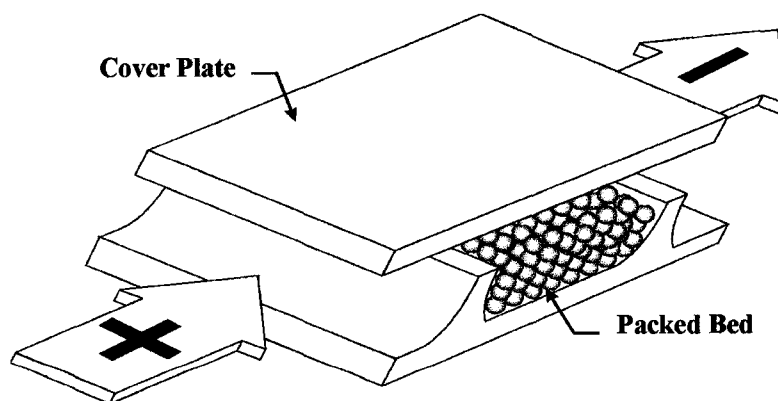
Figure 3.3.   Schematic diagram of packed chamber. Electroosmotic flow is driven by walls and by free silanol groups on particles. Solvent flow direction is indicated for preconcnetration and CEC steps.

86

3.3.2 Column Preparation

In our previous reports,[16, 31, 32] we demonstrated the use of a three-port chip design for trapping micro beads within a microfluidic device. This design was utilized to perform CEC[16], SPE[16] and an immunosorbent assay.[31, 32] In those reports, we used a change in the composition of the buffer system after packing the bed to "lock" the beads within the 330 pL chamber. Eventually, the formation of voids in the packed bed was observed when CEC or SPE were carried out repeatedly with > 50% acetonitrile in the buffer. Such voids can alter peak shape and significantly decrease bed efficiency. One possible reason for the occurrence of these defects is the frequent bed pressurization-depressurization cycles between runs, in addition to the changes in surface charge with solvent composition. Moreover, since ODS beads are hydrophobic, the extent of their agglomeration decreases when buffers with a higher proportion of acetonitrile are used, thus destabilizing the bed. In SPE it is common to replace the beads frequently to avoid the build up of contaminants, so the formation of voids over time is not a problem. However, CEC columns are used repeatedly. To circumvent this problem in CEC, a potential was applied to the bead reservoirs during the runs to direct some solvent flow from the bead channel into the chamber. This step did not always solve the problem completely, especially when the mobile phase was more than 50% organic modifier. We then examined the use of a physical plug, formed by polymerization, to trap the packed beads, using the methacrylate monomer solution described in the Experimental Section. These beds showed improved stability, longer lifetime and better performance. Solvents containing up to 100% acetonitrile could be pumped across the weir, with no loss of

87

packed particles into the bead introduction channel. Such immobilized beds could be used for at least a month without void formation.

The combination of the use of voltage ramping during bed loading, and the polymerization entrapment procedure allowed the use of a chamber constructed with a symmetric bed entrance (Figure 3.1). We previously reported[16] that the symmetric design of chamber inlet suffered from too much solvent backflow to be easily loaded. By actively controlling and ramping down the voltage during packing, the backflow of beads was avoided. The symmetric chamber could be completely packed within 15 - 20 s. Results presented in this chapter used the symmetric chamber with polymer entrapment for CEC, and the asymmetric chamber with "solvent lock" procedures for SPE.

3.3.3 On-Chip Solid Phase Extraction of BODIPY

Preconcentration is a valuable tool that can be used to enhance the sensitivity of microfluidic devices. In this chapter we provide a much more detailed evaluation of the quantitative behavior of the weir-based[16] SPE devices. For SPE the amount of preconcentration is limited by the preconcentration time and the volume of sample available.[11-14] We have used the dye BODIPY to evaluate the effect of these parameters, and dye concentration, on the quantitative performance of these SPE beds. BODIPY exhibits a high affinity for ODS and is an excellent fluorophore. The preconcentration and elution of BODIPY was carried out in three steps, following equilibration of the packed ODS bed with the aqueous buffer. Various concentrations of aqueous BODIPY solutions were placed in reservoir 2 and + 500 V was applied for 2 min, with reservoir 1 grounded and reservoir 3 floating, so that BODIPY was concentrated on the 330 pL ODS

packed bed. The electroosmotic flow (EOF, 0.69 mm/s, 0.25 µL/min) was directed towards reservoir 1, carrying the BODIPY solution onto the SPE bed during the loading step. During this step, no sample breakthrough was observed. A 1 min buffer flush step followed, to wash the sample that remained within the channel onto the bed. Finally, elution buffer replaced the aqueous buffer in reservoir 2, in order to elute the concentrated BODIPY sample for detection downstream of the bed. This was done with + 500 V applied to reservoir 2 while reservoir 1 and reservoir 3 were grounded and floating, respectively. A concentration calibration curve for BODIPY gave a linear response across a concentration range of 1 to 100 pM with slope of 10.66 ± 0.38; intercept of 2.23 ± 2.22 and R^2 of 0.99899 (data not shown). For a 3 min preconcetration time, a concentration limit of detection (CLOD, S/N = 3) of 0.07 pM was obtained by linear extrapolation of the data in Figure 3.4. For the detection system used in the study, the best CLOD we obtained[33] was 30 pM for fluorescein without preconcentration. The concentration ranges studied in this experiment are about a 1000 times lower than those used in previous open tubular[15] or monolithic polymer based[17] microchip SPE studies. To our knowledge this is the first report on sub-picomolar detection limits obtained by SPE on a microchip device.
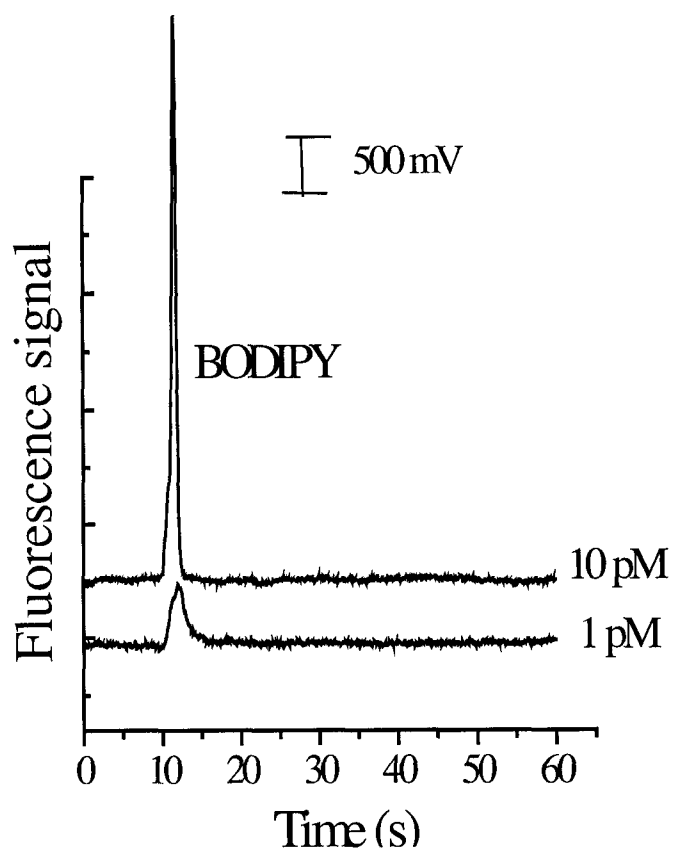
Figure 3.4.   Elution trace of 1 pM BODIPY (S/N = 45) and 10 pM
BODIPY (S/N = 434) obtained after concentrating for 3 min
from pH 8.3 aqueous buffer. Elution was performed with 40
% acetonitrile/60 % pH 8.3 buffer.

90

The effect of preconcentration time was also evaluated. A 10 pM BODIPY solution was concentrated for varying times, with + 500 V applied to reservoir 2 during loading. Linear relationships were observed between the resulting peak areas (slope 0.15 ± 0.02, intercept –0.04 ± 0.06, R^2 = 0.98745) and peak heights (slope 0.62 ± 0.03, intercept 0.00 ± 0.11, R^2 = 0.99761) vs. preconcentration times of 2-6 min. The linearity indicated that we were far from the breakthrough volume[11-14] of the bed at the concentration of BODIPY used. These results indicate that further increasing the preconcentration time would enhance the signal. However, larger concentration enhancement would come at the expense of greater analysis time, and a greater risk of contamination of the ODS bed by other sample components.

To determine the overall capacity of the bed, breakthrough curves were obtained (Figure 3.5). Bed capacity values of 8.1 x 10^{-14} mol of BODIPY or 0.25 mmoles per liter of the ODS packed bed were obtained. This value is about ten times larger than our preliminary estimate previously reported,[16] and is based upon a much more precise experimental procedure. The extraction capacity of an SPE system depends on a number of factors including the nature of the probe, carbon loading of the sorbent, and the quantity and type of SPE phase, so that comparisons to the literature are not exact. Nevertheless, under our conditions, the capacity per unit volume of our column is 8000 times higher than that reported for an ODS modified open tubular solid phase extraction microchip device,[15] but an order of magnitude lower than that of hydrophobic monolithic columns[17] on-chip.

91
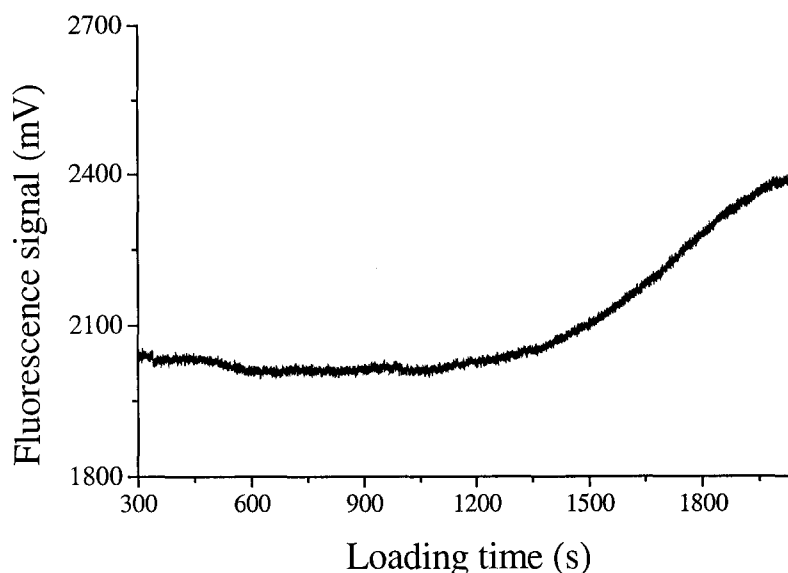
Figure 3.5.   Capacity determination for 330 pL ODS bed using frontal
               analysis. Conditions: probe solution 10 nM BODIPY in 25 mM
               Tris-HCl, pH 8.3 buffer, electroosmotic flow rate 0.20 μL/min,
               fluorescence intensity measured after the bed.

3.3.4 SPE of amino acids

To demonstrate the potential of the SPE bed for amino acid analysis, leucine labeled with

FITC was preconcentrated following the above procedures.   Figure 3.6 shows a

representative elution trace obtained for 1 nM leucine-FITC, concentrated for 2 min by

applying + 500 V to reservoir 2.   During the preconcentration step no sample

breakthrough was observed. The labeled amino acid was eluted from the SPE bed with

90 vol. % acetonitrile to 10% 20 mM NH_4 acetate (pH 4.7), using + 800 V. These results

92

confirm that trace amounts of labeled amino acids can be concentrated in the ODS

packed device and eluted in a later step for further analysis.
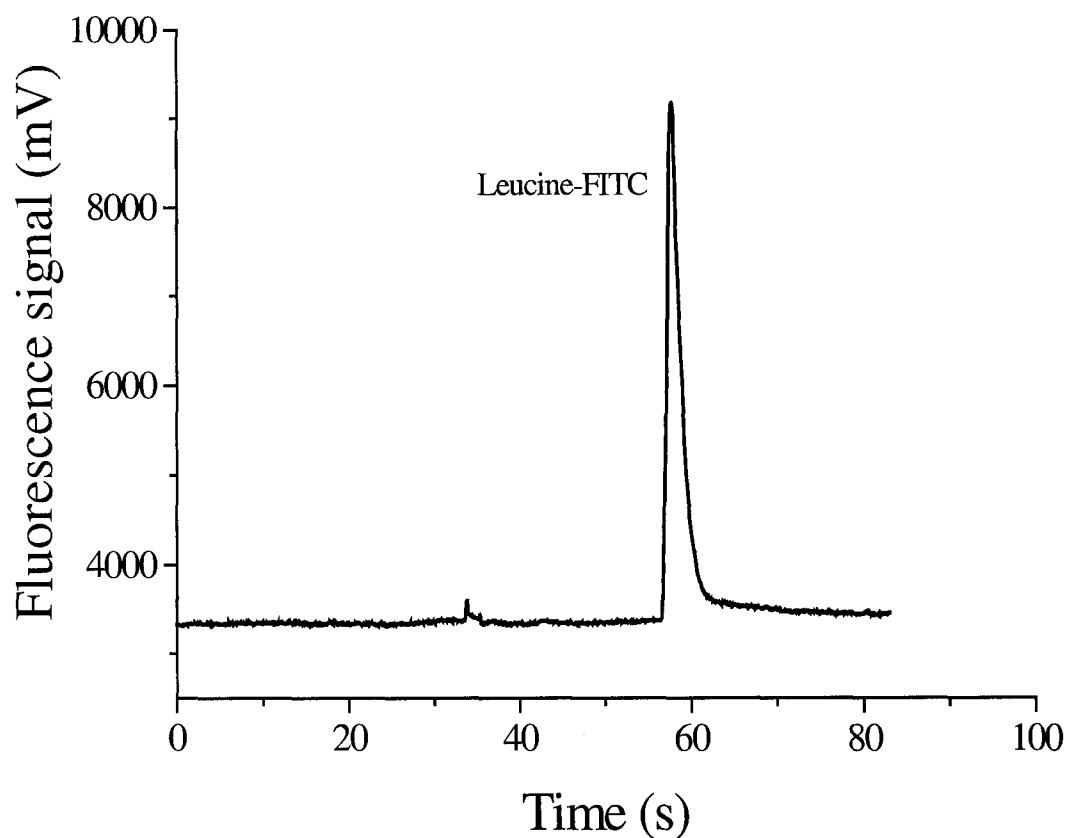
Figure 3.6.   Elution trace obtained for 1 nM leucine-FITC
concentrated for 2 min from pH 8.3 buffer. The sample
was eluted from the ODS bed using 90 % acetonitrile/10
% pH 4.7 buffer.

93

3.3.5 Packed Column CEC On-Chip

Further evaluation of the CEC behavior of these 200-μm long beds is reported here, providing further information about performance relative to the previous preliminary report.[16] Two neutral dyes were used, in order to base performance evaluations on strictly electrochromatographic separation mechanisms. Analysis of a peptide was also performed using trifluoroacetic acid (TFA) and acetonitrile as the eluent, to test the CEC performance under the acidic conditions preferred for peptide separations on surfaces with silanol residues.[34, 35] These separations were evaluated in beds prepared using the polymerization entrapment method, demonstrating improved performance relative to the use of the "solvent lock" method.

Figure 3.7 shows a typical electrochromatogram obtained for CEC separation of a mixture of BODIPY and acridine orange. Actually designed for another purpose, this device lacked an injector, so that samples were first loaded onto the leading edge of the ODS beads in the chromatographic bed using a non-eluting solvent (loading buffer). This approach has the effect of essentially eliminating injector band broadening contributions. Following a buffer flush step, the reservoir solution was changed to 40% acetonitrile/60% 5 mM ammonium acetate buffer, and + 800 V was applied from reservoir 2 to 1, to effect an isocratic elution with a flow rate determined to be 0.37 μL/min. BODIPY was eluted before acridine orange. Since both BODIPY and acridine orange are neutral at pH 8.3, their separation is entirely due to their differential sorption with the ODS phase. The peaks showed a resolution of 1.6 in less than 10 s. The RSD in retention time was < 0.5% for each compound. The RSD for peak heights and peak areas were 3 − 4% (n = 4). Theoretical plate numbers (N) were obtained using the equation,

94

$$N = 5.54 \, (t_{rc}/W_{1/2})^2$$

where t_{rc} is the corrected retention time and $W_{1/2}$ is the peak width at half height. The observed retention time must be corrected for the length of time (6.0 s) required for the elution buffer to reach the packed bed. We estimate about 420, 000 plates/m (N = 84 plates, H = 2.4 μm) for the acridine orange peak. The early eluting BODIPY peak showed N = 23 (115, 000 plates/m) and H = 8.7 μm. The detection zone was about 50 μm long, corresponding to a plate height contribution of about 1 μm. These results are comparable to other values reported for CEC on-chip.[36-39] The reduced plate height (h = H/d_p, where d_p is particle diameter) corrected for off column band broadening was about 1. Various researchers[40-46] have reported reduced plate heights in the range 1–2, and theory predicts a minimum value of just less than 1. We conclude that the fluid dynamics within the bed gives good flow behavior, and uniform flow velocity across the bed cross-section.

In a previous report by Harrison and co-workers,[16] they incorrectly used the observed retention time to calculate the theoretical plates from the packed bed. We do not have an accurate measurement of the time needed for the eluent to reach the bed in the previous study [30% acetonitrile/70% 50 mM ammonium acetate buffer], but a rough estimate of 5.0 s indicates that the number of theoretical plates/m were closer to 50,000–100,000 in that initial study, giving H in the range of 20 μm to 10 μm. Subsequent studies confirmed these values. As a result, we conclude that the use of a polymer plug to stabilize the bed improved the device performance.

95
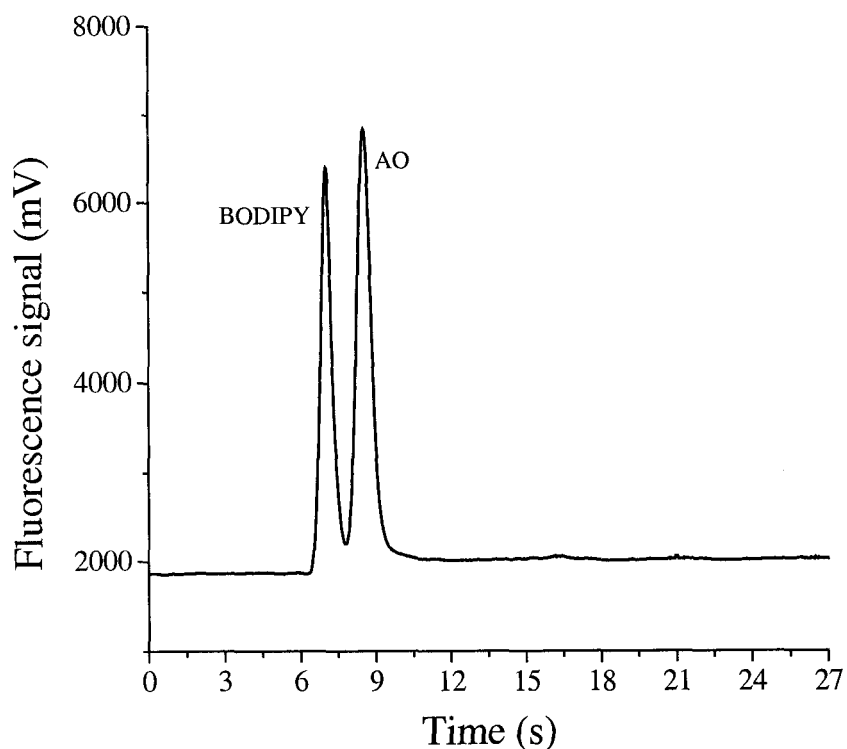
Figure 3.7.   Electrochromatogram for CEC separation of BODIPY
               and acridine orange (AO) using the 200 μm long ODS
               packed bed. Separation was effected using the same
               isocratic mobile phase as in Figure 3.4.   BODIPY
               eluted before acridine orange.

Increasing the separation voltage increased the speed of separation as expected,

dropping the elution time for acridine orange from ~16 s at 500 V to ~ 6 s at 1300 V.

The resolution of the two peaks was 1.8 at 500 V, 1.6 at 800 V and 1.4 at 1300 V. A plot

of $V_{applied}$ versus $1/t_r$ was linear ($R^2 = 0.99966$) from 500 V to 1300 V, but noticeable

deviation from linearity was observed at 1600 V. In fact, applied voltages of greater than

1500 V caused air bubbles at the weirs or in the chamber. This is not unexpected, considering the high electric field strength ($> 8 \times 10^4$ V/cm at 1600 V) we calculate exists at the weir, if we assume the open cross-sectional area of the bead bed is the same as that of the 1 μm deep weir. Bubbles were not observed at 1300 V ($\sim 7 \times 10^4$ V/cm), a field strength that is clearly much higher than the typical upper limit of a few hundred V/cm observed in CEC capillaries with conventional frits. Nevertheless, the decrease in resolution with increasing field likely arises in part from modest Joule heating effects in the bed or weir.

He et al.[47] have pointed out that CEC in microfabricated devices would allow separation of peptide mixtures under isocratic conditions, as opposed to the gradient elution mode used in HPLC. We used Alexafluor labeled angiotensin II to evaluate the bed performance for CEC of a peptide, since this fluorescent dye is not quenched at low pH. The labeled peptide was almost base line separated (resolution = 1.5) from the excess alexafluor using an eluent composition of 0.05% TFA and 26% acetonitrile in water, Figure 3.8. Well formed, Gaussian peaks were observed. In contrast, when the separation was performed with 40% acetonitrile/60% pH 8.3 buffer very extensive tailing was observed (data not shown). The use of acidic elution buffers is important with peptides, to reduce adsorption and tailing effects on silica based stationary phase.[34, 35] Successful use of this TFA buffer on the CEC chip is significant, in that EOF can be reduced at low pH, but the results indicate sufficient pumping action is retained.
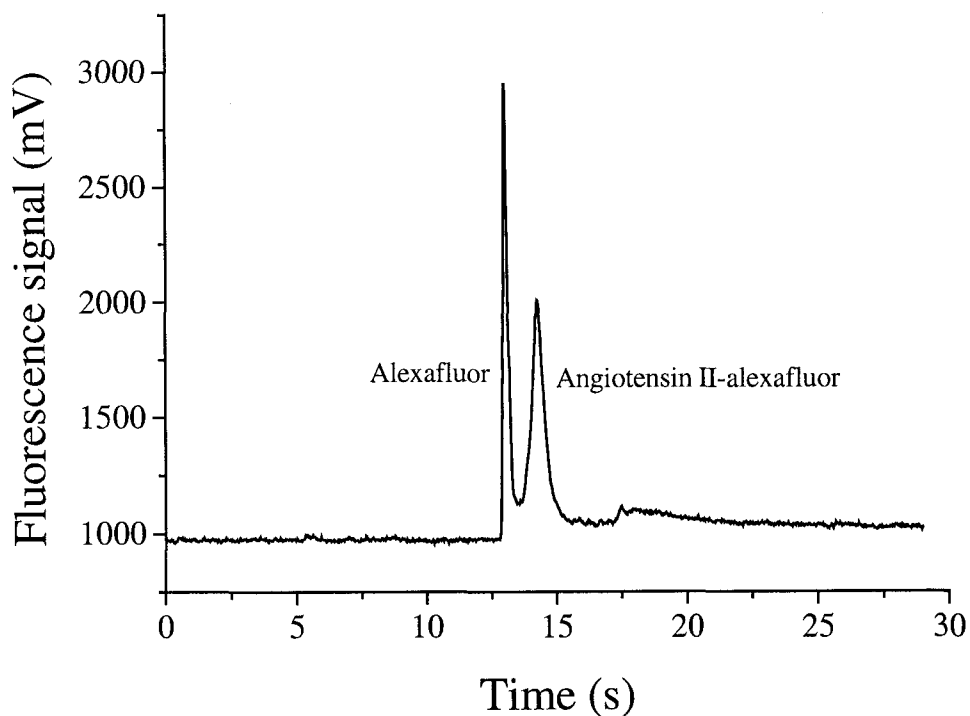
Figure 3.8.   Electrochromatograph showing the separation of angiotensin II-alexafluor from the excess labeling agent by CEC in the 200 µm long bed.   Separation was effected using a mobile phase composed of 0.05 % trifluoroacetic acid and 26 % acetonitrile in water.

3.4 Conclusions

The modified bed packing and bead trapping procedures outlined here extend the usefulness of the weir-based beds significantly, by extending the bed's lifetime for CEC, improving the plate numbers achieved, and increasing the range of bed geometries that may be packed. This report establishes that a sub-nanoliter volume packed bed can perform in a highly reproducible, quantitative and sensitive fashion within a planar

98

microfluidic device. Solid phase extraction within such beds gives a much higher preconcentration factor than has been demonstrated for open-tubular devices with coated channel walls, due to the much higher surface area of the beads. Monolithic polymer beds on-chip show a capacity per unit volume that is about ten times higher than our results, although this likely depends upon the beads used to pack a bed. Importantly, the preconcentration accomplished in the double weirs is in a volume which closely matches the injection volumes used in CE or CEC separations performed on-chip. As the complexity of on-chip processing increases through the integration of multiple sample treatment steps, it will become important that the fluid volumes within each step match those of subsequent steps. This fluid management issue represents a key hurdle for future multi-step integration, so that the ability to integrate a small packed bed for extraction or electrochromatography provides an important tool for addressing this challenge.

3.5 References

(1)   Manz, A.; Graber, N.; Widmer, H. M. *Sens. Actuators B* **1990**, *1*, 244-248.

(2)   Ramsey, J. M.; van der Berg, A., Eds. *Proc. μ-TAS 2001 Symposium*; Kluwer Academic Pub.: Monterey, U.S.A., 2001.

(3)   Kutter, J. P. *Trends Anal. Chem.* **2000**, *19*, 352-363.

(4)   Lichtenberg, J.; de Mello, A. J.; Verpoorte, E. *Talanta* **2002**, *56*, 233-266.

(5)   Jacobson, S. C.; Ramsey, J. M. *Electrophoresis* **1995**, *16*, 481-486.

(6)   Li, J.; Wang, C.; Kelly, J. F.; Harrison, D. J.; Thibault, P. *Electrophoresis* **2000**, *21*, 198-210.

(7)   Lichtenberg, J.; Verpoorte, E.; de Roij, N. F. *Electrophoresis* **2001**, *22*, 258-271.

(8)   Zhang, B.; Liu, H.; Karger, B. L.; Foret, F. *Anal. Chem.* **1999**, *71*, 3258-3264.

(9)   Kaniansky, D.; Masar, M.; Bielcikova, J.; Ivanyi, F.; Eisenbeiss, F.; Stanislawski, B.; Grass, B.; Neyer, A.; Johnck, M. *Anal. Chem.* **2000**, *72*, 3596-3604.

(10)   Prest, J. E.; Baldock, S. J.; Fielden, P. R.; Brown, B. J. T. *Analyst* **2001**, *126*, 433-437.

(11)   Font, G.; Manes, J.; Molto, J. C.; Pici, Y. *J. Chromatogr. A* **1993**, *642*, 135-161.

(12)   Berrueta, L. A.; Gallo, B.; Vicente, F. *Chromatographia* **1995**, *40*, 474-483.

(13)   Bonneil, E.; Waldron, K. C. *J. Chromatogr. B* **1999**, *736*, 273-287.

(14)   Poole, C. F.; Guantilleka, A. D.; Sethuraman, R. *J. Chromatogr. A* **2000**, *855*, 17-39.

(15)   Kutter, J. P.; Jacobson, S. C.; Ramsey, J. M. *J. Microcolumn Sep.* **2000**, *12*, 93-97.

(16)   Oleschuk, R. D.; Shultz-Lockyear, L. L.; Ning, Y.; Harrison, D. J. *Anal. Chem.* **2000**, *72*, 585-590.

(17)   Yu, C.; Davey, M. H.; Svec, F.; Frechet, J. M. J. *Anal.Chem.* **2001**, *72*, 5088-5096.

(18)   Wolfe, K. A.; Breadmore, M. C.; Ferrance, J. P.; Power, M. E.; Conroy, J. F.; Norris, P. M.; Landers, J. P. *Electrophoresis* **2002**, *23*, 727-733.

(19)   Lui, Y.-M.; Sweedler, J. V. *Anal. Chem.* **1996**, *68*, 3928-3933.

(20)   Fan, Z. H.; Harrison, D. J. *Anal. Chem.* **1994**, *66*, 177-184.

(21)   Chiem, N.; Shultz-Lockyear, L. L.; Andersson, P.; Skinner, C. D.; Harrison, D. J. *Sens. Actuators B* **2000**, *63*, 147-152.

(22)   Yan, C.: U.S. Patent, 1995; Vol. 453, pp 163.

(23)   Yan, C.; Dadoo, R.; Zhao, H.; Zare, R. N.; Rakestraw, D. J. *Anal. Chem.* **1995**, *67*, 2026-2029.

(24)   Peters, E. C.; Petro, M.; Svec, F.; Frechet, J. M. J. *Anal. Chem.* **1997**, *69*, 3646-3649.

(25)   Gabriela, S. C.; Remcho, V. T. *Anal. Chem.* **2000**, *72*, 3605-3610.

(26)   Fluri, K.; Fitzpatrick, G.; Chiem, N.; Harrison, D. J. *Anal. Chem.* **1996**, *68*, 4285-4290.

(27)   van den Bosch, S. E.; Heemstra, S.; Kraak, J. C.; Poppe, H. *J. Chromatogr. A* **1996**, *755*, 165-177.

(28)   Seifar, R. M.; Kraak, J. C.; Kok, W. T.; Poppe, H. *J. Chromatogr. A* **1998**, *808*, 71-77.

(29)   Pyell, U. *J. Chromatogr. A* **2000**, *892*, 257-278.

(30)   Shaw, D. J. *Introduction to Colloid and Surface Chemistry, 3rd ed.*; Butterworth: London, 1980.

(31)   Oleschuk, R. D.; Jemere, A. B.; Schultz-Lockyear, L. L.; Fajuyigbe, F.; Harrison, D. J. In *Micro Total Analysis 2000 Symposium*; van der Berg, A., Olthuis, W., Bergveld, P., Eds.; Kluwer Academic Publishers: Enschede, The Netherlands, 2000, pp 11-14.

(32)   Jemere, A. B.; Oleschuk, R. D.; Taylor, J.; Harrison, D. J., Monterey, U.S.A. 2001; Kluwer Academic Pub.; 510-502.

(33)   Chiem, N.; Harrison, D. J. *Anal. Chem.* **1997**, *69*, 373-378.

(34)   Wehr, C. T.; Correia, L.; Abbott, S. R. *J. Chromatogr. Sci.* **1982**, *20*, 114-119.

(35)   Strausbauch, M. A.; Landers, J. P.; Wettstein, P. J. *Anal. Chem.* **1996**, *68*, 306-314.

(36)   Jacobson, S. C.; Hergenroder, R.; Kounty, B. K.; Ramsey, J. M. *Anal. Chem.* **1994**, *66*, 2369-2373.

(37)   Kutter, J. P.; Jacobson, S. C.; Matsubara, N. *Anal. Chem.* **1998**, *70*, 3291-3297.

(38)   He, B.; Tait, N.; Reginer, F. *Anal. Chem.* **1998**, *70*, 3790-3797.

(39)   Ceriotti, L.; de Roij, N. F.; Verpoorte, E. *Anal. Chem.* **2002**, *74*, 639-647.

(40)   Knox, J. H.; Grant, I. H. *Chromatographia* **1991**, *32*, 317-328.

(41)   Smith, N. W.; Evans, M. C. *Chromatographia* **1994**, *38*, 649-657.

(42)   Dittmann, M. M.; Rozing, G. P. *LC-GC* **1995**, *13*, 800 - 808.

(43)   Dittmann, M. M.; Rozing, G. P. *J. Chromatogr. A* **1996**, *744*, 63-74.

(44)   Seifar, R. M.; Kok, W. T.; Kraak, J. C.; Poppe, H. *Chromatographia* **1997**, *46*, 131-136.

(45)   Dadoo, R.; Zare, R. N.; Yan, C.; Anex, D. S. *Anal. Chem.* **1998**, *70*, 4787-4792.

(46)   Chirica, G. S.; Remcho, V. T. *Anal. Chem.* **2000**, *72*, 3605-3610.

(47)   He, B.; Ji, J.; Reginer, F. *J. Chromatogr. A* **1999**, *853*, 257-262.

Chapter 4: Microchip-Based Capillary Electrochromatography using Packed Beds[*]

4.1 Introduction

Separation methods are a key element of many analytical methods, yet the first solution phase on-chip separations were performed using capillary electrophoresis, and variants of electrophoresis have remained the dominant methods studied to date.[1-9] It will be useful to extend the microfluidics toolbox to include a broader range of separation methods. Capillary electrochromatography (CEC),[10-15] a recently developed variant of high performance liquid chromatography (HPLC), is a prime candidate for integration on-chip, since solvent transport in CEC is achieved by electroosmotic flow (EOF) rather than by applied pressure. Previously, we reported the integration of 0.2 mm long columns (330 pL volume) packed with 1.5 μm diameter reversed phase sorbent for solid phase extraction and CEC on-chip.[16-18] These columns, however, lacked an injector and were very short for CEC separations. While the theoretical plates per meter were comparable to those obtained with open tubular CEC on-chip,[14] and with integrated columns packed using monolithic polymers,[19-22] the overall length of our packed beds needed to be increased to improve the separation capability.

This report presents a study of the effect of varying column length for octadecylsilane coated silica beads (ODS), an evaluation of injector performance, and a study of the effect of injector operating parameters. The separation efficiency was examined as a function of column length, injector operation parameters, solvent

---

103

composition and applied electric field. Procedures to pack the columns were developed and tested. In addition, an indirect fluorescence detection method, modified from the procedures developed by Takeuchi and Yeung[23] and by Ceriotti et al.[24] was evaluated using unlabeled amino acids and a neutral dye.

4.2 Materials and Methods

4.2.1 Reagents

Tris(hydroxymethyl)aminomethane (Tris), thiourea, acetonitrile (ACN) (HPLC grade), ethylene dimethacrylate (EDMA), 2,2'-azo-bis(isobutyronitrile) (AIBN), L-arginine and L-leucine were purchased from Sigma-Aldrich Chemical Co. (Milwaukee, WI). 2-(N-Morpholino)ethane sulphonic acid (MES) was from ICN Biomedical Inc. (Aurora, OH), and reagent grade 1-propanol and 1,4-butanediol were obtained from Caledon Laboratories Ltd. (Georgetown, ON) and Eastman Organic Chemicals (Rochester, NY). BODIPY 493/503 (4,4-difluro-1,3,5,7,8-penta methyl-4-bora-3a,4a-diaza-s-indacene) and rhodamine 123 were from Molecular Probes (Eugene, OR), and were prepared as a 0.1 mM stock solution in HPLC grade methanol (Fisher, Fair Lawn, NJ) and in ultra pure water, respectively, while acridine orange (AO) was obtained in a hydrochloride solution (EC No. 2006140, Fluka Chemie GmbH CH-9471 Buchs, Switzerland). All reagents were used as received. All buffers were prepared using ultrapure water prepared with a deionizing system (Millipore Canada, Mississauga, ON) from distilled water, and filtered through a nylon syringe filter (0.2 μm pore size, Nalgene, Rochester, NY) prior to use. Spherisorb ODS-1 particles (ODS beads) were kindly donated by P. Myers (Phase Separations, Flintshire, UK). The beads had a mean pore size of ~ 8 nm, and a particle

diameter ranging from 1.5 μm (high abundance) to 4.0 μm (low abundance), as determined by scanning electron microscopy.

4.2.2 Chip Fabrication and Column Preparation

Chromatographic columns with 1, 2 and 5 mm lengths were fabricated in a quartz plate (2 mm thick, Hoya Corporation, Tokyo, Japan) by Micralyne (Edmonton, Canada), using published procedures.[16, 25, 26] The column was formed between two 1 μm deep weirs, which act as the leading and trailing frits. Flow over the weirs through a 10 μm deep, 100 μm wide channel provided for sample delivery and elution, while a narrow bead introduction channel (10 μm deep, 30 μm wide) was used to deliver packing material,[16-18] as illustrated in Figure 4.1. Channel dimensions were measured using an optical microscopy. Access reservoirs are identified by numbers. After drilling 2 mm diameter access holes on a 2 mm thick quartz cover plate, the etched substrate was thermally bonded to it.[26]

A slurry of ~3 mg/ml of ODS beads in ACN was used to pack the columns. The channels were conditioned with ACN prior to use. The bead slurry was placed in reservoir 5 and a positive high voltage (~1 kV) was applied, with reservoir 1 grounded and negative pressure (house vacuum line) applied on reservoir 2. Effective packing required steadily ramping down the voltage on reservoir 5 to ~80 V as the column filled. Once the column and about 1 mm of the bead introduction channel were packed, reservoirs 1, 3, 4, and 5 were filled with water and the device was flushed for ~5 min. The packed column was monitored under a microscope to ensure that the ACN was replaced by water. The ODS beads visibly agglomerated, and the change in the index of

105

refraction at the water/ACN interface was obvious. Occasionally voids were seen towards the column entrance from the bead introduction channel. In those instances, high voltages (0.6 – 1 kV) were applied for a very short period (1 to 3 s) to increase column density.

In order to fix the packed beads in the column an entrapment polymer was formed *in situ* in the bead introduction channel.[18] The monomer solution was comprised of 200 μL of a mixture of EDMA and the free radical initiator AIBN (2 wt% AIBN per weight of EDMA) in 800 μL of a ternary solvent mixture consisting of 10 wt% H_2O, 40 wt% 1,4-butanediol, and 50 wt% 1-propanol,[27, 28] stored at 4 °C until use. The mixture was purged with N_2 for 15 min to remove dissolved O_2 before use. About 20 μL of the mixture was placed in reservoir 5 and drawn into the side channel using house vacuum, with advancement monitored using a microscope. The suction was stopped before the monomer solution reached the bed, and the chip was cured under UV light (Hg lamp) for about ~5 min. Figure 4.1b shows a photograph of a 1 mm long ODS packed bed, with a polymerized plug in the bead introduction channel seen as a darker region.

106
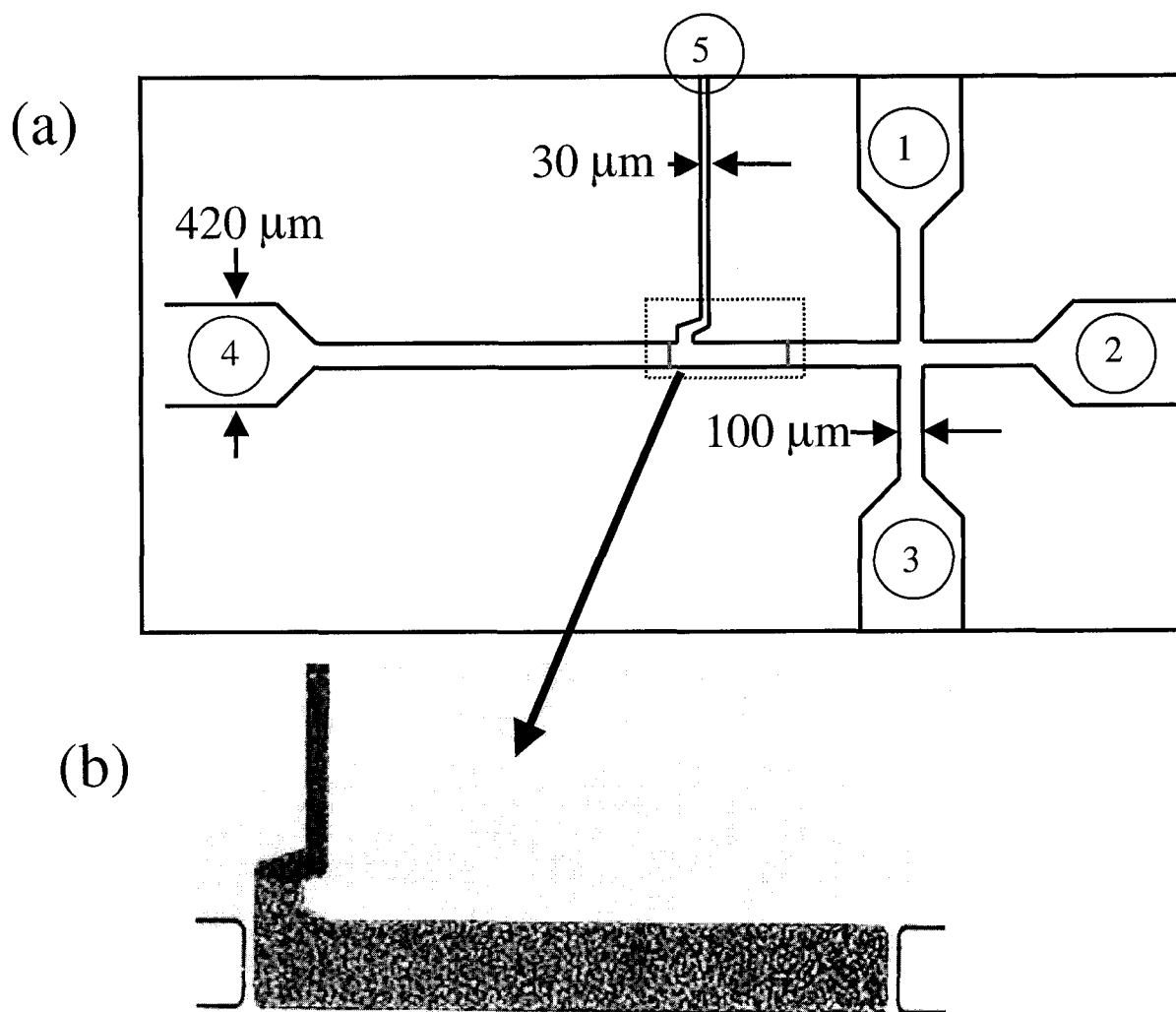
Figure 4.1   a) A schematic drawing of the CEC chip layout, showing
channel widths, and numbering scheme for reservoirs. Black
lines across separation channel indicate the 1-μm deep weirs;
other regions are all 10 μm deep. b) Photomicrograph of
column packed with 1.5 μm diameter ODS beads. The darker
region of the bead introduction channel, which leads to
reservoir 5, is the zone of methacrylate polymerization for
plug formation.

107

4.2.3 Instrumentation

The computer controlled power supply and relay arrangement has been described elsewhere.[29] In-house written LabVIEW programs (National Instruments, Austin, TX) were used for computer control of the voltages and for data acquisition. A previously described laser-induced confocal epifluorescence detection system was used,[30, 31] with the following specific parameters: a 488 nm Ar ion laser (Model 2214-105L, Uniphase, San Jose, CA) operated at 4 mW, a 505DRLP dichroic mirror (Omega, Brattleboro, VT), a 40x, 0.6 N.A. microscope objective (Planachromat LDN 1.2-A; Carl Zeiss Jena, Jena, Germany), an achromat tube lens, f = 200 mm, (Newport, PAC064, Irvine, CA), a 400 µm pinhole, a 530DF 30 (Omega) emission filter and a photo-multiplier tube (PMT) (R1477, Hamamatsu, Bridgewater, NJ). The detector was positioned either upstream or downstream of the column, with the weir just out of the field of view. The PMT was biased to 500 - 600 V, while the PMT signal was amplified (10^7 gain trans-impedance amplifier), filtered (active 25 Hz Butterworth filter, house built) and collected on a MacIntosh IIci using a National Instruments NB-MIO16 A/D board at a sampling frequency of 50 or 100 Hz. Peaks were analyzed using Igor Pro Software (WaveMetrics, Inc., Lake Oswego, OR).

4.2.4 Chip Operation

The CEC columns were conditioned with ACN, 25 mM Tris-HCl (pH 8.0) buffer mixtures (60 - 80% ACN) used as the mobile phase, prior to sample injection. Samples were prepared in the same buffer mixture. Sample injection was performed in a floating side channel configuration, by applying –1 kV across the sample (# 1) and sample waste

108

(# 3) reservoirs for 5 – 30 s, with the sample at ground. Separation was done with negative high voltage (0.5 – 5 kV) on waste reservoir 4 while buffer reservoir 2 was grounded. Reservoirs 1 and 3 were at relatively low negative voltages (~1/4 of the separation voltage) in order to prevent leakage of analyte from the cross channels during separation. Separations were performed at room temperature.

For indirect fluorescence detection, the ODS column was conditioned with ACN, 10 mM MES (pH 6.7) buffer mixtures (either 50 or 70% ACN by volume), followed by the mobile phase, consisting of the same buffer with 8 or 10 nM BODIPY as the probe. Samples were prepared in the same buffer mixtures from 1 mM (amino acids) or 13 mM (thiourea) aqueous stock solutions.

To evaluate column performance, the flow rate was first measured with the detector located at the upstream entrance to the column. The time required for sample to travel from the injector cross to the column head was then evaluated as a function of applied field, and the linear velocity was converted to volumetric flow rate using the channel cross section. While the electroosmotic flow rate (EOF) is known to differ between the packed column and the open channel,[32, 33] conservation of mass requires that the volumetric flow rates be equal in the two regions. In calculating the theoretical plate height, H, time spent off-column is not relevant. Because the bed lengths were so short, the time spent between the injector and the column head artificially increased the number of theoretical plates. We subtracted the time spent in this effective dead volume from the total elution time before calculating N and H.[18]

109

4.3 Results and Discussions

The chip layout illustrated in Figure 4.1, incorporating a cross injector for formation of a sample plug, and a 1 μm-deep double weir structure for trapping 1.5 μm diam. reversed phase octadecylsilane-coated silica (ODS) beads, was used to form a CEC column. The three arms of the cross injector were designed to have similar flow resistance, in order to create a symmetric injector for reduced leakage effects. The entrance weir for the bed was located 1 mm downstream of the injector and bed lengths of 1, 2 and 5 mm were designed in different layouts. A bead introduction channel[16] with a narrow cross section and a long path length provided a means to pack the bed. The bead introduction channel was designed to have a significantly higher resistance to flow[34] than the weirs and channels forming the separation flow manifold, in order to reduce flow into that channel when performing separations.

Electrokinetic packing of ODS columns 1 mm or longer proved to be difficult, in contrast to previous results for the packing of a 0.2 mm long bed.[16-18] In the initial stages of packing, the bed filled uniformly and rapidly. For a 1 mm long column solvent recirculation and backflow as a result of the back pressure developed at the head of the column caused the beads at the head to begin swirling about, preventing further packing. Similar results were seen with 2 and 5 mm columns, occurring after ~1 mm of the bed was packed. The backflow problem was eliminated by the application of suction at the separation buffer reservoir 2. Negative pressure alone also worked for packing, but was slower, and the bead introduction channel was more prone to plugging in this mode. The combination of electrokinetic and hydrodynamic flow was used by Stol et al.[35] to prepare robust, well-packed capillary columns. We found that packing the chip beds additionally

110

required the electrokinetic force be ramped to lower values as the packed bed length increased. The bead beds were permanently trapped by photo-initiated polymerization of a methacrylate monomer, within the bead introduction channel, as can be seen in the photograph in Figure 4.1b. The use of photo rather than thermal initiation gave much more rapid column preparation times.[18, 19] While almost all the 1 and 2 mm beds formed in this fashion were stable, only about 1/3 of the 5 mm long beds performed reliably. Visual inspection showed that voids would appear in the failed columns when running separations. These voids appeared after polymerization of the methacrylate plug, despite achieving a dense, uniform bed during packing and subsequent equilibration with water.

All our results were obtained using the design with the bead introduction channel located at the downstream weir. However, devices were fabricated with that channel positioned at either the upstream or downstream ends of the column, or at both ends. When using a device with two bead introduction channels at both ends of the column, we could not easily keep the beads trapped during packing. When using a device with an upstream bead introduction channel alone, the sample loading and injection procedures described were unreliable. This problem was anticipated, and is assumed to result from the large pressure head required to flow solvent through the packed bed, meaning that leakage out the bead introduction channel becomes significant when it is at the upstream end.

4.3.1   Column Efficiency

Figure 4.2 shows a typical electrochromatogram obtained for the separation of a test mixture of BODIPY, rhodamine 123, and acridine orange (AO) in the 1 mm ODS

111

column. Peaks were identified by comparing their retention times with those of standards run individually. Rhodamine 123 is a monocation, while BODIPY and AO are neutral at pH 8.0. In CZE, the electrophoretic mobility of rhodamine 123 will add with the EOF making it the first to elute from a CZE column. In this experiment, however, the cation eluted between the two neutral compounds, indicating that it was their differential interaction with the ODS phase that dominated the separation. With 500 V applied, plate numbers (N) of 330 (330, 000 plates/m; height equivalent to a theoretical plate, H = 3.0 μm) for BODIPY, 360 (360, 000 plates/m, H = 2.8 μm) for rhodamine 123, and 244 (244, 000 plates/m; H = 4.1 μm) for AO were obtained. The resolution (R) and plate numbers achieved are much higher than those we observed for the 0.2 mm long column (N = 23 for BODIPY and 84 for AO; R = 1.6 for the pair vs 7.3 with the 1 mm column).[18] However, that short column was operated under different injection and buffer conditions, so that a completely quantitative comparison is not possible.

Figure 4.2 shows separations performed on the three different column lengths using the same separation voltage. The data in Table 4.1 show that the resolution and number of plates increased as the column length increased. In CEC the column efficiency is a function of volumetric flow rate, just as in HPLC. To evaluate performance, the flow rate was first measured as a function of applied field upstream of the column, as described in Section 4.2.4. A plot of EOF velocity (mm/s) upstream of the column versus applied voltage (0.5 to 4 kV), yielded a linear response for all column lengths {slope = (2.00 ± 0.09) x 10^{-3} mm/Vs; intercept = 0.27 ± 0.21 mm/s; R^2 = 0.9967 for a typical 1 mm long column}. Figure 4.3 shows the similar trends observed in the van Deemter plots for all three column lengths, providing a quantitative comparison. For

112

the neutral dyes H increased with flow rate, indicating resistance to mass transfer contributes significantly to dispersion in the flow range studied. The cationic dye showed a slightly different trend, staying approximately constant with flow rate. This could be due to the mixed mechanism of separation for the cation; both electrophoresis and sorption interaction with the stationary phase plays role. For the 1 and 2 mm columns, the plate heights observed are similar to those reported for CEC in ODS packed capillaries using similarly sized particles (1.5 – 1.8 μm diam.).[12, 36-38] The 2 mm column gave ~1.8 times more plates than the 1 mm column, when operated at constant flow rate. Figure 4.3 illustrates that, at the same flow rate, the plate height was essentially the same for the neutral dyes in both the 1 and 2 mm columns. The 5 mm long column showed the highest plate numbers, but H increased significantly relative to the shorter columns. We believe this problem is due to voids, since these were often observed in the failed 5 mm long columns. Knox[39] has suggested that the non-linear increasing dependence of H on velocity can arise from velocity dependent dispersion due to uneven flow profiles outside the particles in CEC. He suggests better packing reduce this effect, consistent with our conclusion that the 5 mm columns are not as well packed.

Our current packing procedure utilized a limited range of pressure values (about 0.5 to 0.9 bar), and pressure was applied only during loading and equilibration, not during formation of the polymer plug in the bead introduction channel. Stol et al.[35] found it necessary to use up to 200 bar of packing pressure, and to maintain that pressure while forming the frits to trap the bed. Even more vigorous conditions have been used to pack CEC and capillary LC columns.[40] Consequently, higher packing pressures than used in this study may be required to routinely obtain efficient columns longer than 2 mm.

113
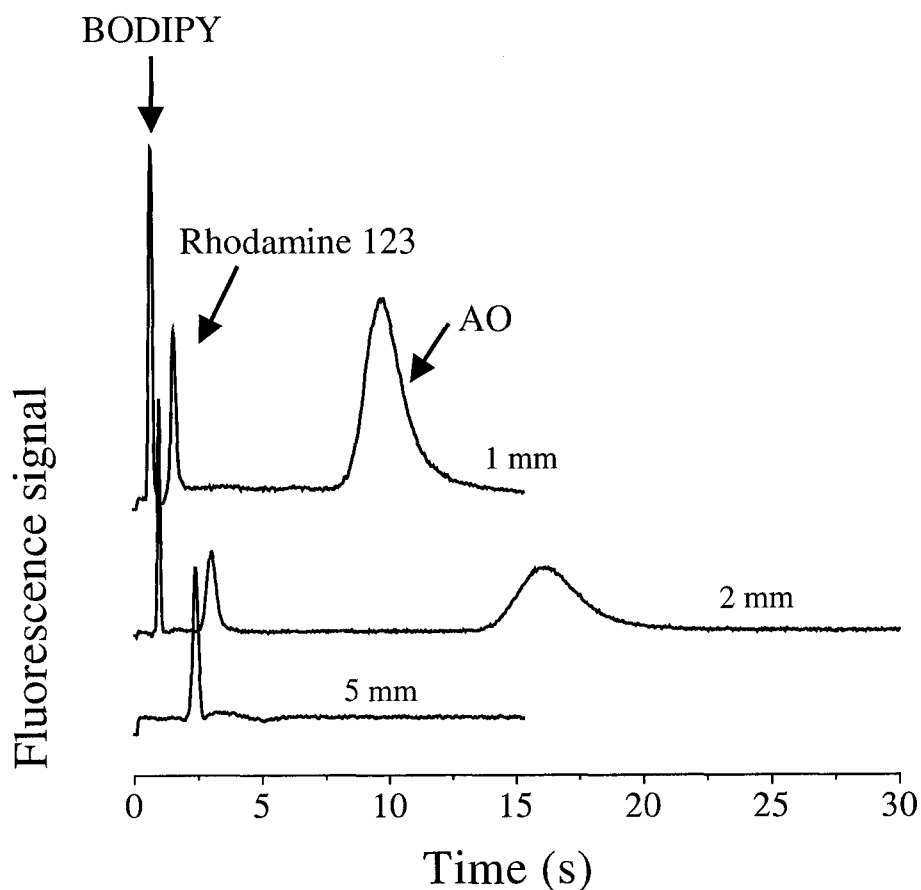
Figure 4.2   Electrochromatograms showing separations at 2 kV on three ODS column lengths, using fluorescence detection.   Injection was performed for 10 s, at −1 kV. The dyes eluted in the order BODIPY, rhodamine 123 and acridine orange.   Mobile phase was 80% acetonitrile and 20% 25 mM Tris-HCl, pH 8.0.   Column lengths are indicated.   Traces are slightly offset, fluorescence intensity scales differ for each trace. Conditions: 1 mm column, 600 V PMT bias, 10 nM BODIPY, 12 nM rhodamine 123, 8 nM AO; 2 mm column, 550 V bias PMT, 6 nM in each dye; 5 mm column, 550 V PMT bias, 6 nM BODIPY with no other dyes.

114

Table 4.1a.   Theoretical plate numbers obtained for the three ODS columns.   The mobile phase consisted of 70% ACN and 30% 25 mM Tris (pH 8.0).   Sample was injected for 10 s at 1 kV and 2 kV was applied during separation

Analyte	N (1 mm column)	N (2 mm column)	N (5 mm column)
BODIPY	185	330	425
Rhodamine 123	268	370	-
Acridine Orange	130	215	-

Table 4.1b   Peak resolution between two peaks as a function of column length measured at a flow rate of 4.2 nL/s. The mobile phase contained 70% ACN.

Column length, mm	Peak resolution between		
	BODIPY-Rhodamine 123	Rhodamine 123-AO	BODIPY-AO
1	3.9	4.5	5.1
2	4.8	5.3	6.4

Figure 4.3 van Deemter plot (H vs flow rate) for three ODS column lengths and three dyes: (square) BODIPY, (circle) rhodamine 123, (triangle) acridine orange (AO). Injection was performed for 10 s, at −1 kV. Mobile phase was 80% acetonitrile and 20% 25 mM Tris-HCl, pH 8.0. Only BODIPY was run in the 5 mm column.

116

4.3.2 Effect of Sample Loading

Sample loading and injection of the sample plug onto the column is a key factor in controlling separation efficiency. A large plug contributes too much to band broadening, while a small plug m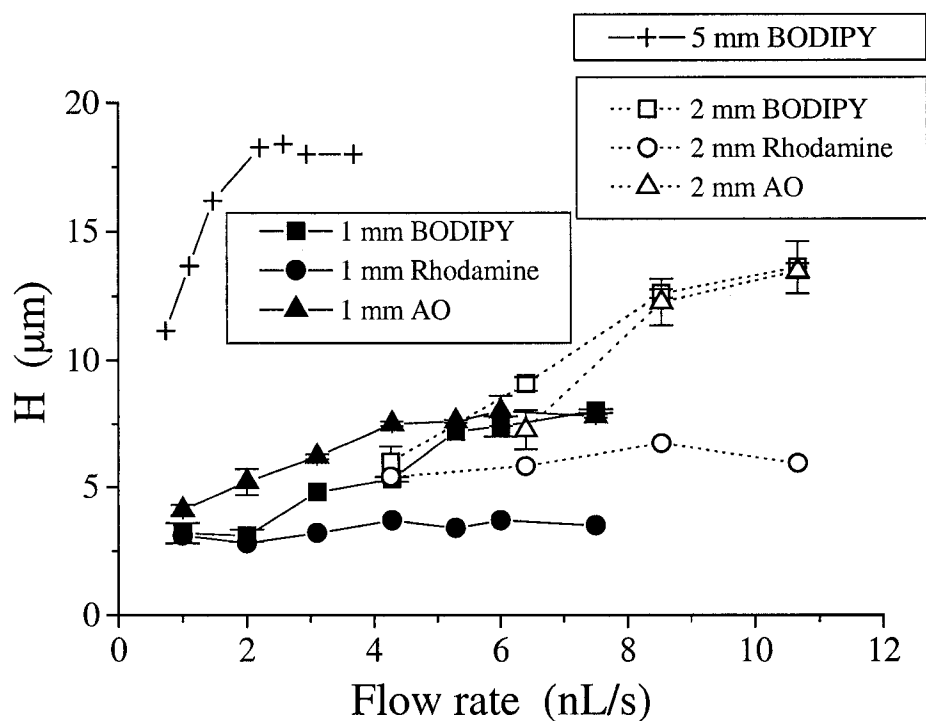ay not provide enough sample. The cross injector is known to show substantial leakage when the side channels are left floating, leading to much larger plugs than expected from the geometry of the intersection.[4, 25] By carefully controlling the time of injection this effect can be made reproducible and used to increase the amount injected. Alternatively, the voltage on all channels at the injector intersection can be controlled in order to shape the injected plug and minimize its size.[2, 4] A study of the width of the sample plug before reaching the CEC column head was performed, establishing that peak area increased with injection time. This is consistent with previous leakage studies of the cross injector in a purely electrophoretic device, which showed a nearly linear increase in peak area at short injection times, with a negative curvature after 30 to 60 s of injection.[4, 25] In contrast, a study of the full width at half maximum for the CEC peak downstream of the column showed no significant dependence on injection times between 5 and 30 s. Peak width varied by 3.8 % for BODIPY and by 1 % for the other two dyes as a function of injection time (n = 15 each). At any one injection time the variation in peak width was 5% for BODIPY, 1 % for Rhodamine 123, and 2 % for AO (n = 15 each), so any changes were within experimental error. At the same time, the peak height downstream of the column increased rectilinearly with injection time for all three dyes. For example, BODIPY gave a peak height which increased with a slope of 155 ± 6 mV/s, an intercept of 2100 ± 80 mV, and an R^2 value of 0.998 (n = 5). Peak area increased approximately linearly, with some negative curvature above 20 s injection time.

117

The above effects can only be explained by zone focusing due to solute enrichment at the head of the ODS column, since the sample is prepared in the running buffer to eliminate electrophoretic stacking effects. Our results are consistent with those reported by Pyell et al.[41] and by Chen et al.[41, 42] for CEC in packed capillary columns. Similar observations were made by Cergo et al.[43] for CEC with open tubular CEC columns. The consequence of these observations for the microchip device was that voltage controlled injections were not required to achieve high levels of performance and reproducibility, and that relatively high quantities of sample could be injected.

4.3.3   Column and Device Reproducibility

Reproducibility of column performance is critical for routine analytical use, and can also provide a diagnostic of the column's condition. A study performed with a 2 mm column gave peak height and area RSD values of 2.5 and 3.3%, respectively, as average values for the three dyes (n = 15). The resolution varied by 2.6% between the various dye combinations (n = 5). The RSD for the dye retention times was 1% (n = 6) over one day, and 3% (n = 30) over 5 days, indicating stable EOF in the absence of surface active sample components. Different 1 or 2 mm columns showed retention time variations of 3 or 4 % (n = 6), respectively, indicating reproducible column to column packing and behavior. While a column lifetime evaluation was not performed, many of the 1 and 2 mm columns were used for more than four weeks. Typical column failure involves clogging of the weir by particles from the sample or the buffer solution used. The packed columns themselves did not show any change in packing uniformity or a change in electroosmotic flow during their use.

118

4.3.4 Column Performance as a Function of Eluent Strength

Solvent composition is an important parameter in CEC, just as in HPLC.[44] We varied the composition between 60 - 80 % acetonitrile (ACN), the remainder being the aqueous buffer, while maintaining all other operating parameters constant except the ionic strength. Figure 4.4 shows several separation traces as a function of composition for a 2 mm long column. As the ACN content decreased from 80 - 60%, the separation times increased. This trend is consistent with a decrease in elution strength for hydrophobic solutes, along with a decrease in EOF associated with an increase in ionic strength and a decrease in the ratio of dielectric constant to viscosity of the mobile phase at lower percent ACN. The resolution between the three dyes improved as the ACN content decreased, due to greater differences in migration rates. In contrast, the efficiency decreased as the ACN content decreased, leading to a 20 – 25 % increase in H for BODIPY and rhodamine 123. The latter effect is consistent with the results of Seifar et al.[36] on a 1.8 μm diameter ODS capillary column, and is attributed to the increase in the contribution of the mass transfer term to plate height that results from an increase in capacity factor. Acridine orange shows the opposite behavior, decreasing H by a factor of 1.5 with decreasing ACN content, perhaps due to specific interactions with the stationary phase.
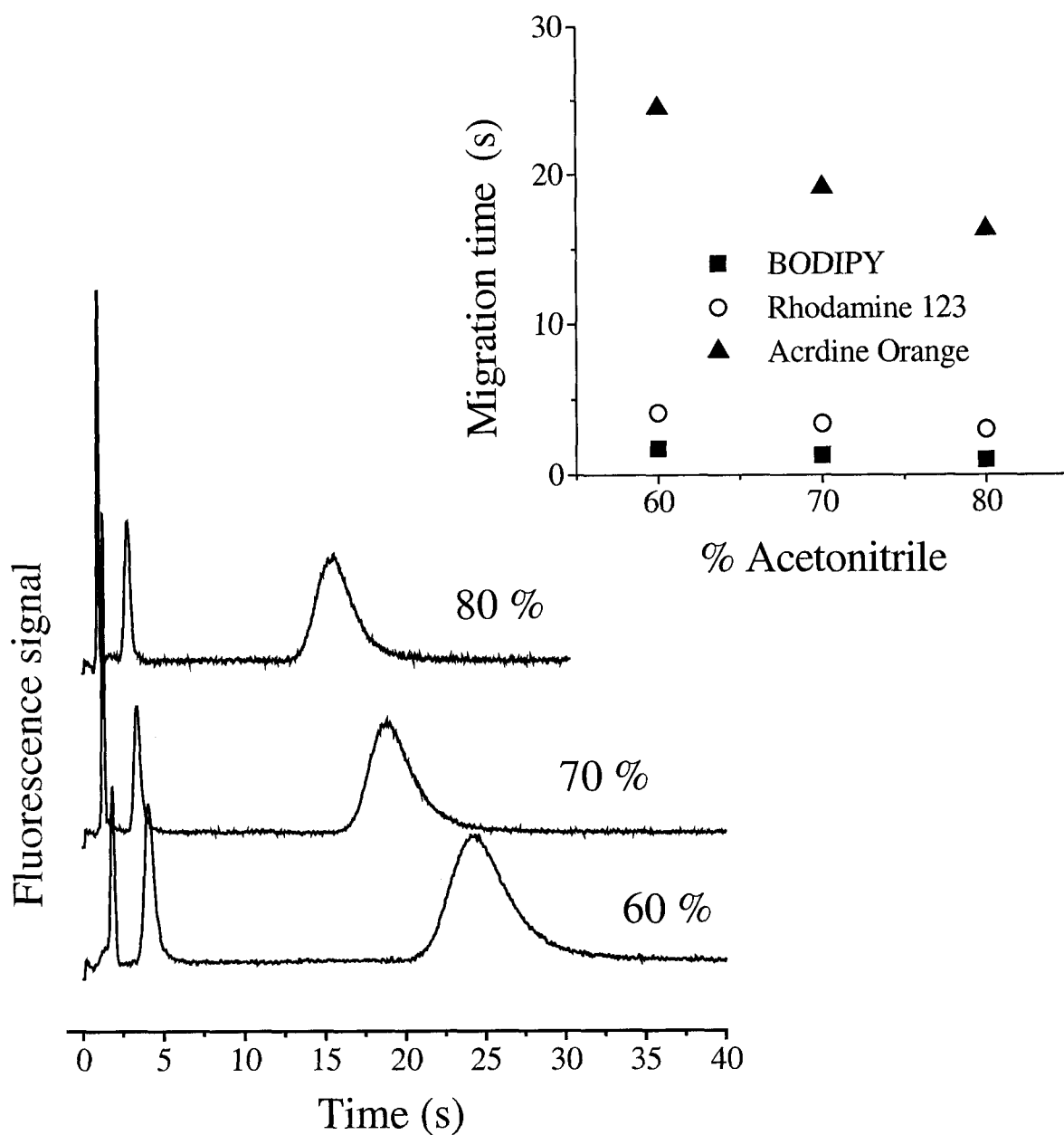
119

Figure 4.4   Electrochromatograms showing separations at 2 kV on a 2 mm long column, using three different mixtures of acetonitrile and 25 mM Tris-HCl, pH 8.0. Injection was performed for 5 s, at −1 kV for the two upper traces and 10 s for the lower trace. Error bars were all smaller than symbols shown in the inset. The dyes were 6 nM each. Traces are offset.

120

4.3.5 Indirect Laser Induced Fluorescence Detection

Detection in narrow bore channels presents significant challenges. Recently, indirect detection has been adapted to CEC[24, 45] as a means to extend the range of measurable analytes. A detectable probe is included in the mobile phase and distributed to the hydrophobic adsorbent used as stationary phase. Injected solutes affect the distribution of the detectable probe by binding or displacement in such a way that a detector response is obtained also for solutes that are devoid of inherent detectable properties. Previous CEC studies[24, 45] have used ionic dyes, similar to those used for indirect detection in capillary electrophoresis (CE)[46-50]. However, there is no need to use a charged dye when displacement occurs through competition for sites on the stationary phase. A neutral dye should avoid problems with peak fronting and tailing associated with a poor mismatch between the electrophoretic mobility of the analyte and the dye. The neutral dye BODIPY appeared to be a good candidate for use in indirect detection, because, while it is hydrophobic, it is relatively weakly retained, and shows good separation performance on ODS beads. A study of indirect detection was performed with this dye using a 1 mm column for the analysis of thiourea and of amino acids.

The inset in Figure 4.5 shows a typical electrochromatogram for thiourea in 70 % ACN, 30% 10 mM MES buffer, pH 6.7, with 10 nM BODIPY in the buffer. A negative displacement peak is seen. Thiourea has been commonly used as a neutral marker in CEC, however Ludtke et al.[51] have shown that thiourea is weakly retained by the ODS phase so it is a poor choice for a neutral marker. In this experiment, thiourea elutes close to the system peak since it is weakly retained by the ODS beads. By varying the flow rate using the separation voltage (0.5 to 2.5 kV), a van Deemter plot could be obtained, as

121

shown in Figure 4.5. The plot shows a minimum at 6 nL/s, indicating that longitudinal diffusion was significant at lower flow rates, in contrast to the results obtained with direct fluorescence detection. Separation efficiencies obtained for thiourea were similar to those observed for fluorescent dyes using direct detection. For example, the trace in Figure 4.5 gave a plate height of 3.6 μm (N = 278 plates or 278, 000 plates/m), which also compares favorably with 5 μm reported for on-chip CEC of thiourea using 3 μm ODS beads.[24]

Previously we have detected fluorescein labeled amino acids separated using a 0.2 mm long ODS bed.[18] However, an indirect detection method using a neutral dye would eliminate the demand for labeling, and for matching mobilities as required in CE, and make the analysis of amino acids on-chip more straightforward.[47, 48, 50] Figure 4.6 shows baseline resolution of native arginine and leucine on a 1 mm ODS column, using indirect fluorescence detection with 8 nM BODIPY present in 50% ACN, MES buffer, pH 6.7. Increasing the applied field strength increased the speed of analysis (13 s at 1 kV and 3 s at 4 kV), while still providing baseline resolution. A detection limit (S/N = 3) of 10 μM was obtained for the two amino acids. This value is 3 times lower than reported for indirect detection limits for on-chip CE of amino acids.[47] Despite the fact that the detection sensitivity was lower than that achievable by labeling the amino acids with fluorescein isothiocyanate, circumventing sample preparation and the difficulties inherent with tagging complex samples make this technique attractive for a variety of assays where sensitivity is not critical. The detection limit we report here is well within the range for many amino acid concentrations expected in biological fluids such as urine and serum.[52]
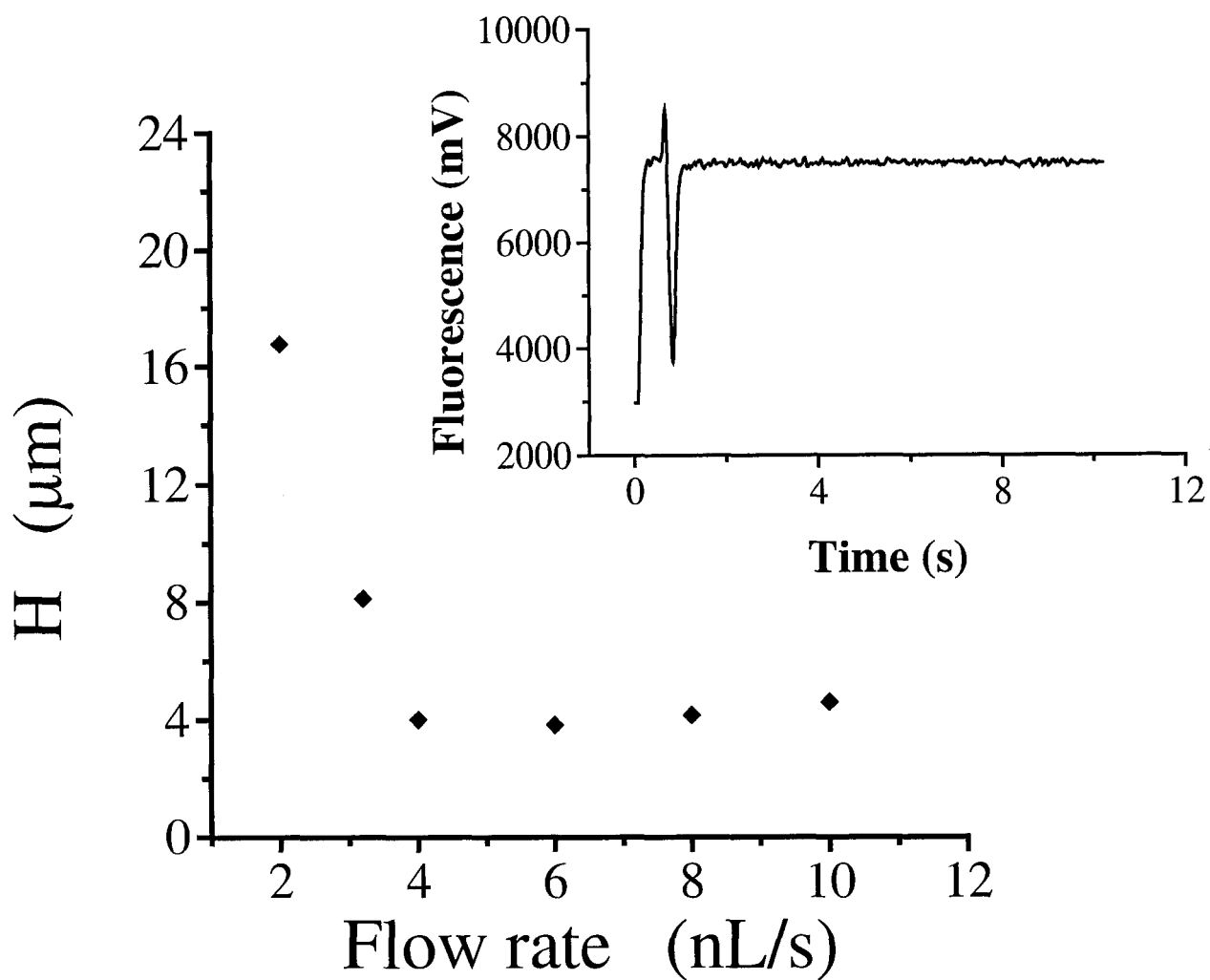
Figure 4.5   van Deemter plot obtained with a 1 mm ODS column for indirect detection of 13 mM thiourea in 70% ACN, 10 mM MES (pH 6.7) buffer, with 10 nM BODIPY present in both sample and running buffer.   Inset shows a typical electropherogram for thiourea, obtained at 1.5 kV.   Injections were performed for 10 s, at –1 kV.

123

(A)

0.8 kV

1 kV

2 kV

4 kV

Fluorescence

Time (s)

(B)

10000

8000

6000

4000

2000

0

Fluorescence (mV)

System peak

Arginine   Leucine

Time (s)
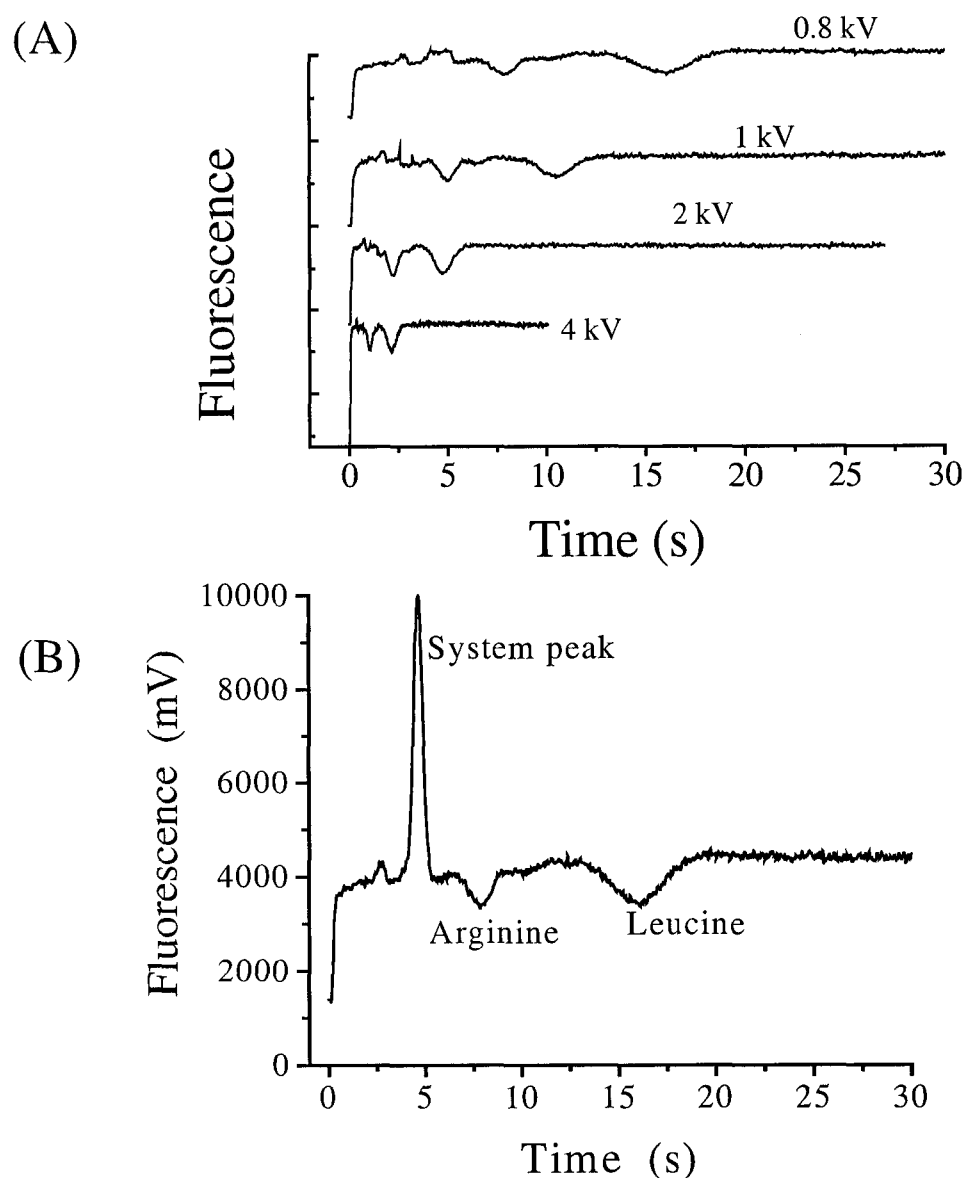
Figure 4.6   (A) Electrochromatograms showing indirect detection of unlabeled 90 μM arginine and 100 μM leucine in a 1 mm long ODS column, run at several separation voltages. Injection was performed for 10 s, at −1 kV. Mobile phase was a mixture of acetonitrile and MES, pH 6.7 (1:1, v/v) containing 8 nM BODIPY in both sample and running buffers. Traces are slightly offset and have been background subtracted. The lower trace (B) shows the raw data generated at 0.8 kV separation voltage.

124

4.4　Conclusions

Our results demonstrate that packed beds with 1 and 2 mm column lengths can be readily prepared within a microchip, and that their performance is directly comparable to conventional packed CEC columns, and to both open tubular and monolithic columns formed on chip. The cross injector works quite effectively for forming sample plugs for the column. In fact, the zone focusing effect which often occurs in CEC makes floating-side-channel injections quite effective within the chip, in contrast to the behavior of the cross injector when used in CZE chips. The 1 and 2 mm columns show good reproducibility from chip to chip, and over time, indicating they are robust. Columns with a 5 mm length proved more difficult to prepare routinely, and we suspect that longer columns could be even more difficult to pack with our current methods. Thus, the challenges associated with preparing longer columns on-chip appear to be the same as those associated with packing conventional CEC capillaries, so that similar, more vigorous packing methods will likely be needed to prepare longer packed columns on-chip. Nevertheless, for sample clean up or separation and analysis of simple mixtures, the current device should prove to be quite effective. Finally, the use of a neutral dye for indirect fluorescence detection in CEC should provide a convenient method for extending the range of analytes that can be determined on-chip, while avoiding many of the peak distortion effects associated with the use of charged dyes in a electrokinetically pumped system.

125

4.5   References

(1)   Harrison, D. J.; Manz, A.; Fan, Z. H.; Lüdi, H.; Widmer, H. M. *Anal. Chem.* **1992**, *64*, 1926-1932.

(2)   Harrison, D. J.; Fluri, K.; Seiler, K.; Fan, Z. H.; Effenhauser, C. S.; Manz, A. *Science* **1993**, *261*, 895-897.

(3)   Wooley, A.; Mathies, R. A. *Proc. Natl. Acad. Sci. U.S.A.* **1994**, *91*, 11348-11352.

(4)   Jacobson, S. C.; Hergenroder, R.; Kounty, B. L.; Warmack, R. J.; Ramsey, J. M. *Anal. Chem.* **1994**, *66*, 1107-1113.

(5)   Jacobson, S. C.; Ramsey, J. M. *Electrophoresis* **1995**, *16*, 481-486.

(6)   Kutter, J. P.; Jacobson, S. C.; Ramsey, J. M. *J. Microcolumn Sep.* **2000**, *12*, 93-97.

(7)   Chiem, N.; Harrison, D. J. *Anal. Chem.* **1997**, *69*, 373-378.

(8)   Effenhauser, C. S.; Bruin, G. J. M.; Paulus, A. *Electrophoresis* **1997**, *18*, 2203-2213.

(9)   Bruin, G. J. M. *Electrophoresis* **2000**, *21*, 3931-3951.

(10)   Jorgenson, J. W.; Luckas, K. D. *J. Chromatogr.* **1981**, *218*, 209-216.

(11)   Knox, J. H.; Grant, I. H. *Chromatographia* **1991**, *32*, 317-328.

(12)   Yammamoto, H.; Baumann, J.; Erni, F. *J. Chromatogr.* **1992**, *593*, 313-319.

(13)   Yan, C.; Dadoo, R.; Zhao, H.; Zare, R. N.; Rakestraw, D. J. *Anal. Chem.* **1995**, *67*, 2026-2029.

(14)   Jacobson, S. C.; Hergenroder, R.; Kounty, B. K.; Ramsey, J. M. *Anal. Chem.* **1994**, *66*, 2369-2373.

(15)   Colon, L. A.; Guo, Y.; Fermier, A. *Anal. Chem.* **1997**, *69*, 461A-467A.

(16)   Oleschuk, R. D.; Shultz-Lockyear, L. L.; Ning, Y.; Harrison, D. J. *Anal. Chem.* **2000**, *72*, 585-590.

(17)   Oleschuk, R. D.; Jemere, A. B.; Schultz-Lockyear, L. L.; Fajuyigbe, F.; Harrison, D. J., in: van der Berg, A., Olthuis, W., Bergveld, P. (Eds.), *Proc. μ-TAS Systems 2000*; Enschede, The Netherlands 2000; Kluwer Academic Publishers; p. 11-14.

(18)   Jemere, A. B.; Oleschuk, R. D.; Ouchen, F.; Fajuyigbe, F.; Harrison, D. J. *Electrophoresis* **2002**, *23*, 3537-3544.

(19)   Yu, C.; Svec, F.; Frechet, J. M. J. *Electrophoresis* **2000**, *21*, 120-127.

(20)   Ericson, C.; Holm, J.; Ericson, T.; Hjerten, S. *Anal. Chem.* **2000**, *72*, 81-87.

(21)   Fintschenko, Y.; Choi, W.-Y.; Ngola, S. M.; Shepodd, T. J. *Fresenius J. Anal. Chem.* **2001**, *371*, 174-181.

(22)   Throckmorton, D. J.; Shepodd, T. J.; Singh, A. K. *Anal. Chem.* **2002**, *74*, 784-789.

(23)   Takeuchi, T.; Yeung, E. S. *J. Chromatogr.* **1986**, *366*, 145-152.

(24)   Ceriotti, L.; de Roij, N. F.; Verpoorte, E. *Anal. Chem.* **2002**, *74*, 639-647.

(25)   Fan, Z. H.; Harrison, D. J. *Anal. Chem.* **1994**, *66*, 177-184.

(26)   Fluri, K.; Fitzpatrick, G.; Chiem, N.; Harrison, D. J. *Anal. Chem.* **1996**, *68*, 4285-4290.

(27)   Peters, E. C.; Petro, M.; Svec, F.; Frechet, J. M. J. *Anal. Chem.* **1997**, *69*, 3646-3649.

(28)   Gabriela, S. C.; Remcho, V. T. *Anal. Chem.* **2000**, *72*, 3605-3610.

(29)   Seiler, K.; Harrison, D. J.; Manz, A. *Anal. Chem.* **1993**, *65*, 1481-1488.

(30)   Ocvirk, G.; Tang, T.; Harrison, D. J. *Analyst* **1998**, *123*, 1429-1434.

(31)   Taylor, J.; Picelli, G.; Harrison, D. J. *Electrophoresis* **2001**, *22*, 3699-3708.

(32)   Cikalo, M. G.; Bartle, K. D.; Myers, P. *J. Chromatogr. A* **1999**, *836*, 25-34.

(33)   Chodhary, G.; Horvath, C. *J. Chromatogr. A* **1997**, *781*, 161-183.

(34)   Attiya, S.; Jemere, A. B.; Tang, T.; Fitzpatrick, G.; Seiler, K.; Chiem, N.; Harrison, D. J. *Electrophoresis* **2001**, *22*, 318-327.

(35)   Stol, R.; Mazereeuw, M.; Tjaden, U. R.; van der Greef, J. *J. Chromatogr. A* **2000**, *873*, 71-77.

(36)   Seifar, R. M.; Kraak, J. C.; Kok, W. T.; Poppe, H. *J. Chromatogr. A* **1998**, *808*, 71-77.

(37)   Dadoo, R.; Zare, R. N.; Yan, C.; Anex, D. S. *Anal. Chem.* **1998**, *70*, 4787-4792.

(38)   Xin, B.; Lee, M. L. *Electrophoresis* **1999**, *20*, 67-73.

(39)   Colon, L. A.; Maloney, T. D.; Fermier, A. M. *J. Chromatogr. A* **2000**, *887*, 43-53.

(40)   Pyell, U.; Rebscher, H.; Banholczer, A. *J. Chromatogr. A* **1997**, *779*, 155-163.

(41)   Chen, J. R.; Zare, R. N.; Peters, E. C.; Svec, F.; Frechet, J. M. J. *Anal. Chem.* **2001**, *73*, 1987-1992.

(42)   Crego, A. L.; Martinez, J.; Marina, M. L. *J. High Resol. Chromatogr.* **2000**, *23*, 373-378.

(43)   Bartle, K. D.; Myers, P. *J. Chromatogr. A* **2001**, *916*, 3-23.

(44)   Bailey, C. G.; Wallenborg, S. R. *Electrophoresis* **2000**, *21*, 3081-3087.

(45)   Melanson, J. E.; Boulet, C. A.; Lucy, C. A. *Anal. Chem.* **2001**, *73*, 1809-1813.

(46)   Munro, N. J.; Huanh, Z.; Finegold, D. N.; Landers, J. P. *Anal. Chem.* **2000**, *72*, 2765-2773.

(47)   Kuhr, W. G.; Yeung, E. S. *Anal. Chem.* **1988**, *60.*, 1832-1834.

(48)   Yeung, E. S. *Acc. Chem. Res.* **1989**, 22, 125-130.

(49)   Yeung, E. S.; Kuhr, W. G. *Anal. Chem.* **1991**, *63*, 275A-282A.

(50)   Sharpira, E.; Blitzer, M. G.; Miller, J. B.; Africk, D. K. In *Biochemical Genetics:*

A Laboratory Manual; Oxford University Press: New York, 1989, pp 96-97.

Chapter 5: Integrated Packed Column Size Exclusion Electrochromatography

5.1 Introduction

Capillary electrochromatography (CEC) is a recently developed variant of HPLC, which combines the advantages of HPLC (selectivity) and CE (efficiency). Compared to conventional pressure driven HPLC, CEC column efficiencies are higher due to the plug like mobile phase flow profile induced at the surface of the stationary phase by an applied electric field.[1-6] In addition, with CEC, smaller stationary phase particles can be used since there is no pressure limitation. Application of CEC for the separation of a variety of compounds including proteins,[7-9] peptides,[10-12] and pharmaceuticals[13] is documented in the literature. To date CEC, however, is predominantly performed in reversed-phase and ion exchange modes. Size-based separations of molecules have not been fully exploited in CEC, excluding capillary gel electrophoresis,[14, 15] which depends on sieving rather than a size exclusion mechanism. Typical HPLC separation of macromolecules (synthetic polymers and biopolymers) involves the use of size exclusion chromatography (SEC) in which analytes are separated according to their size or hydrodynamic volume in solution.[16] When a polydisperse material passes through a column of porous beads, the movement of small molecules is retarded in the pores, while larger molecules pass through the column unimpeded. Recently, electrically driven size exclusion chromatography (SEEC), using conventional capillaries packed with 5 µm particles, with pore sizes ranging from 100 Å up to 1000 Å, has been demonstrated for the separation of standard synthetic polymers with molecular weight between 310, 000 and 1000 Dalton.[17-20] These reports have exhibited 2-3 times higher plate numbers in SEEC, compared to

130

pressure-driven SEC for the same solutes. The high efficiency of SEEC is attributed to a homogeneous flow velocity distribution over the column cross-section and the possibility of generating and controlling an intraparticle flow much better than in SEC. Since polymers naturally have low diffusion coefficients, low mass transfer within the pores seriously limits the separation efficiency and speed in pressure-driven SEC, so that analysis times well over an hour are not uncommon.[16]

Integration of SEC on microchip would address the increasing desire for high speed and high-throughput SEC systems for both synthetic and biopolymers.[21] However, to the best of our knowledge there is no report on integrated SEC. In this chapter the feasibility of an on-chip based packed column SEEC for biological polymers, using a previously described microchip design[22] to retain packing materials, is described.

5.2   Materials and Methods

5.2.1 Reagents

Acetonitrile (ACN) (HPLC grade), ethylene dimethacrylate (EDMA), 2,2'-azo-bis(isobutyronitrile) (AIBN), fluorescein isothiocyanate labeled IgG (FITC-IgG, Mol. Wt. ~150 kDa) and FITC-insulin (Mol. Wt. ~6 kDa) were purchased from Sigma-Aldrich Chemical Co. (Milwaukee, WI). FITC-IgG was obtained in solution, which according to Sigma could be used in direct immunofluorescence assay up to 64 x dilution while the FITC-insulin was obtained as a lyophilized powder. FITC-IgG was diluted 50 x in the running buffer before use. A stock solution of 5.3 μM FITC-insulin was prepared in 20 mM NaH_2PO_4 pH 6.7 buffer. Sodium dihydrogen orthophosphate (monobasic) was from BDH Chemicals (Toronto, ON), and reagent grade 1-propanol and 1,4-butanediol were

131

obtained from Caledon Laboratories Ltd. (Georgetown, ON) and Eastman Organic Chemicals (Rochester, NY). All reagents were used as received. Buffers were prepared using ultrapure water prepared with a deionizing system (Millipore Canada, Mississauga, ON) from distilled water, and filtered through a nylon syringe filter (0.2 μm pore size, Nalgene, Rochester, NY) prior to use.

A guard column of Biosep-SEC 2000 beads (5 μm in diameter and 145 Å pore size) was obtained from Phenomenex (Torrance, CA). The SEC beads were removed from the guard column and kept in a 20 mM NaH_2PO_4, pH 6.7 buffer containing 10% methanol at 4 °C.

5.2.2   Chip Fabrication and Column Preparation

The chip layout, fabrication and operating protocols were described in Chapter 4. The column was formed between two 2 μm deep weirs, which act as the leading and trailing frits. Flow over the weirs through a 20 μm deep, 170 μm wide channel provided for sample delivery and elution, while a narrow bead introduction channel (20 μm deep, 50 μm wide) was used to deliver packing material. After drilling 2 mm diameter access holes on a 600 μm thick, Corning 0211 glass cover plate, the etched substrate was thermally bonded to it.[23]

The channels were conditioned with water prior to use. Slurry of SEC beads in 20 mM NaH_2PO_4 (pH 6.7) was fed into the column using a mixed electrokinetic and house-vacuum packing technique described in Chapter 4. At the beginning of the packing, 1.2 kV was applied between the beads reservoir and the sample or sample waste reservoir while a house-vacuum was applied in the buffer reservoir, as discussed in Chapter 4. The

132

applied voltage was ramped down to ~100 V as the column was packing. Once the column and about 1 mm of the bead introduction channel were packed, the bead introduction channel and the column were vacuum flushed with ACN for ~5 min. The packed column was monitored under a microscope to ensure that the buffer was replaced by ACN. The SEC beads, being hydrophilic, agglomerated. Occasionally voids were seen towards the column entrance from the bead introduction channel. In those instances, high voltages (0.6 − 1 kV) were applied for a very short period (1 to 3 s) to increase column density. The packed beads in the column were then entrapped using the polymer plug technique described in Chapters 3 and 4.

5.2.3 Instrumentation

The computer controlled power supply and relay arrangement has been described elsewhere. [24] In-house written LabVIEW programs (National Instruments, Austin, TX) were used for computer control of the voltages and for data acquisition. A previously described laser-induced confocal epifluorescence detection system was used, [25, 26] with the following specific parameters: a 488 nm Ar ion laser (Model 2214-105L, Uniphase, San Jose, CA) operated at 4 mW, a 505DRLP dichroic mirror (Omega, Brattleboro, VT), a 40x, 0.6 N.A. microscope objective (Planachromat LDN 1.2-A; Carl Zeiss Jena, Jena, Germany), an achromat tube lens, f = 200 mm, (Newport, PAC064, Irvine, CA), a 400 µm pinhole, a 530DF 30 (Omega) emission filter and a photo-multiplier tube (PMT) (R1477, Hamamatsu, Bridgewater, NJ). The detector was positioned either upstream or downstream of the column, with the weir just out of the field of view. The PMT was biased to 500 - 550 V, while the PMT signal was amplified (10^7 gain trans-impedance

133

amplifier), filtered (active 25 Hz Butterworth filter, house built) and collected on a MacIntosh IIci using a National Instruments NB-MIO16 A/D board at sampling frequency of 50 or 100 Hz. Peaks were analyzed using Igor Pro Software (WaveMetrics, Inc., Lake Oswego, OR).

5.2.4 Chip Operation

The SEEC column was conditioned for 30 min with the mobile phase prior to sample injection. The mobile phase was composed of 10 mM NaH_2PO_4 (pH 6.7, adjusted with 0.1 M NaOH) containing 0.25 mM (0.008 %) SDS, 0.01% Tween 20 and 10 or 50% ACN. Samples were prepared in the same buffer mixture. Sample injection was performed in a floating side channel configuration discussed in Chapter 4 by applying -0.6 kV across the sample and sample waste reservoirs for 3 – 20 s, with the sample at ground. Separation was done with negative high voltage (0.1 – 0.8 kV) on separation waste reservoir while the buffer reservoir was grounded. The sample and sample waste reservoirs were at relatively low negative voltages (~1/4 of the separation voltage) in order to prevent leakage of analyte from the cross channels during separation. Separations were performed at room temperature.

To evaluate the column performance, the flow rate was first measured with the detector located at the upstream entrance to the column. The time required for sample to travel from the injector cross to the column head was then evaluated as a function of applied field, and the linear velocity was converted to volumetric flow rate using the channel cross section (3000 μm^2). While the linear flow velocity is known to differ between the packed column and the open channel,[11, 27] conservation of mass requires that

134

the volumetric flow rates be equal in the two regions. In calculating the theoretical plate height, H, time spent off-column is not relevant. Because the column length was so short, the time spent between the injector and detector artificially increased the number of theoretical plates. We subtracted the time spent in this effective dead volume from the total elution time before calculating N and H. [28]

5.3   Results and Discussions

5.3.1   Selection of Mobile Phase

True SEC depends upon the accurate separation of molecules by size, with no or minimal interaction of sample with the packing surface. The BIOSEP 2000 stationary phase used in this study, originally designed for pressure-driven SEC, is coated with a hydrophilic agent to minimize protein-stationary phase interactions. According to the manufacturer of the product,[29, 30] the particles are fully covered with the coating, so that there are essentially no residual sites remaining from the silica. In order to undergo SEEC, however, the packing material is required to support electroosmotic flow (EOF). As discussed in Chapter 1 of this thesis, essential for the generation of EOF is the presence of charge on the capillary wall as well as the packing particles, and the presence of ions in the mobile phase. The open segments, before and after the packed column, can generate EOF at an appropriate pH; however, the packed SEC column will generate little or no EOF. This will cause undesired band broadening due to pressure imbalance that arise from the difference in EOF driving force between the open segments and the packed column.[31] Moreover, there will be no or minimum pore flow required to transport molecules through the pores in order for the proteins to be separated according to their

135

size. An attempt to separate FITC-insulin from FITC-IgG by SEEC using a 20 mM

NaH$_2$PO$_4$, pH 6.7 buffer containing 0.01% Tween 20 was not successful. The retention

times of the proteins were irreproducible and the mixture was barely separated. Thus, in

order to perform SEEC separation of a test mixture of these proteins, it was required to

induce charge on the stationary phase by dynamically modifying the beads with a

charged surfactant.

The use of sodium dodecylsulphate (SDS) and cetyltrimethylammonium bromide

(CTAB) in surfactant-mediated reversed-phase CEC[32-35] as well as SEEC[17] has been

reported. Using up to 5 mM (0.15 wt %) SDS in the mobile phase was found to stabilize

the current and the flow in both reversed-phase CEC[32-35] and SEEC.[17] It is well known

that SDS adsorbs well on reversed phase packing materials and dynamically modifies the

surface.[36, 37] Badal et al.[38] and others have reported that SDS, being negatively charged,

does not coat the negatively charged silica glass. However in the presence of a neutral

surfactant, Badal et al.[38] noted a change in the EOF velocity in a glass microchip channel

as a function of SDS concentration, suggesting that the neutral surfactant adsorbs on the

silica surface first so that SDS would adsorb with it. These results suggest SDS or other

anionic surfactants could be used to introduce charge to the SEEC column, and so create

EOF. In order to investigate this, 0.25 mM SDS was added to the mobile phase. Indeed

the stability of the current and the reproducibility of the system improved significantly,

and separation of the test mixture was possible. The neutral surfactant was still used,

since it is generally thought to reduce non-specific adsorption of proteins on most

surfaces.[39, 40] The use of such low concentration of SDS has dual advantages: most

proteins do not precipitate at low concentration of SDS,[41] and high concentrations of SDS

136

in the mobile phase alters the molecular weight range of proteins that can be separated by the stationary phase.[29, 30]

Figure 5.1 shows typical electrochromatograms obtained for the separation of a test mixture of FITC-IgG (pI 7.5)[42] and FITC-insulin (pI 5.4)[43] in the 2 mm SEEC column using two different proportions of ACN. Peaks were identified by comparing their retention times with those of standards run individually. The high molecular weight FITC-IgG eluted prior to FITC-insulin, as expected. Detection of the mixture at the head of the column (1 mm from the injector) showed only a single peak, leading us to conclude that separation by differential electrophoretic mobility alone is impossible with a 1 - 2 mm column length, although the proteins carried different charges at the pH we used. In Figure 5.1a, the compounds were base line resolved in less than 10 s with a theoretical plate number of 88 (44, 000 plates/m; height equivalent to a theoretical plate, H = 23 μm) for FITC-insulin. The study was performed with 200 V applied for separation (that gave a volumetric flow rate of 0.6 μL/min), using 10% ACN in the mobile phase. Increasing the proportion of ACN to 50% rendered a better performance with 278 plates (139, 000 plates/m; H = 7.2 μm) for FITC-insulin with 300 V applied (corresponding flow rate was 43.2 nL/min), Figure 5.1b. Under the run conditions used in this experiment, the migration times of the proteins varied by an average RSD of 1.8%, n = 20.

With the 50% ACN buffer composition, an additional signal, some impurity peak that did not show up with 10% ACN buffer system, was also recorded. Further increasing the composition of ACN in the mobile phase, however, was not successful since the proteins precipitated at higher proportions of ACN. However, an attempt was

137

made to separate the protein mixture using 100% ACN as the mobile phase with the sample being prepared in 50% ACN buffer system. This resulted in a slight increment in efficiency (71, 000 plates/m) compared to 10% ACN and a longer retention window, as seen in Figure 5.2. Protein precipitation, however, was evident in the column. Visual observation of the SEEC column, under a 488 nm laser, revealed the column fluorescing. As can be seen from relative peak intensities of the two proteins, the high molecular weight protein (FITC-IgG) precipitated to a greater extent than FITC-insulin.

The increase in efficiency on going from 10% to 50% ACN could suggest that hydrophobic interaction of the proteins with the packing material as well as the glass surface occurs at low % ACN. At the same time, increasing the ACN proportion from 10% to 50% decreased the flow rate by ~ 76%. The drastic decrease in flow velocity at 50% ACN could be attributed to the modification of the surface by SDS. It has been reported that the adsorption of SDS decreases when increasing the proportion of ACN.[36, 37] Thus, the number of negative charges on the surface of the beads decreases with increasing acetonitrile content of the buffer. As discussed in Chapter 1 of this thesis, this will result in lower electroosmotic flow. Therefore, the difference in N could also have been due to the flow velocity dependence of SEEC separation efficiency.[17] Results presented below show the effect of velocity can be quite significant.

Stol et al.[19] observed that the retention window in SEEC is strongly influenced by the ionic strength of the solvent used. They showed that 1 mM LiCl gave larger separation factors for synthetic polymers at high molecular weights (>100, 000 Da) than did 10 mM LiCl. At higher ionic strengths, the retention window decreases and eventually disappears. This effect was attributed to changes in the flow in the pores of the stationary

138

material. With increasing ionic strength of the mobile phase, the electrical double layer thickness decreases and therefore, the flow inside the pores increases.[44] When the pore-to-interstitial flow velocity becomes equal, no size separation can be observed anymore. Stol et al.'s[19] study, and the theoretical analysis by Venema et al.[45] suggest lower ionic strength is preferred for better separations. This suggests that the 5-9 mM hydrogen phosphate buffer (in 50% to 10% ACN) used in this study is on the high side for optimal resolution. However, it is well known in SEC separation of proteins that relatively high ionic strength is preferred to minimize protein adsorption. Consequently, the buffer concentration we selected for these initial studies represents a compromise ionic strength.

5.3.2 Effect of Sample Volume on Efficiency

Sample injection was accomplished via the floating side channel procedure described in the Experimental. As discussed in Chapter 4, the shorter the injected sample plug the less it contributes to band broadening. Figure 5.3 shows the effect of injection time (proportional to sample injection volume) on the efficiency of the column for FITC-insulin. Unlike what we noted for reversed-phase CEC in Chapter 4, the SEEC column efficiency deteriorated rapidly for injected amounts exceeding a certain volume. Consequently sample injection was made for 5 sec. In SEEC there is no retention of solute molecules by the column packing. As a result, there is no sharpening of the component peaks as they are applied to the column.
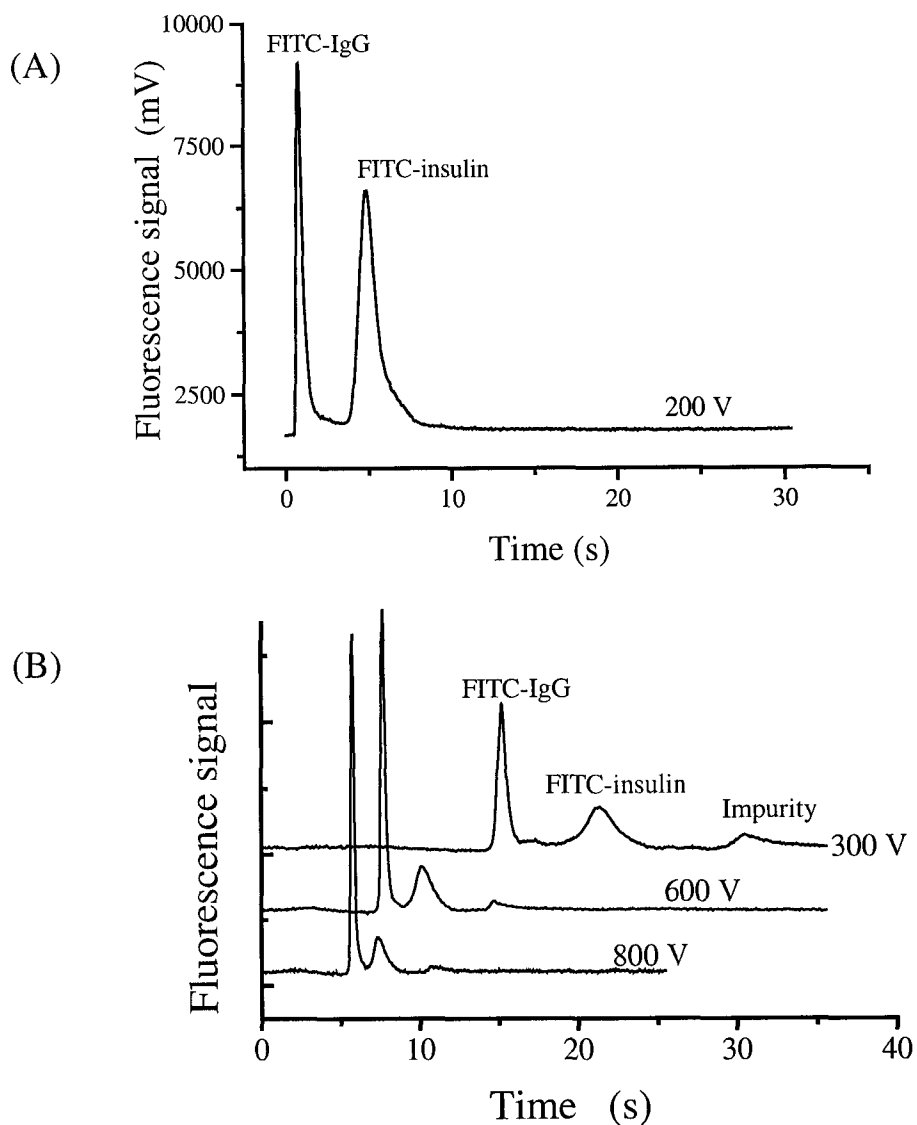
139

(A)

(B)

Figure 5.1   Electrochromatograms of FITC-insulin and FITC-IgG under different run conditions. Conditions: (A) 50 x diluted FITC-IgG and 8 nM FITC-insulin, mobile phase was 10% ACN in 10 mM NaH_2PO_4 buffer, pH 6.7 (with 0.25 mM SDS and 0.01% Tween 20. (B) 50 x diluted FITC-IgG and 6 nM FITC-insulin, mobile phase was 50% ACN, 10 mM NaH_2PO_4 buffer, pH 6.7 (with 0.25 mM SDS and 0.01% Tween 20). Injection was made for 5 s using –600 V applied. Separation voltages are indicated. Traces are slightly offset.
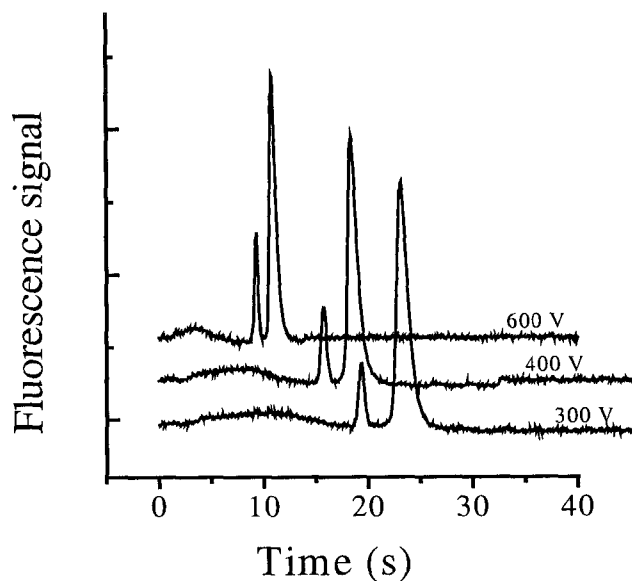
140

Figure 5.2 Electrochromatograms of 8 nM FITC-insulin and FITC-IgG. Conditions: Sample in 50% ACN/50% aqueous buffer, while pure ACN was used as the mobile phase. Sample was injected for 5 sec with –600 V applied. Separation voltages are indicated. Traces are slightly
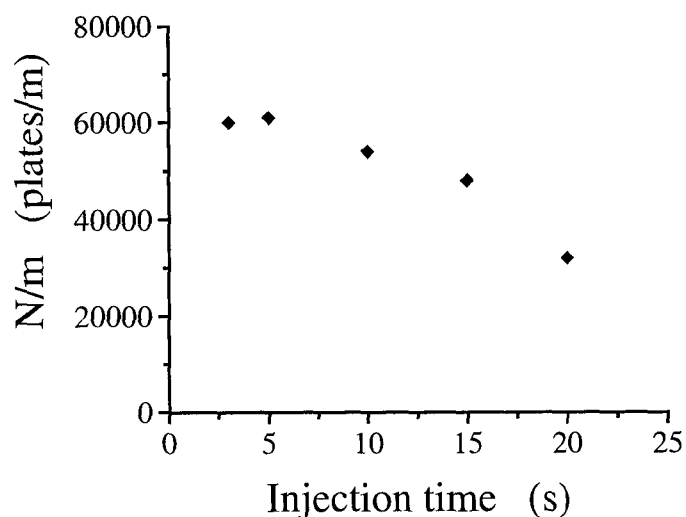

Figure 5.3 Plot of column efficiency vs injection time. Conditions: 6 nM FITC-insulin in 10% ACN, 10 mM NaH_2PO_4, pH 6.7 buffer (with 0.25 mM SDS and 0.01% Tween 20). Injection was made with –600 V applied between sample and sample waste reservoirs in a floating side configuration. Separation voltage was 100 V.

141

5.3.3 Role of Solvent Velocity on Efficiency

In SEEC, column efficiency is a function of volumetric flow rate, just as in HPLC, and this is controlled with the applied electric field magnitude. To evaluate performance, the flow rate was first measured as a function of applied field upstream of the column, as described in the Section 5.1.4. A plot of flow velocity (mm/s) upstream of the column versus applied voltage (0.3 to 0.8 kV), yielded a linear response with a slope of $(3.1 \pm 0.07) \times 10^{-3}$ mm/Vs and an intercept of 0.05 ± 0.03 mm/s; $R^2 = 0.9994$ with 50 % ACN in the mobile phase. Figure 5.4a is the van Deemter plot of this column for FITC-insulin. H remained essentially the same as the flow rate was increased, indicating that no significant resistance to mass transfer contribution to band broadening. However, a similar study with 10% ACN showed that H increased almost linearly with the flow rate (Figure 5.4b), suggesting resistance to mass transfer contributes significantly to dispersion at the flow rates studied. The best separation performance in 10% ACN was obtained at 100 V and gave 120 plates (60,000 plates/m; H = 16.7 µm) for FITC-insulin.

The significant difference in the efficiency of the SEEC column between 10% and 50% ACN buffers has several possible origins: (a) the low ionic strength and lower solvent polarity increase the double layer thickness relative to 10% ACN, causing a greater difference between velocity in the pores versus in solution, giving more efficient separation; (b) the much higher velocity in 10% ACN may mean that resistance to mass transfer in the stagnant mobile phase becomes much more pronounced, consistent with the observation that SEEC efficiency can depend strongly on flow velocity.[17] This point is supported by the linearly rising van Deemter plot, see Figure 5.4b; (c) effects due to

difference in solvent composition that change protein/surface interaction or swelling of

the particles and pores may also play a role.
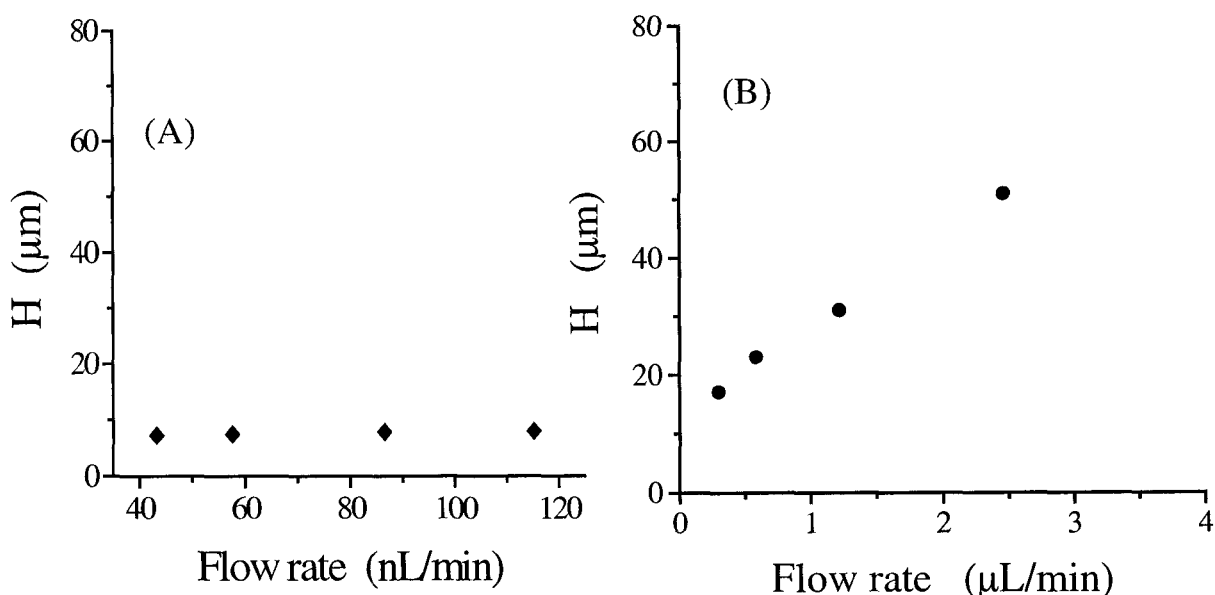
Figures 5.4.   van Deemter plot of plate height vs flow rate for 6 nM (A) and 8

nM (B) FITC-insulin using a mobile phase composed of 10 mM

NaH_2PO_4 pH 6.7 buffer, 0.25 mM SDS, 0.01% Tween 20 plus (A)

50% ACN and (B) 10% ACN. Sample was injected for 5 sec with

–600 V applied. Separation voltage ranged from 0.1 kV to 0.8 kV.

5.4 Conclusions

The present study demonstrates the feasibility of integrating packed column SEEC on

microchips for biopolymers. Rapid separation of proteins has been demonstrated.

Although the absolute plate numbers are not high, the plates/m are comparable with

capillary based SEEC and with conventional SEC. This study shows that SEEC on-chip

can be performed using packed beds, and further extends the range of on-chip separation

methods.

143

5.5 References

(1)   Pretorius, V.; Hopkins, B. J.; Schieke, J. D. *J. Chromatogr.* **1974**, *99*, 23-30.

(2)   Jorgenson, J. W.; Luckas, K. D. *J. Chromatogr.* **1981**, *218*, 209-216.

(3)   Seifar, R. M.; Kraak, J. C.; Kok, W. T.; Poppe, H. *J. Chromatogr. A* **1998**, *808*, 71-77.

(4)   Colon, L. A.; Maloney, T. D.; Fermier, A. M. *J. Chromatogr. A* **2000**, *887*, 43-53.

(5)   Colon, L. A.; Guo, Y.; Fermier, A. *Anal. Chem.* **1997**, *69*, 461A-467A.

(6)   Bartle, K. D.; Myers, P., Eds. *Capillary Electrochromatography*; RSC, 2001.

(7)   Pesek, J. J.; Matyska, M. T.; Mauskar, L. *J. Chromatogr. A* **1997**, *763*, 307-314.

(8)   Ericson, C.; Hjerten, S. *Anal. Chem.* **1999**, *71*, 1621-1627.

(9)   Zhang, B.; Huang, X.; Zhang, S.; Horvath, C. *Anal. Chem.* **2000**, *72*, 3022-3029.

(10) Palm, A.; Novotny, M. V. *Anal. Chem.* **1997**, *69*, 4499-4507.

(11) Chodhary, G.; Horvath, C. *J. Chromatogr. A* **1997**, *781*, 161-183.

(12) Walhagen, K.; Unger, K. K.; Hearn, M. T. W. *J. Chromatogr. A* **2000**, *887*, 165-185.

(13) Vanhoenacker, G.; Van den Bosch, T.; Rozing, G.; Sandra, P. *Electrophoresis* **2001**, *22*, 4064-4103.

(14) Fujimoto, C. *Anal. Chem.* **1995**, *67*, 2050-2053.

(15) Fujimoto, C.; Kino, J.; Sawada, H. *J. Chromatogr. A* **1995**, *716*, 107-113.

(16) Wu, C.-S., Ed. *Handbook of Size Exclusion Chromatography, Chromatographic Science Series*; Marcel Dekker, Inc.: New York, 1995.

(17) Venema, E.; Kraak, J. C.; Tijssen, R.; Poppe, H. *Chromatographia* **1998**, *48*, 347-354.

(18) Peters, E. C.; Petro, M.; Svec, F.; Frechet, J. M. J. *Anal. Chem.* **1998**, *70*, 2296-2302.

(19) Stol, R.; Poppe, H.; Kok, W. T. *J. Chromatogr. A* **2000**, *887*, 199-208.

(20) Ding, F.; Stol, R.; Kok, W. T.; Poppe, H. *J. Chromatogr. A* **2001**, *924*, 239-249.

(21) DeFrancesco, L.; Harris, C. M. *Anal. Chem.* **2002**, *74*, 275A - 278A.

(22) Jemere, A. B.; Oleschuk, R. D.; Harrison, D. J. *Anal. Chem.* **2002**, *Submitted.*

(23) Chiem, N.; Shultz-Lockyear, L. L.; Andersson, P.; Skinner, C. D.; Harrison, D. J. *Sens. Actuators B* **2000**, *63*, 147-152.

(24) Seiler, K.; Harrison, D. J.; Manz, A. *Anal. Chem.* **1993**, *65*, 1481-1488.

(25) Ocvirk, G.; Tang, T.; Harrison, D. J. *Analyst* **1998**, *123*, 1429-1434.

(26) Taylor, J.; Picelli, G.; Harrison, D. J. *Electrophoresis* **2001**, *22*, 3699-3708.

(27) Cikalo, M. G.; Bartle, K. D.; Myers, P. *J. Chromatogr. A* **1999**, *836*, 25-34.

(28) Jemere, A. B.; Oleschuk, R. D.; Ouchen, F.; Fajuyigbe, F.; Harrison, D. J. *Electrophoresis* **2002**, *23*, 3537-3540.

(29) Ahmed, F.; Modrek, B. *J. Chromatogr.* **1992**, *599*, 25-33.

(30) http://www.phenomenex.com/.

(31) Rathore, A. S.; Horvath, C. *Anal. Chem.* **1998**, *70*, 3069-3077.

(32) Seifar, R. M.; Kok, W. T.; Kraak, J. C.; Poppe, H. *Chromatographia* **1997**, *46*, 131-136.

(33) Ye, M.; Zou, H.; Liu, Z.; Ni, J.; Zhang, Y. *Anal. Chem.* **2000**, *72*, 616-621.

(34) Tegeler, T.; El Rassi, Z. *Electrophoresis* **2002**, *23*, 1217-1223.

(35) Hilmi, A.; Luong, J. H. T. *Electrophoresis* **2000**, *21*, 1395-1404.

(36) Knox, J. H.; Laird, G. R. *J. Chromatogr.* **1976**, *122*, 17-34.

145

(37) Kraak, J. C.; Jonker, K. M.; Huber, J. F. K. *J. Chromatogr.* **1977**, *142*, 671-688.

(38) Badal, Y. M.; Wong, M.; Chiem, N.; Salimi-Moosavi, H.; Harrison, D. J. *J. Chromatogr. A* **2002**, *947*, 277-286.

(39) Chiem, N.; Harrison, D. J. *Anal. Chem.* **1997**, *69*, 373-378.

(40) Chiem, N.; Harrison, D. J. *Clin. Chem.* **1998**, *44*, 591-598.

(41) Tanford, C. *The Hydrophilic Effect: Formation of Micelles and Biological Membranes*; Wiley: New York, 1980.

(42) Righetti, P. G.; Tudor, G.; Ek, K. *J. Chromatogr.* **1981**, *220*, 115-194.

(43) Voet, D.; Voet, J. G. *Biochemistry*, 2nd ed.; John Wiley & Sons, Inc.: New York,, 1995, pp. 77.

(44) Jacobson, S. C.; Alarie, J. P.; Ramsey, M. J., in van der Berg, A., Ramsey, M. J. (Eds.) *Proc. of μ-TAS 2001 Symposium*, Monterey, CA, USA 2001; Kluwer Academic Pub.; pp. 57-59.

(45) Venema, E.; Kraak, J. C.; Poppe, H.; Tijssen, R. *J. chromatogr. A* **1999**, *837*, 3-15.

Chapter 6: Summary and Suggestions for Future Work

6.1   Conclusions from the Thesis Work

As stated in Chapter 1, one of the goals of this work is to demonstrate packed column electro-driven separations on-chip. The objective was achieved and the details have been presented in Chapters 3-5. The other goal of this work was the development of a portable, integrated, automated, immunoassay system, which has been presented in Chapter 2. The purpose of this chapter is to summarize some of the main conclusions gained from this thesis work and to suggest future directions of research projects based on results obtained in this thesis work. The conclusions drawn will be presented in the order of the chapters.

In Chapter 2, we described a microchip-based CE instrument, the DARPA box (Figure 2.2), for biochemical analysis. In this project we undertook to produce, test and characterize an automated and portable microchip platform, plus peripheral subsystems that would perform a complete immunoassay. The overall size of the instrument was 30 x 35 x 50 cm. The system enabled performance of the key elements in analytical processing: sampling, injection, mixing, detection and elimination within 3-5 minutes. The unit has a detection limit of 69 pM which is lower than that we achieved using the Beckman CE machine (0.1 nM) for the same fluorescent indicator, Cy5 dye. A linear calibration curve for the direct assay of ovalbumin with Cy5-labeled anti-ovalbumin was obtained with very good day-to-day (~3% RSD for migration time) and chip-to-chip (~2% RSD for migration time) reproducibility. The work presented in this chapter shows

147

that integrated devices hold great promise as a simple, compact and automated immunoassay systems suitable for point-of-care testing and environmental monitoring.

In Chapters 3-5, we described the development of integrated packed column capillary electrochromatography. Columns of various lengths were packed with stationary phases to perform SPE, CEC and SEEC. Various methods of securing the packed columns were tested. The use of a polymer plug to fix the bed gave columns that could be used with the greatest range of conditions, and the best performance. In SPE, we have preconcentrated amino acids, peptides and neutral fluorophores with a very low detection limit (70 fM BODIPY). CEC columns for reversed phase chromatography were developed that showed up to 360 plates. This corresponds to 360, 000 plates/m, which is comparable to most CEC methods. The packing technique described in this thesis works well for up to 2 mm long columns. Comparison of the 1 and 2 mm columns using neutral analytes under a similar flow rate condition showed the plate numbers increased by close to two for the 2 mm column, as would be expected for a two-fold length increase. A 5 mm ODS column did not perform ideally, although it showed an increased plate number compared to the 2 mm column. The packed beds were also extended to show that size exclusion could be performed on chip using electrokinetic pumping. The integration of a variety of techniques based on packed beds that are complementary to CE will expand the ability of microfluidics to analyze compounds and perform assays that were previously beyond the scope of microchip-based devices.

148

6.2　Future Suggestions

A few suggestions towards exploring further the packed column electrochromatography study presented in this thesis will be put forward.

6.2.1　Improvement for Integrated Packed Column Electrochromatography

The lessons learned in Chapter 3 were applied to fabricate longer chromatographic columns, as discussed in Chapter 4. In the latter chapter and in Chapter 5, we described the development of packed column reversed phase and size exclusion electrochromatographic techniques using 1 - 5 mm long columns. Analyzing complex sample mixtures using on-chip CEC may require still longer columns, and as noted, the 5 mm column did not behave ideally. From chromatographic theory we know that the number of theoretical plates increases linearly with increasing separation length, if the operating parameters remain unchanged. As shown in Chapter 4, the packing strategy described in this thesis, namely the combination of electrokinetic and house-vacuum packing, works well for up to 2 mm long columns. However, packing 5 mm long columns was a challenge. Thus further research is needed to develop alternative packing techniques to pack ≥ 5 mm long columns. One possibility is to adapt the high-pressure packing techniques used in packing conventional capillary columns for CEC.[1-5] The second alternative is to use columns in series and use the packing technique described in this thesis. Figure 6.1 shows a three-column system. The columns could be fabricated as described in Chapters 3 and 4, with each column ~ 4 mm long. First, column 3 could be packed by applying vacuum at reservoir E, with the bead slurry in reservoir F and voltage applied between reservoirs F and A. Then column 2 could be packed by applying

149

vacuum at reservoir D, with a bead slurry at reservoir E and a voltage applied between reservoirs E and A. Finally, column 1 would be packed following a similar approach, by having a bead slurry in reservoir D and vacuum at reservoir A, with voltage applied from reservoir D to reservoir B or C. A similar process could be done for continuous column packing. The packed columns could then be secured using the polymer plug technique described in Chapters 3 and 4. Sample injection and electrochromatographic separation could then be executed like the one column system discussed in Chapters 4 and 5. This design would solve the problem of packing long columns (≥ 5 mm) using the method described in this thesis and a wide variety of bead-based electrically driven separation techniques, such as affinity chromatography, strong anion and strong cation exchange chromatography, normal phase chromatography, etc, could be integrated on the chip design shown in Figure 6.1.

6.2.2 Gradient Elution in Integrated Packed Column Electrochromatography

In order to exploit the full potential of the integrated CEC system for successfully separating a wide variety of complex samples, it will be necessary to develop the capability of gradient elution, as in HPLC.[6] Unlike in isocratic elution, during a gradient chromatographic run the proportion of the stronger eluent is increased gradually and in a controlled manner. Qiu and Harrison,[7] and Kutter et al[8] have demonstrated controlled electrokinetic solvent mixing for integrated systems. Figure 6.2 shows a chip design that could be used to perform gradient CEC on microchips. The column or columns in tandem could be packed with reversed phase particles using the packing protocol

150

developed in this work. Gradient elution of sample components could be performed by gradually increasing the voltage applied on the acetonitrile reservoir, say reservoir 1, while the voltage in reservoir 2 (the aqueous buffer reservoir) is maintained constant.
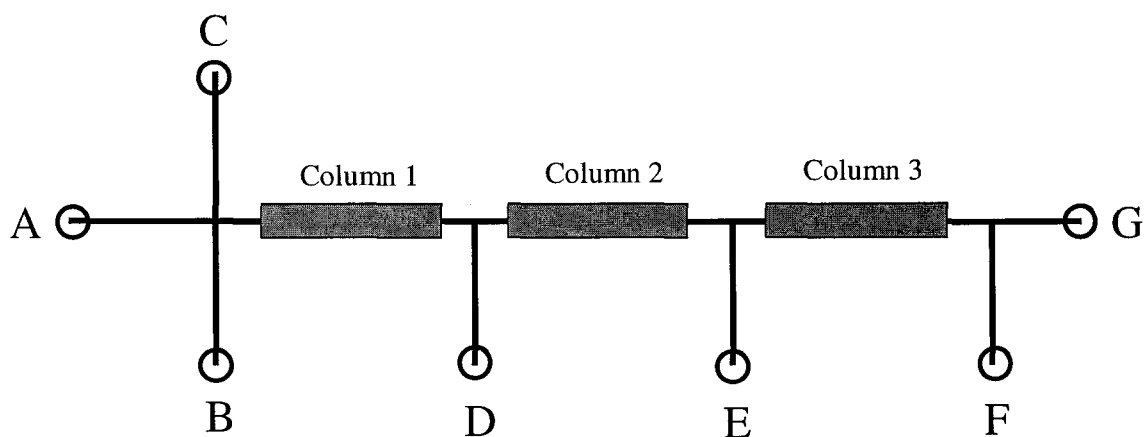

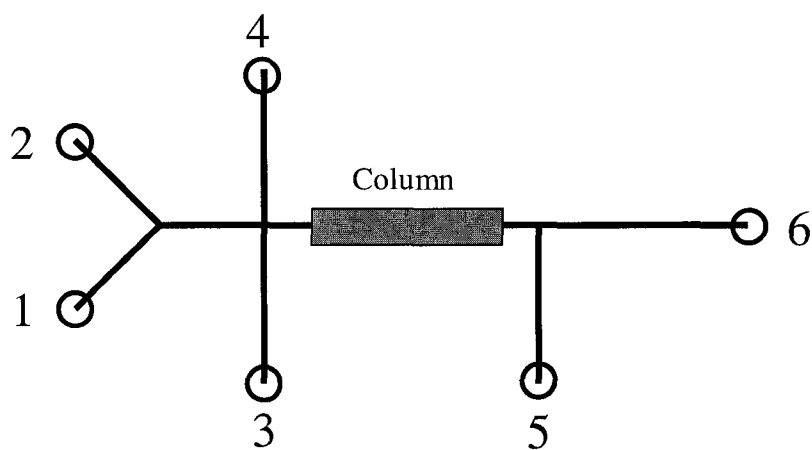Figure 6.1   Schematic representation of columns in tandem for electrochromatography.

Figure 6.2   Schematic representation of a gradient elution electrochromatographic column.

151

6.2.3 Integration of Multidimensional Electrochromatography

A natural extension of the single packed column study demonstrated in this work would be the integration of multidimensional separation techniques on-chip. Multidimensional separation systems are of interest because of their increased peak capacity and resolution over single-dimensional separation methods. According to Gidding's[9] the peak capacity of a two-dimensional (2D) system is the product of the peak capacities of the independent one-dimensional methods, provided that the separation techniques used in the two dimensions are orthogonal, i.e., the separation techniques are based on different physicochemical properties of the sample. The peak resolution is the square root of the sum of the squares of the resolution of the individual techniques. A number of coupled column separation schemes for performing comprehensive 2D analyses have been documented in the literature.[10-13]

Microfluidic devices possess great potential for multidimensional separations because high efficiency separations can be achieved and small sample volumes can be manipulated with minimal dead volumes between interconnecting channels. The chip design depicted in Figure 6.1 could also be used to undergo multidimensional electrochromatography by packing the columns with different stationary phases. By way of example, I will explain the possibility of integrating a 2D elctrochromatographic separation method using size exclusion and reversed phase beads packed in a chip design that has only two serially connected columns, columns 1 and 2 in Figure 6.1. Columns 1 and 2 could be packed with SEC and ODS beads, respectively, as discussed above. Components of a sample mixture will then be separated according to their size in the first column. If the eluting peak from this column consists of multiple components that have

152

similar size but different hydrophobicities, they will be separated in the second column by reversed phase mechanism. Otherwise, components of similar hydrophobicity but different size would elute already separated by the SEC column, using the reversed phase column to sharpen the peak, increasing the concentration, prior to detection. Because of the unlikely possibility that any two components of a mixture will have the same size and hydrophobicity, such a system offers substantially higher chromatographic resolution.

6.3 References

(1)   Venema, E.; Kraak, J. C.; Poppe, H.; Tijssen, R. *J. chromatogr. A* **1999**, *837*, 3-15.

(2)   Rebscher, H.; Pyell, U. *Chromatographia* **1994**, *38*, 737-743.

(3)   Chodhary, G.; Horvath, C. *J. Chromatogr. A* **1997**, *781*, 161-183.

(4)   Stol, R.; Mazereeuw, M.; Tjaden, U. R.; van der Greef, J. *J. Chromatogr.A* **2000**, *873*, 71-77.

(5)   Crego, A. L.; Martinez, J.; Marina, M. L. *J. High Resol. Chromatogr.* **2000**, *23*, 373-378.

(6)   Jandera, P.; Churacek, J. *Gradient Elution in Column Liquid Chromatography*; Elsevier: Amsterdam, 1985.

(7)   Qiu, C. X.; Harrison, D. J. *Electrophoresis* **2001**, *22*, 3949-3958.

(8)   Kutter, J. P.; Jacobson, S. C.; Matsubara, N. *Anal. Chem.* **1998**, *70*, 3291-3297.

(9)   Giddings, J. C. *J, High Resolut. Chromatogr.* **1987**, *10*, 319-323.

(10)   Gottschlich, N.; Jacobson, S. C.; Culbertson, C. T.; Ramsey, J. M. *Anal. Chem.* **2001**, *73*, 2669-2674.

(11)   Washburn, M. P.; Wolters, D.; Yates, J. R. *Nature Bitotechnology* **2001**, *19*, 242-

247.

(12)   Opitek, G. P.; Jorgenson, J. W. *Anal. Chem.* **1997**, *69*, 1518-1524.

(13)   Liu, H.; Lin, D.; Yates, J. R. *BioTechniques* **2002**, *32*, 898-912.